

ASPECTS ON INVERSE SCATTERING
FROM ROTATIONALLY SYMMETRIC BODIES

Francis Vandenberghe

A Dissertation
in
Electrical Engineering

Presented to the Faculty of Graduate Studies and Research of the
University of Manitoba
in Partial Fulfillment of the Requirements for the
Degree of Doctor of Philosophy

1972



RESUME

On considère le problème inverse de la diffusion par des objets parfaitement conducteurs à géométrie rotationnelle (cylindre circulaire, elliptique, sphère et ellipsoïde prolongé). Toutes les informations relatives à la géométrie de ces diffuseurs sont emmagasinées dans les coefficients du développement qui entre dans la représentation du champ diffusé.

Cette propriété est à la base de la théorie présentée ici. On accède à ces coefficients par une technique d'inversion en utilisant les composantes transversales du champ diffusé supposées connues en amplitude, phase et polarisation pour un nombre fini de direction de mesures. Afin d'obtenir le maximum de précision lors de cette inversion, on optimise le déterminant associé à la matrice du champ diffusé et exprimé sous forme analytique en fonction de ses singularités. Toute technique de mesure appropriée devra tenir compte des contraintes fondamentales résultant de cette optimisation. En supposant qu'une partie finie du développement soit connue avec une précision suffisante, il est possible de déterminer la configuration géométrique des différents diffuseurs en exprimant leurs rayons de courbure en fonction d'un nombre fini de coefficients contigus du développement. Ceci peut se faire d'une façon exacte dans les cas du cylindre circulaire et de la sphère. On trouve aussi des relations entre coefficients contigus de type électrique ou magnétique relatives au problème inverse de la diffusion. Ces mêmes concepts sont alors employés pour approcher les rayons de courbure du cylindre elliptique et de l'ellipsoïde prolongé. On n'a pas trouvé de re-

sultats exacts pour ces géométries, les relations existant entre les coefficients du développement et ces diffuseurs étant ici beaucoup plus complexes que dans les cas précédents. Une méthode, statistique et itérative, utilisant les propriétés des sections efficaces mono-statiques est alors présentée. On recommande son emploi dans les cas où la précision obtenue sur les coefficients est insuffisante. Cela arrive notamment d'une part, lorsque le rayon de courbure électrique est beaucoup plus grand que l'unité, ce qui augmente l'ordre de la matrice; d'autre part lorsque l'angle solide d'observation est petit, ce qui rend la matrice du champ diffusé quasi-singulière. Ce problème de la précision étant considéré comme très important, la deuxième partie de la thèse décrit une nouvelle méthode d'optimisation qui prévoit la localisation exacte des directions de mesures pour lesquelles l'inversion de la matrice du champ diffusé est possible. Cette nouvelle méthode est particulièrement bien adaptée pour optimiser des déterminants du type de Vandermonde impliquant des fonctions bornées.

ABSTRACT

The approach considered in this study of the inverse problem of scattering will be based on the assumption that all information pertaining to the scattering geometry is contained in the expansion coefficients representing the scattered field. This approach will be applied to rotationally symmetrical perfectly conducting scatterers, namely, the circular and elliptic cylinders, spheres and prolate spheroids. These expansion coefficients are recovered via a matrix inversion procedure from the transverse scattered field, which is known in amplitude, phase and polarization, for a limited number of non-identical aspect angles. To achieve maximum accuracy in the inversion, the closed form root factorized representation of the determinants associated with the particular scattered field matrix are optimized with emphasis placed on the basic constraints for any suitable technique limiting the measurements to a finite observation domain. Assuming that the required truncated set of expansion coefficients is found with a sufficient degree of accuracy, it is then shown that the geometrical configuration of the various bodies can be determined by expressing the main radii of curvature in terms of a finite set of contiguous expansion coefficients. For the particularly simple cases of the circular cylinder and the sphere, exact formulae are attainable in order to retrieve the associated electrical radius. Furthermore, it was found that in these cases, unique relationships exist between contiguous expansion coefficients of both electrical and/or magnetic types. The same concepts are applied to obtain approximate re-

sults for the recovery of the main radii of curvature of the elliptic cylinder and the prolate spheroid. Exact formulae have not yet been developed for these more complicated geometries, due to the complex inter-relationship between the associated expansion coefficients and the geometry. An averaging iterative method is presented employing the relationship between the magnitude of the scattered field and the illuminated area of the scatterer. This alternative is recommended whenever there is an insufficient degree of accuracy in the recovery of the expansion coefficients. This usually occurs when the electrical radius of curvature is larger than unity, which increases the size of the scattered field matrix and/or when the observation domain is restricted to a small solid angle, which produces pseudo-singular behaviour of the matrix. Since these aspects of accuracy are considered highly important, a separate section puts forward in detail a novel optimization procedure, in order to alleviate this problem. The theorems resulting from the optimization procedure determine the exact values of the bistatic aspect angles at which measurement data must be compiled in order to obtain maximum accuracy in the inversion of the scattered field matrix. This novel method is anticipated to be well suited to optimize determinants of the Vandermonde type whose elements are band-limited functions.

ZUSAMMENFASSUNG

Ein besonderer Angriff des inversen Streuungsproblems für rotationssymmetrische, unendlich leitende Streukörper (kreisförmiger und elliptischer Zylinder, Kugel und verlängertes Rotations-Ellipsoid) wird untersucht. Die Behandlung stützt sich auf die Annahme, dass alle notwendigen Daten, die die Geometrie des Streukörpers beschreiben in den Koeffizienten der Reihenentwicklung des betreffenden Streufelds enthalten sind. Diese Entwicklungskoeffizienten werden durch eine Matrixinversionsmethode vom transversalen Streufeld bestimmt, das in Amplitude, Phase und Polarisation für eine beschränkte Anzahl verschiedener Messrichtungspunkte als gegeben angenommen wird. Um höchste Genauigkeit der Matrixinversion zu garantieren, wird die geschlossene analytische Wurzelardarstellung, der für das behandelte Streuungsproblems zutreffenden Determinante optimisiert, und grundlegende Zwangsbedingungen der Messpunktverteilung, die für geeignete Messverfahren zutreffend sind, wurden besonders klargestellt. Mit der Annahme, die notwendige, beschränkte Anzahl von Entwicklungskoeffizienten mit hinreichender Genauigkeit gefunden zu haben, wird dann gezeigt, dass die Geometrie der behandelten Streukörper so bestimmt werden kann, dass die Hauptkrümmungsradien durch eine endliche Anzahl kontiguerter Entwicklungskoeffizienten ausgedrückt werden können. Für die besonders einfachen Fälle des kreisförmiger Zylinders und der Kugel konnten exakte, geschlossene Ausdrücke für die zutreffenden elektrischen Krümmungsradien formuliert werden. Weiterhin hat sich herausgestellt, dass eindeutige Beziehungen zwischen kontiguerter Entwicklungskoeffizienten des elek-

trischen und oder auch des magnetischen Types für diese beiden besonderen Fälle existieren. Die gleichen Hypothesen wurden auf die Inversionsprobleme des Ellipsoids angewandt um angenäherte Kriterien für die Bestimmung der elektrischen Hauptkrümmungsradien zu erhalten. Exakte, geschlossene Formulierungen konnten für diese komplizierteren Geometrien jedoch, wegen der komplexen Abhängigkeit der assoziierteren Entwicklungskoeffizienten von der Geometrie, nicht gefunden werden. Deshalb wird eine statistische iterative Methode eingeführt wobei von bekannten Beziehungen des monostatischen Streuungsquerschnitts Gebrauch gemacht wird um die elektrischen Hauptkrümmungsradien zu bestimmen. Dieses Annäherungsverfahren wird besonders für jene Fälle empfohlen, in denen die Genauigkeit nicht hinreichend ist. Solches ist gewöhnlich der Fall, wenn der elektrische Krümmungsradius sehr gross ist und damit eben die Ordnung der Matrix rasch zunimmt, und oder auch wenn der Beobachtungsbereich recht begrenzt ist, wodurch pseudo-singuläres Matrixverhalten auftritt. Weil diese Gesichtspunkte der Genauigkeit als besonders wichtig betrachtet werden müssen, wurde Teil B dem Hauptkörper der Dissertation hinzugefügt. Das Resultat dieses Optimisationsverfahren wurde in zwei Lehrsätze zusammengefasst, die die genauen Werte jener Messrichtungspunkte bestimmen für die genaue Messwerte nötig sind um höchste Genauigkeit in der Inversion der Streuungsmatrix zu erhalten. In dieser algebraischen Analyse wird ein neuer Optimisationsprozess für Determinanten, die sich als Vandermondsche von Funktionen begrenzten Gültigkeitsbereiches ausdrücken lassen, in Einzelheiten behandelt.

ACKNOWLEDGEMENTS

I am primarily indebted to the members of my advisory committee, which consisted of Professors W. M. Boerner, M. A. K. Hamid, H. R. Coish and E. Bridges for their guidance and direction in my post-graduate study program.

In particular, innumerable hours of consultation and discussion with Dr. W. M. Boerner, who suggested and supervised the dissertation, have provided inspiration, not only for this project, but for a life-time of personal quest. The amount of time consumed by his constructive criticism of the research, from its halting beginnings right up to the final draft, is a debt which can never be repaid.

I also wish to acknowledge my gratitude to the many professors at the University of Manitoba and elsewhere, particularly Dr. L. Shafai, who provided many helpful comments in applying numerical computation methods, and also Dr. M. A. K. Hamid, from whose help I profited in the earlier stages. In short, the entire host of my study colleagues and friends must be commended for their continuous encouragement and support which provided an essential stimulus for the development of this dissertation.

Last, not least, I wish to express my sincere gratitude to Professor V. H. Weston, who supervised Dr. W. M. Boerner during his post-doctoral

studies at the University of Michigan (Radiation Laboratory, Ann Arbor, Michigan); and who accepted to referee this thesis. Without his highly recognized contributions to the international scientific community, as a pioneer in the study of problems of electromagnetic inverse scattering, this thesis would never have been attempted.

Finally, I wish to express my appreciation for the financial support of the "International Rotary Foundation, the University of Manitoba, and the National Research Council of Canada", without whose help, it would have been impossible to complete this research.

The computation work was performed with the facilities of the University of Manitoba Data Processing Centre.

I acknowledge with pleasure my debt to Miss Jane MacIsaac for the care she has bestowed in doing the proof-reading.

In conclusion, I would like to thank Miss Carol McQuarrie for her skillful typing of the final version of the thesis.

Francis Vandenberghe

TABLE OF CONTENTS

	<u>PAGE</u>
RESUME	i
ABSTRACT	iii
ZUSAMMENFASSUNG	v
ACKNOWLEDGEMENTS	vii
TABLE OF CONTENTS	ix
LIST OF FIGURES	xiii
LIST OF TABLES	xiv
LIST OF SYMBOLS	xv
INTRODUCTION	1
<i>chapter one</i> SURVEY OF THE LITERATURE	4
1.1 Synopsis	4
1.2 Critical Evaluation of the Literature	10
1.3 Formulation of the Problem	27
<u>PART A</u>	
<i>chapter two</i> THE CIRCULAR CYLINDER	31
2.1 Introduction	31
2.2 Matrix Formulation of the Far Scattered Field Components	33
2.3 Closed-Form Solution and Optimization of the Determinant Associated with the Matrix $[\phi(N)]$	37
2.3.1 Closed-Form Solution of the Determinant $ \phi(N) $	37
2.3.2 Optimization Procedure	38
2.3.3 Computational Results	42
2.4 Derivation of the Equivalent Electrical Radius	42
2.4.1 Introduction	42

	<u>PAGE</u>
2.4.2	TM Case: $\delta = 0$ 45
2.4.3	Mixed Case TM-TE: $0 < \delta < \pi/2$ 46
2.4.4	TE Case: $\delta = \pi/2$ 49
2.5	Computation of k_a from the Exact Values of the a_n and b_n Coefficients 52
2.6	Computation of k_a from the Coefficients' Values Obtained after Inversion of $[\phi(N)]$ 59
2.6.1	Introduction 59
2.6.2	Accuracy Dependence upon the Order of Truncation M 60
2.6.3	Formulation of $(a_n, n \geq 4)$ in Terms of $a_0, a_1, a_2,$ and a_3 61
2.6.4	Accuracy Dependence upon the Domain of Observation 63
2.7	Iterative Averaging Method Developed to Retrieve the Electrical Radius of Curvature of the Cylinder 64
2.7.1	Introduction 64
2.7.2	Iterative Averaging Method 67
2.7.3	Flow Chart and Computational Results 71
2.8	Conclusions 72
<i>chapter three</i> THE ELLIPTICAL CYLINDER 76	
3.1	Introduction 76
3.2	Formulation of the Far Field 77
3.3	Inversion Procedure 82
3.4	Reduction of Equations (3.2.10) and (3.2.12) 82
3.4.1	Review of the Notations 82
3.4.2	Reduction of Equation (3.2.12) 83
3.4.3	Reduction of Equation (3.2.10) 85
3.4.4	Preliminary Conclusions 86
3.4.5	Analysis of $-\sum_{n=0}^{\infty} A_1^{2n+1} ce_{2n+1}(0) \cdot \gamma_{2n+1}(\xi_0)$ 86
3.4.6	Limiting Case of the Circular Cylinder 89
3.5	Retrieval of the Axis of the Cylinder by Employing an Iterative Averaging Method 90
3.6	Conclusions 97

	<u>PAGE</u>
<i>chapter four</i> THE SPHERE	99
4.1 Introduction	99
4.2 Formulation of the Far Scattered Field	100
4.3 Closed-Form Solution and Optimization of the Determinant Associated with the Matrix $[F_m]$	107
4.3.1 Decomposition of the Determinant Associated with $[F_m]$ into its Polar and Azimuthal Parts	107
4.3.2 $\text{Det} \cdot [\phi_m(\phi_\mu)] = \phi_m(\phi_\mu) $	108
4.3.3 $\text{Det} \cdot [\Theta_m(\theta_{\mu,\nu})] = \Theta_m(\theta_{\mu,\nu}) $	109
4.3.4 Summary and Interpretation of the Closed-Form Solution of the Determinant $ F_m(\theta_\mu, \phi_\mu) $	109
4.4 Optimization Procedure	110
4.5 Determination of the Equivalent Radius of Curvature of the Sphere	119
4.5.1 Introduction	119
4.5.2 Derivation	120
4.5.3 Computation of ka from the Exact Values of the a_n and b_n Coefficients	125
4.6 Conclusions	125
<i>chapter five</i> THE PROLATE SPHEROID	129
5.1 Introduction	129
5.2 Matrix Formulation of the Scattered Field	130
5.3 Retrieval of the Parameters of the Generating Ellipse	134
5.3.1 Computation of the K_j and \bar{K}_j Coefficients	134
5.3.2 Retrieval of the Parameters of the Generating Ellipse	135
5.4 Conclusions	137

<u>PART B</u>	<u>PAGE</u>
<i>chapter six</i> OPTIMIZATION PROCEDURE	141
6.1 Introduction	141
6.2 Formulation of the Problem	143
6.3 Optimization Procedure	145
6.4 Optimization of the Determinant $ \phi(N) $ as Given by Equation (2.3.2)	149
6.5 Optimization of the Determinant Associated with the Geometries Representing the mth Degree Multipole Cases	160
6.6 Relevance to Measurement Techniques	163
<i>chapter seven</i> SUMMARY AND CONCLUSIONS	164
BIBLIOGRAPHY	172
APPENDICES	177
A.1 Retrieval of the Polarization Angle δ	177
A.2 Properties of the Vandermonde Determinant	180
A.3 Formulation of a_0 and a_2 in Terms of the b_n Coefficients	182
A.4 Formulation of $(a_{n+4}, n \geq 0)$ in Terms of (a_0, a_1, a_2, a_3)	186
A.5 Formulation of the Far Scattered Field from an Elliptic Cylinder	190

Leaf xvii omitted
in page numbering.

LIST OF FIGURESPAGE

Figure 1	Geometry for Plane Wave Incidence	34
Figure 2	Measurement Aspect Angles	40
Figure 3	Co-ordinates for the Optimization Procedure	41
Figure 4	Block Diagram of the Iterative Averaging Method	69
Figure 5	Flow Chart of the Iterative Averaging Method	70
Figure 6	Co-ordinates Used for the Elliptic Cylinder	79
Figure 7	Receiver Directions for the Reduction of Equation (3.2.12)	84
Figure 8a, 8b, 8c, 8d	Comparison of the Backscattered Field from an Elliptic Cylinder and a Circular Cylinder of Identical Radius of Curvature	91 - 94
Figure 9	Scattering Geometry for the Sphere	101
Figure 10	Measurement Polar Angle Used for Geometries Representing the mth Degree Multipole Cases	112
Figure 11	"Pseudo-Singular" Distribution of Aspect Angles	117
Figure 12	Stable Distribution of Aspect Angles	118
Figure 13	Prolate Spheroid Scattering Geometry for Nose-on Incidence	132
Figure 14	Characteristic Equation for the Evaluation of the Eccentricity	138

<u>LIST OF TABLES</u>	<u>PAGE</u>	
Table 1	Verification of the Optimization Procedure	43 - 44
Table 2	Tabulation of a_n and b_n Coefficients for $ka = 1.0, 5.0, n$ and 10.0	53 - 55
Table 3	Expansion Coefficients a_2 as Given by (2.2.5b) and by (A.3.17)	56
Table 4	Determination of ka for the TM, TM-TE, and TE Cases	57
Table 5	Determination of ka for the TE Case Employing the Approximation $a_0 \approx - (1 + b_0)$	58
Table 6	Retrieval of the Electrical Radius of the Cylinder From the Iterative Averaging Method	73
Table 7	Determination of the Axes of an Elliptic Cylinder	96
Table 8	Expansion Coefficients a_0 and a_1 as Given by (4.5.9) and (4.5.13)	126
Table 9	Determination of ka for the TM, TM-TE, and TE Cases	127

LIST OF SYMBOLS

Greek Alphabet:

α, β	Wedge limiting angles
α_0	$= a_0 - b_0$
α_1	$= a_0 - b_1$
$\alpha_{2n}, \beta_{2n+2}, \gamma_{2n+1}, \delta_{2n+1}$	Constants used in the formulation of the field scattered from an elliptic cylinder
δ	Polarization angle
$\Delta_{\mu\nu}$	Geodesic distance between two points
∇^2	Laplacian operator
ϵ_0, μ_0	Characteristics of the propagation medium
ϵ_n	$\begin{cases} 1, n=0 \\ 2, n>1 \end{cases}$
θ_r	Polar angle
θ_{ma}, θ_{mb}	Limiting measurement aspect angle of the cone of observation
θ_a, θ_b	Limiting computational aspect angles
θ_{0r}	Computational aspect angle
θ_{MC}	Half-cone measurement angle
λ	Wavelength
μ, ν	Integers
ξ_0	Inverse of the eccentricity of the generating ellipse of the elliptic cylinder
(η, ξ, z)	Elliptic co-ordinate system
π	Pi (3.14159265)
ρ	$= ka$

ρ_m, s_m, C_m, S_m	Constant multipliers used in the formulation of the field scattered from an elliptic cylinder
σ	Cross section
ϕ, ϕ_r	Bistatic measurement angles
ϕ_0	Computational axis angle
ϕ_a	Half-wedge angle
ϕ_ω	Centre wedge angle
$[\phi(N)]$	Matrix of order N
ω	Angular speed
$\omega_{\mu\nu}$	Element in a Vandermonde determinant
ω_i	Column vector in a Vandermonde matrix

Latin Alphabet:

a	Radius of the cylinder or of the sphere
\hat{a}	Invariant axis of the observation cone
a_n, b_n, a_n'', b_n''	Associated expansion coefficients
$a_{\mu\nu}$	Difference term of expansion coefficients $a_\mu - a_\nu$
a, b	Axes of the elliptic cylinder
$A_\mu, B_\mu, C_\mu, T_\mu, U_\mu, L_\mu, M_\mu, N_\mu$	Coefficients
A_n^m, B_n^m	Coefficients of the Mathieu functions
$a_{o,m,n}^e, b_{o,m,n}^e$	Expansion coefficients in the scattered field formulation for the sphere case
$a_{o,mn}^e, b_{o,mn}^e$	
$b_{\mu\nu}$	$= b_\mu - b_\nu$
ce_m, se_m	Even and odd solution of order m of the regular Mathieu differential equation

P_n^m	Associated Legendre polynomial of order n and degree m of the first kind
q	Parameter used in the Mathieu functions
Q_n	Legendre polynomial of order n of the second kind
Q_n^m	Associated Legendre polynomials of order n and degree m of the second kind
R	Range
(R_c, θ_c, ϕ_c)	Co-ordinates of the c th receiver
S_n^e	Sum of the exact magnitude of the back-scattered fields evaluated at n aspect angles
$S_n^{\text{appr.}}$	Sum of the approximate magnitude of the back-scattered fields evaluated at the same n aspect angles as for S_n^e
T_n, U_n	Functions of multiplied expansion coefficients
u_k, u_r	Normalized cosines
v_k	$= u_k^2$
V	Potential function
x_r	$= \cos \phi_r$, ϕ_r azimuthal angle
X	Column vector of associated expansion coefficients
(x, y, z)	Cartesian co-ordinate system
$\hat{x}_0, \hat{y}_0, \hat{z}_0$	Unit vectors in a cartesian co-ordinate system
Z_ν	Bessel function

P_n^m	Associated Legendre polynomial of order n and degree m of the first kind
q	Parameter used in the Mathieu functions
Q_n	Legendre polynomial of order n of the second kind
Q_n^m	Associated Legendre polynomials of order n and degree m of the second kind
R	Range
(R_c, θ_c, ϕ_c)	Co-ordinates of the c th receiver
S_n^e	Sum of the exact magnitude of the back-scattered fields evaluated at n aspect angles
$S_n^{\text{appr.}}$	Sum of the approximate magnitude of the back-scattered fields evaluated at the same n aspect angles as for S_n^e
T_n, U_n	Functions of multiplied expansion coefficients
u_k, u_r	Normalized cosines
v_k	$= u_k^2$
V	Potential function
x_r	$= \cos \phi_r$, ϕ_r azimuthal angle
X	Column vector of associated expansion coefficients
(x, y, z)	Cartesian co-ordinate system
$\hat{x}_0, \hat{y}_0, \hat{z}_0$	Unit vectors in a cartesian co-ordinate system
Z_ν	Bessel function

The world of our sight is like
the habitation in prison, the fire-
light there to the sunlight here,
the ascent and the view of the upper
world is the rising of the soul into
the world of mind; put it so and you
will not be far from my own surmise,
since that is what you want to hear;
but God knows if it is really true.

(from "The Cave" Book VII of the
Republic - Plato)

INTRODUCTION

The goal of science is to extend our human faculties to limitless horizons. Researchers have been endeavouring since the turn of the century to devise equipment specially designed to identify objects that we cannot see with the naked eye. Visual identification of objects by scattered light is an everyday experience and the mechanism whereby the eye perceives shapes is relatively well understood. With the appearance of Doppler-radar, sonar-operated systems, Fourier optics and aperture synthesis, it is now possible to localize and attain a good resolution of otherwise remote objects. These systems are employed extensively in the fields of air traffic control, oceanography, telemetry, satellite tracking, remote sensing, etc.

However, no-one has yet succeeded in displaying actual configuration of objects illuminated by radar, although several attempts were initiated in the last few decades. Numerous techniques were developed and tested in order to increase the ability of radar-operated systems to portray remote objects. These techniques organised the accumulation of radar data to reach its full potential, comparable in its development to that of software techniques for the computer. These techniques are the epitome of radar information as the most powerful extension of visual perception.

Research in the field of inverse scattering is directed towards this

goal of target identification. The following survey of the literature puts in evidence the lack of a general method of target identification. Presuming the existence of such an overall technique, there is also no indication of its development in the near future despite prodigious efforts devoted to this end.

In practical applications, various radar signatures are simultaneously considered for any specific case encountered. Correlation of these signatures usually allows a significant reduction of ambiguity in the objectification of the body shape. In the light of the previous remarks, any contribution to this extremely complicated problem will bring substantial insight into the problem of scattering and aid to define the ultimate goal of defining the shape of remote objects.

Within this framework, then, the present thesis will be strictly concerned with the objectification of the shape of rotationally symmetrical bodies of revolution, for which separation into orthogonal functions has been well-established. The shapes we will consider are: the circular cylinder, the elliptic cylinder, the sphere and the prolate spheroid, which we will assume to be perfectly conducting bodies. Various factors dictate the choice of these particular geometries: the circular cylinder and the sphere have important applications in radar and antenna theories, and the elliptic cylinder and the spheroid are often used as models for the development and testing of approximate methods. Finally, since the exterior form of these scatterers is a level surface in a system of

orthogonal co-ordinates, this investigation will be confined within the realm of classical electromagnetic theory.

*chapter one*SURVEY OF THE LITERATURE1.1 SYNOPSIS

The theory of diffraction and scattering was developed for the express purpose of gaining insight into the interaction of propagating waves with known obstacles. In its most general implications, this theory compares the behaviour of a non-stationary system as time tends towards zero with its asymptotic behaviour, as time tends towards infinity via a scattering matrix. This scattering matrix, which relates the properties of the system to the nature of the scatterer, constitutes the sole observable data when the scatterer is remote, or otherwise inaccessible to direct observation. Lately, with the advent of radar tracking and identification, it has become essential to extract that information pertaining to the shape and material constituents of the scatterer directly from the scattering matrix. This incentive has opened up an entirely new area of research: that of the inverse theory and technique of diffraction and scattering in the field of electromagnetics.

The inverse theory deals with the problem of recovering the shape of the scatterer from bistatic data for a given incident field, both of which are compiled in the scattering matrix. However, the delineation of the shape of the scatterer can be accomplished only if the scattered field data is related to a given co-ordinate system. This data will

then be expressed in terms of its co-ordinate variables, and the associated vector wave functions suitable for the problem at hand.

Though the inverse scattering field has generated an intense amount of interest in the past few years, the demand for new basic model techniques is as strong as ever, since the formulation of a general overall model technique seems increasingly unfeasible, owing to extensive mathematical complications. For this reason, only those shapes easily amenable to rigorous mathematical treatment will be considered within the scope of this thesis: namely, the circular and elliptic cylinders, the sphere and the prolate spheroid, for which the direct problem of scattering has been resolved. While none of these shapes represent the elaborate geometries one encounters in practice, the results of the present investigation of the inverse scattering field will prove highly encouraging to all those engaged in areas of target identification and structural pattern recognition.

As an initial approach to the inverse problem of scattering, the far scattered field will be expanded in terms of the associated vector wave functions. The transverse far scattered field components for non-identical aspect angles will then be related by means of the far scattered field matrix to the truncated set of the unknown expansion coefficients, which we assume to be extractible from the scattering matrix. The associated expansion coefficients are further determined by a matrix inversion technique which imposes severe restrictions on the distribution of

aspect angles. The matrix inversion procedure is inherently unstable, however, due to the particular properties of the wave functions employed; these instabilities can be examined from the properties of the determinant associated with the scattered field matrix. To avoid these instabilities, a novel determinate optimization procedure has been developed to deal with the closed-form solution of these determinants. (This optimization procedure and its relevance to any suitable measurement technique is presented in Part B. In particular, it is shown that when the derived optimization constraints are satisfied, the expansion coefficients can be recovered with maximum accuracy.) Assuming, therefore, that the scattered field matrix can be inverted, the prime objective of this thesis is to demonstrate the recovery of the electrical radii of curvature of that particular perfectly conducting scatterer under consideration, from a limited set of contiguous expansion coefficients (as analysed in Part A). In addition, within the course of the analysis, unique relationships between contiguous expansion coefficients of the magnetic and/or the electric type, and fundamental properties of vector wave expansions have been derived. These may be favourably employed for improving the accuracy of the recovered expansion coefficients and are, therefore, considered highly relevant to the inverse problem of scattering.

However, this approach does not ascertain total accuracy in all cases. For example, when the electrical radius is very much greater than unity, or, when the domain of observation is restricted to a small solid angle,

the inversion of the matrix remains a very long and involved operation. Therefore, an alternative approach had to be put forward; the concept implied in this alternative will base itself upon the fact that the backscattered field depends on the radius of curvature of the illuminated area of the scatterer. When the associated expansion coefficients cannot be reduced to a simple form, as was possible in the cases of the circular cylinder and the sphere, this alternative method will be expressly employed, in order to obtain a reasonable degree of accuracy.

This thesis will be divided up into two major sections. Part A will be mainly concerned with the retrieval of the radii of curvature of the various scatterers; Part B will be reserved for the optimization procedure.

Part A is further divided into four chapters, each of which deals with a different scattering geometry.

Chapter one consists of a selective critical survey of the latest articles on the problem of inverse scattering. However, due to the large amount of research in this area still considered classified information, this survey makes no claim to completely exhaust the field.

Chapter two devotes itself to the problem of the perfectly conducting circular cylinder. In dealing with this problem, we will include:

- (i) The formulation of the far scattered field in terms of circular wave functions
- (ii) The recovery of the electrical radius for the TE, TM and mixed polarization cases
- (iii) A detailed discussion of optimum locations of bistatic angles, in order to avoid the instabilities inherent in the matrix inversion procedure.

There arises a definite problem in obtaining good accuracy here, due to the truncation of the infinite series representing the scattered field, and the matrix inversion procedure. This problem will be reviewed in detail. A description of the iterative averaging method is also presented, in order to obtain the degree of accuracy necessary to retrieve the shape of the circular cylinder.

Chapter three applies the theory developed at length in *chapter two* to the case of the elliptic cylinder. In particular, the difficulty of recovering the contour of the cylinder utilizing the first method is demonstrated. This is due to the complexity of the Mathieu functions involved in the formulation of the far scattered field. Therefore, the alternative method is also applied in this case of the elliptic cylinder.

A further application of the inverse scattering model to the three dimensional case is reviewed in *chapter four*. This chapter points out the similarity existing between the far scattered field and the associated expansion coefficients in both the spherical and the cylindrical cases.

Once again, in order to recover the associated coefficients, we must avoid the inherent instability in the matrix inversion procedure by employing the optimization procedure for the m th degree of multipole geometries. This is invaluable in determining the location of the optimum directions of measurement.

The method of shape recovery for the prolate spheroid is proposed in *chapter five*. This will be predominantly based on the representation of the far field as given by Stevenson⁽⁴⁵⁾. However, this study will be limited by a lack of tabulated data, to a purely theoretical analysis.

Part B is strictly concerned with the optimization procedure essential to accurately recover the scatterer shapes examined in Part A. As it is not, strictly speaking, included in the field of inverse scattering, it has been thought to reserve its development to a separate section of the thesis. This optimization procedure deals with the closed-form representation of the determinants associated with the various scattered field matrices. Of tantamount importance is the derivation of this novel determinate method, which can be used to optimize any analytical and band-limited expression written in terms of a factorized root expansion of its singularities.

Part B is followed by five appendices. *Appendix A.1* presents a method to recover the polarization angle from the expansion coefficients in the case of the circular cylinder.

Appendix A.2 is a brief reminder of the properties of the Vandermonde determinant.

Appendix A.3 formulates the expansion coefficients associated with the TM case, in terms of the expansion coefficients associated with the TE case, for the circular cylinder.

Appendix A.4 formulates the TM coefficients in terms of the first five coefficients for the circular case.

Appendix A.5 derives the far field scattered by the elliptic cylinder in terms of the Mathieu functions.

1.2 CRITICAL EVALUATION OF THE LITERATURE

The classical problem of scattering and diffraction of electromagnetic waves by an object originates within the field of optics. Research carried out so far on this problem primarily concerns itself with the formulation of the scattered and diffracted field when the scatterer and the sources (i.e. the incident field) are known. To determine the field scattered by the object, we must find the difference between the total field which exists when the object is present and the field existing in the object's absence. We then add the scattered field to the incident field to find the diffracted field.

The inverse scattering problem arises naturally as the situation is reversed, that is, when the nature of the scattering body is unknown, and the only information available is the incident and scattered fields. These fields are given in terms of a fixed co-ordinate system whose origin lies within the scatterer.

A variety of problems fall under the general heading of inverse scattering and diffraction, due to the diverse interests of those engaged in this field. Therefore, we will divide our review into three major approaches: The first approach will be largely theoretical; the second numerical; and the third mainly concerned with those practical applications and experimental work of the type usually conducted under the supervision of the Departments of Defense.

The purely theoretical approach endeavours to acquire the maximum data about the distribution of sources of finite extent from the far scattered field, which originated from those very same sources.

The second approach attempts to discover methods of resolving simpler problems of inverse scattering, such as identification of bodies of revolution by employing certain approximations, which then lead to numerical results. These methods also specify the conditions adequate in order to determine techniques of measurement, thus eliminating redundant data, and cutting down on computation time.

The last approach deals essentially with estimating from radar data the size, configuration and characteristics of target motion, such as the generalized vector of motion, which encompasses angular velocities of axial rotation and tumbling, and the inclination of the target axis relative to its mass-center trajectory.

Although there is a lack of precise terminology about what exactly is inferred by the inverse scattering problem (I.S.P.), the two latter approaches center on the common problem of determining the shape and material constituents of unknown scatterers from far field data when the transmitted field is given and the received far scattered quantities are known in amplitude, phase and polarization. The problem is usually investigated by resorting to two techniques often found in the literature: continuous wave inverse scattering (C.W.I.S.) and pulse wave inverse scattering (P.W.I.S.).

However, when the scattering geometry is non-stationary, the problem also involves the description of the orbital vector of target motion.

The orbital vector of motion includes:

- (i) the translatory vector, giving direction of spinning;
- (ii) the spin vector, determining spinning rate; and
- (iii) a third vector, outlining the direction and rate of tumbling;

all three of which are specified in terms of a stationary fixed time-space reference system. The translatory vector of motion is usually determined by monostatic wave-operated Doppler radar systems, whereas

the spin vector and the vector describing the direction and time rate of tumbling must be determined from inverse scattering.

These three approaches will be covered in sequence, emphasizing the problem of ascertaining target shape. However, the last approach will only be briefly sketched as most of the work in this area is unavailable.

The last few decades have seen an important development in the theoretical analysis to the inverse scattering problem. Studies on the far field produced by a known scatterer have led to research on the inverse problem: to what extent does a knowledge of the far field arising from finite sources determine the distribution of these same sources? This problem, first examined by Saunders⁽⁴⁰⁾ and Weyl⁽⁵⁹⁾, was further investigated by Müller^(36,37) and Wilcox⁽⁶⁰⁾ in the scalar and vector cases. They discovered that the far scattered field determines the radius of the minimum sphere enclosing the sources generating this same field. However, the extension of these sources within this minimum sphere is not uniquely specified; for instance, if the sources are distributed over a certain volume in such a manner that the far field can be expressed in a finite number of surface harmonics, as in the case of the sphere, an identical far field can be obtained from sources inside an infinitesimal sphere around the origin. These results also follow from an expansion theorem given by Wilcox⁽⁶⁰⁾ for the vector case. They are also verified by Atkinson⁽³⁾ while an equivalent expansion theorem was propounded by Karp⁽¹⁹⁾ for the scalar case. The one-to-one

relationship between the far field and the sources is nevertheless established by assuming that the integral:

$$\iiint_{\text{source}} |j|^2 dv$$

is minimal. In this formula, "j" represents the currents originating from dipole densities on lines, surfaces, or domains within the minimum sphere.

It is worthwhile, at this stage, to note that the inverse scattering problem for the scalar case is well known in non-relativistic quantum mechanics. The time-independent Schroedinger equation:

$$\nabla^2 u + k^2(1 - V)u = 0$$

which describes the quantum mechanical scattering has the same form as the Helmholtz equation:

$$\nabla^2 u + \frac{k^2}{\eta^2} u = 0$$

In these formulae, "u" represents the wave function or probability amplitude of particles moving in a potential "V", "k" being the wave number and "η" the relative impedance. The problems resolved so far in quantum mechanics are one-dimensional. They can be treated by the perturbation theory in which "V" must always be smaller than unity. This method could be carried over into electromagnetic theory, for the one-dimensional case, by replacing $(1 - V)$ by $1/\eta^2$. However, in scattering from remote objects, $\eta = 1$ everywhere outside the object and zero inside the object, implying that "V" would be by no means smaller everywhere as compared to unity. Consequently, these methods are in general inappropriate.

However, using a slightly modified technique, a group of one-dimensional problems has been successfully treated by Moses and de Ridder⁽³⁵⁾ and Kay⁽²¹⁾. In his paper, Kay considers the feasibility of recovering for all x a function potential $V(x)$ associated with the following differential equation:

$$\frac{d^2 u(x,k)}{dx^2} + k^2 [1 - V(x)] u(x,k) = 0$$

from the reflection coefficient $r(k)$ known for all real k . He demonstrates that this is indeed possible whenever $r(k)$ is a rational function of k . Bargmann⁽⁴⁾ found in addition that potentials for the radial Schroedinger equation of quantum mechanics, as well as for the radial corresponding wave equation, can be explicitly determined under identical conditions. Faddeyev⁽¹³⁾ also presented an extensive bibliography of the quantum mechanics inverse scattering problem.

A three-dimensional scalar problem is similarly treated by Petrina⁽³⁸⁾. The scattering body is assumed to be homogeneous and isotropic; so that the Helmholtz equation is satisfied with a wave number k_1 inside the body, and with a wave number k_0 outside the body. Petrina indicates further that the relation between the scattering amplitude and the shape of the scattering body is:

$$\left. \frac{\partial f(k_0, k_1, \tau)}{\partial (k_0^2)} \right|_{k_0^2 = k_1^2} = - \frac{1}{4\pi} \iiint_{\text{body}} e^{j\tau \cdot s} ds$$

The integration is to be performed over the volume of the scattering body using:

$$\underline{\tau} = \underline{k}_0 - \frac{k_0}{|\underline{R}|} \underline{R}$$

with " \underline{k}_0 " being the wave vector of the incident plane wave and \underline{R} being in the direction of observation. The integral on the right-hand side can be considered as the Fourier transform of a function which is equal to unity inside the scatterer and vanishes outside. Thus, knowledge of the left hand side for all $\underline{\tau}$ determines the shape of the scatterer.

Some properties for two-dimensional, acoustically soft and hard obstacles are given by Karp⁽²⁰⁾. He forms determinants with elements f_{ij} , where $f_{ij}=f(\theta_i, \theta_j)$ represents the far diffracted field at infinity, at an angle of observation θ_i for an angle of incidence θ_j . He deduces the necessary and sufficient geometrical conditions relative to the shape of the scatterer for the vanishing of such determinants, when the boundary conditions are fulfilled. Furthermore, he proves that if $f(\theta_i, \theta_j)$ depends only upon the difference $(\theta_i - \theta_j)$, the scatterer must be a circle.

Whenever the target under investigation is stationary but not of a simple form, like the infinite circular cylinder or the sphere, approximations must be made to obtain actual numerical solutions. These approximations result from the fact that the shape of the body is either not a level surface in any co-ordinate system, or that the formulation of the solution to the direct problem is too complex to be exploited for the inverse study. This has been reviewed from the standpoint of the inverse scattering problem by Altman, Bates and Fowle⁽²⁾. In parti-

cular, they show that for good conductors, the direct solution is given through the following integral equations of the second kind:

$$\begin{aligned} \underline{H}_s \Big|_P &= \frac{1}{4\pi} \iint_{\text{scatterer}} \hat{n} \times (\underline{H}_i + \underline{H}_s) \times \nabla \left[\frac{e^{+jkR}}{R} \right] \cdot \underline{ds} \\ \underline{E}_s \Big|_P &= \frac{1}{4\pi} \iint_{\text{scatterer}} \left\{ + j\omega\mu [\hat{n} \times (\underline{H}_i + \underline{H}_s)] \frac{e^{+jkR}}{R} - \right. \\ &\quad \left. \frac{1}{j\omega\epsilon} [\hat{n} \cdot \nabla \times (\underline{H}_i + \underline{H}_s)] \nabla \left[\frac{e^{+jkR}}{R} \right] \right\} \cdot \underline{ds} \end{aligned}$$

where \underline{H}_s assumes its value on the surface S inside the integral sign, "R" being the distance from the point of observation to the vector surface element \underline{ds} , \hat{n} being the normal vector pointing outward from S , with μ and ϵ being the characteristic constants of the medium.

In a numerical approach, if one is given the far field $E_s \Big|_{\infty}$ and $H_s \Big|_{\infty}$ at a sufficient number of bistatic receiver locations, the problem is reversed and becomes that of determining the shape of the scatterer. Various techniques have been proposed employing the method of continuous wave inverse scattering (C.W.I.S.), in order to approximate the overall structure of the unknown target. For instance, the inversions of \underline{E}_s and \underline{H}_s can be carried out in some restricted cases under physical or geometrical optics approximations.

In particular, Altman et al⁽²⁾ demonstrate that, if the body is a flat plate of arbitrary shape, and if the scattered field falls within a small solid angle, the shape of this plate can be recovered. This is done

using the two-dimensional Fourier transform of the scattered field as a function of aspect angles and using physical optics or the Kirchhoff approximations. These approximations assume that the body dimensions and the wavelength are smaller than the range and that the total H field equals $2H_i$ on the body surface in the illuminated region and equals zero in the shadow region.

The inverse scattering problem associated with the geometrical optics approximations ($k \rightarrow \infty$) has been investigated by Lewis⁽²⁸⁾ and Keller⁽²³⁾ for doubly curved convex bodies of revolution whose axis of symmetry is known. From a given scattering amplitude and reflection coefficient at the specular point, the specular point being that region perpendicular to the radar line of sight, Altman et al⁽²⁾ have obtained explicit formulae to determine the illuminated surface area of two-dimensional geometries. In the three-dimensional case, the bistatic radar cross section is proportional to the reflection coefficient and the product of the principal radii of curvature R_1 and R_2 . When the Gaussian curvature $G = \frac{1}{R_1 R_2}$ of a particular surface is given for all directions of the normal to the surface, the shape recovery is entitled Minkowski's problem, and has a unique solution for smooth convex bodies. For a singly curved body of revolution (i.e. cone, cylinder, etc.) whose axis of symmetry has been determined, the geometrical optics method no longer applies, since one principal radius of curvature becomes infinite. In this case, an approximate method originated by Blasberg, is described in Altman et al⁽²⁾. Using the geometrical optics approximations, they

demonstrate that the backscattering is proportional to the Fourier transform of a function $\sqrt{r(x)} e^{2jkr(x)}$. In this expression $r(x)$ is the radius of the cross section as a function of x along the axis of revolution. This function is valid only for small values of that angle formed by the direction of propagation of the incident plane wave and the direction perpendicular to the axis of revolution, the three directions being coplanar. Using this modified technique, they prove the inverse Fourier transform to be a function of $\sqrt{r(x)} e^{2jkr(x)}$ for x inside the body and zero outside, provided that the backscattering field falls within a small solid angle, as in the case of flat bodies.

Recently, using Kirchhoff approximations, Lewis⁽²⁸⁾ found a general method for solving the inverse diffraction problem, when the backscattering field is known at all aspect angles and frequencies. His method, based on Bojarski's identity⁽⁹⁾, states that the characteristic function $\gamma(x)$ defining the target where $\gamma(x) = 1$ inside and zero elsewhere, is a Fourier transform of that gamma function $\Gamma(\frac{2\omega}{c})$ related to the backscattering field. He shows that only partial recognition is possible, when data is restricted to a frequency band and a limited cone of aspects. However, his results are somewhat limited in their application since $\Gamma(\frac{2\omega}{c})$ must be measured near the front and the rear of the target.

The site of intense involvement in inverse scattering since 1965 has been the University of Michigan Radiation Laboratory where V. H. Weston and his research associates have developed a good variety of inverse

scattering techniques. As regards the one-to-one source field relationship, they first of all examined the interdependence of the shape and material characteristics of the scattering body with the radius of the minimum sphere. The equivalent sources are enclosed by this minimum sphere, whose radius is given as the radius of convergence of the far field expansion in Wilcox's paper⁽⁶⁰⁾. It is shown in particular that one can obtain different minimum spheres enveloping the target by changing the origin of the co-ordinate system. This report essentially contributes a unique theoretical explanation of the recovery of scatterer shapes of convex configuration, under specific boundary conditions. These conditions require that the total E field vanishes on the surface if the body is a perfect conductor or that E and H are related by the equation of the Leontovich type:

$$\underline{E} - [\underline{E} \cdot \hat{n}] \cdot \hat{n} = \eta \sqrt{\frac{\mu_0}{\epsilon_0}} \hat{n} \times \underline{H}$$

where \hat{n} is the unit outward normal to the surface and η is the relative impedance of the body.

In the light of the foregoing results, and in order to apply boundary conditions, Weston and Bowman⁽⁵⁶⁾ have developed a technique for the recovery of the near field in terms of the far field data. This technique bases itself upon the representation of the far scattered field in terms of plane waves. An integral representation of the near field over a complex unit sphere has been derived for this purpose. The expression of the field in the far zone is then extended by analytical

continuation into the complex polar angle plane. The solution is best suited for the high frequency case since the integral may then be evaluated by the stationary phase method. Weston, Bowman and Ar⁽⁵⁷⁾ examine the possibility of recovering the near field into cavity regions, using an analytical continuation procedure in order to define the contour of the scattering geometry. They derive further the necessary boundary condition $\underline{E}_T \times \underline{E}_T^*$ valid for perfect conductors. This condition correctly portrays the scattering surface when expressed at two different frequencies, as is demonstrated⁽⁴⁹⁾ for a perfectly conducting sphere. This necessary boundary condition $\underline{E}_T \times \underline{E}_T^*$, though not sufficient is superior to the condition $|\underline{E}_i| - |\underline{E}_s| = 0$ since $\underline{E}_T \times \underline{E}_T^*$ is applicable far into the shadow region, whereas $|\underline{E}_i| - |\underline{E}_s|$ represents the geometrical optics approximations usually restricted to a narrow cone around the specular point. Both conditions also yield maximum accuracy when the incident polarization is parallel to the generatrix of the scatterer.

In a more recent publication dealing with the three-dimensional vector problem, Weston and Boerner⁽⁵⁵⁾ show that the total field produced by a plane wave incident on a scattering body can be expressed as the sum of two contributions: the incident field and the Fourier transform of a quantity related to the scattering matrix. They deduce⁽⁵⁵⁾ the following equation which is valid for all points in space, including the interior of the scattering body.

$$\underline{E}(\underline{x}, \underline{k}) = \underline{E}_i(\underline{x}, \underline{k}) + \frac{1}{\sqrt{(2\pi)^3}} \int_{-\infty}^{\infty} \frac{e^{j\underline{p} \cdot \underline{x}}}{p^2 - k^2} \overleftrightarrow{T}(\underline{p}, \underline{k}) \cdot d\underline{p}$$

where $-\infty < p < \infty$, " \underline{k} " is the direction of the incident wave and $\overleftrightarrow{T}(\underline{p}, \underline{k})$ is a measurable function proportional to the far scattered field in the direction \underline{p} related to the scattering matrix. They also examine what can be recovered about the body, when the measurements of the far field can only be carried out within a limited domain of aspect angles. In particular, they show that the near field representation can be determined by a matrix inversion for rotationally symmetric scatterers and end-on incidence. In this case, the far scattered field components are represented by a series expansion into spherical vector wave functions. These components are best displayed as the matrix formulation:

$$[E] = [A] \cdot [X]$$

where X represents the unknown expansion coefficients. The matrix $[A]$ is inverted in order to recover these coefficients and the near field is deduced accordingly. Unfortunately, this process involves instability and definite loss of accuracy. Following this line of thought, the direct problem is studied in detail by Waterman and McCarthy⁽⁴⁹⁾. They have gone so far as to develop a documented computer program to evaluate the scattered field originating from perfectly conducting symmetric bodies. The method is based on the generation of elements of an $N \times N$ matrix, followed by subsequent inversion to solve for the unknown surface currents on the scatterer which are obtained via an integro-differential equation.

In a recent paper, Imbriale and Mittra⁽¹⁵⁾ applied a technique similar to that of Weston and Boerner⁽⁵⁵⁾. They employ a process of analytical continuation with translations of the co-ordinate origin to obtain the near field representation; and geometrical optics boundary conditions to define the body shape contour. In particular, they demonstrate that the knowledge of the incident and scattered field at only one frequency was indeed sufficient to recover the size, shape and location of the scatterer. They limited their study to elliptic, circular cylinders and conducting strip geometries.

When the overall structure of the scatterer is known, the subsequent problem consists in defining the material characteristics of the body. Although the P.W.I.S. method is more suitable for this purpose, some important details about those characteristics are acquired by using the monostatic-bistatic cross section theorem. This theorem states that for bodies of sufficient smoothness⁽²²⁾, the bistatic cross-section for transmitter direction \underline{k} and receiver direction \underline{n}_0 is equal to the monostatic cross section for the transmitter-receiver direction $(\underline{k} + \underline{n}_0)$ with $\underline{k} \neq 0$ in the limit of vanishing wavelengths. It is then demonstrated in (58) that for poor conductors, or perfect conductors coated with a material of a high refraction index, the impedance of the coating, apart from the sign of the imaginary part, can be determined from the knowledge of the bistatic cross sections $\sigma_{\perp}(\underline{k}, \underline{n}_0)$ and $\sigma_{\parallel}(\underline{k}, \underline{n}_0)$. This is possible when both transmitting and receiving antennae are linearly polarized, perpendicular or parallel to the plane defined by the vectors $(\underline{k}, \underline{n}_0)$.

Freedman describes a convenient method⁽¹⁴⁾ for the identification of uniformly coated scatterers, using pulse waves, which requires only one or two mono-/bistatic receivers. In this method, for an incoming modulated pulse wave, the scattered field in any arbitrary direction in the lit region results in the superposition of image pulses. These pulses are generated at the scatterer discontinuities, with pulse magnitude being proportional to generating discontinuity size and pulse phase depending on the total associated path.

The echoes or image pulses for various shapes are then considered for the high frequency case with Kennaugh and Moffat⁽²⁴⁾ who give a more sophisticated treatment. Mitzner⁽³³⁾ approaches the transient problem by subdividing the scattering surface of a smooth target into incremental belts. These belts are aligned in such a way with the incoming wave front that the pulse response can be analysed in terms of the body shape so decomposed. This is performed using an integral equation coupled with a general set of boundary conditions describing the local scattering surface. In general, this analysis of the pulse returned from a target does yield more information pertaining to the properties of the scatterer than the pure C.W.I.S. method as was demonstrated in (5) for the dielectric strip. It is especially shown here that the leading wave front indicates some properties about the composition of the strip, as the trailing returned pulse is related to its thickness.

However, in the last few years, it has been demonstrated⁽³⁹⁾ that the

C.W.I.S. method could feedback as much information as the P.W.I.S. method as to the direct problem of scattering when the C.W.I.S. method operates at high frequency and bases itself on scattering centers (i.e. localized sources). Models for the inverse solution are presently investigated in order to identify the various scattering centers from the far scattered field. These centers, when compared to a catalogue of direct problem solutions, should lead to target recognition.

Although it is difficult to separate the numerical approach from that approach used by the Departments of Defence, since both make recourse to computerized solutions, it is still possible to point out salient features which characterize the latter. In this area, information on space vehicles is of top priority. This information can be limited to a simple signature, such as a cross section obtained at a single polarization, frequency or bistatic angle, or to more complex signatures such as cross sections measured under various conditions of polarization, frequency, bistatic angles, etc.... This information is then used to identify the space object. Based on the assumption that physically similar vehicles exhibit equivalent signatures, the size and shape of those vehicles are estimated via comparative studies with known results contained in catalogues constructed under geometrical optics approximations. Of course, these hypotheses all predicate the meaningfulness of the signature representation. A more reliable degree of recognition is attained by increasing the resolution of the radar system. The practical solution often displays a choice between the better equipped ground radar stations or more sophisticated signatures

requiring either highly trained cross section analysts or sophisticated computerized decision-making processes.

Experimentally, technicians are dealing with scattering matrix measurements of various vehicle models, representing a vast spectrum of geometrical complexity. These techniques could have been part of our review of the numerical approach as they use the scattering phase centers concept to identify objects and as they necessitate retrieval of cross sections at various polarizations. The purpose of most of the investigation in this area is to determine adequate signatures of space objects. The simpler signatures are used as this makes for significant reduction in computer storage and analysis time; if the sophisticated signatures were used, this would result in heavy computer storage, lengthy decision-making and complicated comparative programs, though eliminating ambiguity in target recognition. However, studies in this area are for the most classified information; we can only speculate that more than one signature is employed for better discrimination with subsequent theoretical verification.

Both of these aspects are introduced and explained by Crispin et al⁽¹⁰⁾ who determine the complete scattering matrix for several aspects for Jupiter C, with or without the tail fins, and also for the Jupiter C nose cone. They observed that reasonably adequate matrix data could be obtained in the laboratory by measuring $\sigma(AA)$, $\sigma(A,B)$, $\sigma(B,B)$ and any two of the three phases associated with these amplitudes where

$\sigma(I,J)$ denotes the cross section measured when the transmitted energy has the polarization J, and the receiver polarization is along I. The symbols A and B designate two mutually orthogonal directions. A representative list of classified papers on the measurement of scattering matrices of laboratory models is given along with a display of the block-diagram of the measurement equipment.

In conclusion, there is obviously much to be gained by orientating research towards additional theoretical and experimental work relative to various scattering geometries. Further investigation would be advantageous, to optimize the methods used in reducing the measured data necessary to objectify the scatterer. Analysis should also be carried out to estimate the accuracy, particular to any employed techniques, needed to predict with sufficient reliability the shape of the target. Finally, experimental methods should be developed in accordance with the requirements imposed by the various theoretical methods. Those primary aims have been the concern of many authors and experimenters; however, it is felt that a continued effort towards providing more and more reliable information along these lines is still highly desirable.

1.3 FORMULATION OF THE PROBLEM

This thesis presents a solution to the inverse scattering problem as applied to axially symmetric conducting bodies of revolution embedded in a uniform homogeneous and isotropic medium of electric permittivity ϵ , magnetic permeability μ , and zero conductivity. It is assumed that

for a given transmitted field, the measured far scattered field components can be accurately obtained in amplitude, phase and polarization, for a sufficient number of bistatic receiver locations. If the scatterer possesses only one axis of revolution, then the incident plane wave will be propagated along the larger dimension of the body, in a direction perpendicular to its axis of revolution. In this case, the three-dimensional problem is then reduced to the two-dimensional scalar problem. In the general vector problem case, we consider the incident plane wave as propagating along the negative \hat{z} -axis of a spherical coordinate system, whose origin lies at the center of the unknown scatterer. The choice of time harmonic fields, with time dependence factor omitted throughout, is justified by the fact that this is a typical practical condition; and by the fact that an arbitrary field can always be decomposed into the sum of mono-chromatic waves by Fourier analysis.

In addition, we know from Wilcox's expansion⁽⁶⁰⁾ that the scattered field can arise from a set of equivalent sources located inside the scatterer. Hence, the scattered field can be represented in terms of orthogonal functions outside the sphere of minimum radius enclosing the scattering object. Therefore, the origin of any co-ordinate system used in this problem must be identical with the center of this sphere outside which the representation of the fields is convergent. The infinite series representing the scattered fields as a sum of orthogonal functions multiplied by associated expansion coefficients are then truncated to some order whose lower bound depends upon the larger di-

mension of the body. These coefficients are related to the shape of the scatterer.

The interdependence between these coefficients and the salient features of the scatterer has been acknowledged for many years; nonetheless, it has not been exploited to the extent that it deserves in its ability to portray the body shape. To resume, all the information concerning the scattering geometry is contained in these coefficients and this cognizance constitutes the basic concept underlying the method described in this thesis and applied throughout. The problem consists, then, in recovering these coefficients and to extract from their knowledge the desirable information.

Therefore, in order to have access to the geometrical features of the scatterer, these coefficients are first recovered via a matrix inversion procedure. Relationships between the wave functions used in the formulation of the scattered field are next exploited in order to relate them analytically with the radius of curvature of the object.

However, if the analytical expression of these coefficients is too sophisticated to extract that radius of curvature or if the coefficients are inaccurately retrieved due to the inversion procedure, another method must be developed to alleviate numerical difficulties.

An iterative averaging method is thus presented which bases itself

upon the dependency of the backscattered field magnitude with the impact area that is the vicinity of the specular point. In this new approach, the inverse scattering problem is considered as the synthesis of a system which includes the obstacle and the backscattered field and whose parameter " ka " is unknown. This perspective was apparently ignored in the literature, yet it could result in the practical implementation of system of target identification.

This purely numerical method gives this dissertation the counter-poise to its purely theoretical aspects. They are both complementary and any initial work on this problem of target recognition ought to include them with their respective contribution to unity and thoroughness.

PART A

*chapter two*THE CIRCULAR CYLINDER2.1 INTRODUCTION

The selection of this particular geometry among many others results from various considerations. First, there is a large amount of theoretical and experimental data published on the scattering by a cylinder, which will be necessary at a later stage in this investigation since no experimental work could be carried out as yet. Secondly, the circular cylinder constitutes a practical model for the testing of methods of more general applicability. In the field of inverse scattering, its analysis generated an incentive to undertake and develop similar studies on other geometries. Finally, it is a shape of considerable interest in practical applications such as the portrayal of missiles, shells, etc.

Therefore, the inverse problem of scattering for a circular cylindrical scattering geometry is first considered, namely, the shape of an unknown, perfectly conducting, cylindrical scatterer must be determined from bistatic field data for a given incident plane wave. This choice of a plane wave incidence as a primary field results from a practical consideration; in radar scattering, the target is usually illuminated by a source located at infinity. Although measurements are usually performed strictly within the Fraunhofer region, the present analysis is valid in all spatial regions.

The transverse electric field components are first related to a properly truncated number of expansion coefficients in matrix formulation. These coefficients are then obtained from the scattered field components and the inverted scattered field matrix. To avoid instability in this inversion procedure, a novel optimization technique is derived, which maximizes the determinant associated with the scattered field matrix.

The equivalent electrical radius of curvature "ka" of the cylinder is next recovered from a set of contiguous expansion coefficients. Simple formulae exist in all polarization cases where only four coefficients are necessary in the TM as well as the mixed TM-TE cases and five in the TE case. Such recurrence expressions for "ka" result from the definition of the expansion coefficients and the recurrence relationships between three contiguous Bessel functions as shown in (7).

Although the expressions derived for the retrieval of "ka" are restricted only to circular cylindrical scatterers, the technique developed in this chapter (7) may be extended to other scattering geometries (8) without requiring inverse boundary conditions (52) or methods of analytical continuation (31, 54).

The problem of accuracy is reviewed next, in connection with both the order of truncation of the infinite series expressing the far scattered field and the matrix inversion procedure. An iterative statistical

method is presented which is based on the dependence of the magnitude of the far scattered field with the local geometry of the illuminated area. Within the framework of this new method, the inverse scattering problem is considered as a synthesis of a system which includes the scatterer, the back scattered field and the connection between that field and the curvature of the scatterer. The terminology of system synthesis is hence used throughout. This alternative technique enables the recovery of the circular cylinder with excellent accuracy and therefore is recommended whenever the measurement bistatic angles are confined within a small wedge angle.

2.2 MATRIX FORMULATION OF THE FAR SCATTERED FIELD COMPONENTS

We will now consider the case of a plane electromagnetic wave which is normally incident on a smooth, perfectly conducting circular cylinder of electrical radius ka , with "k" being the wave number ($\frac{2\pi}{\lambda}$) and "a" the radius of the cylinder. The three-dimensional vector problem is hence reduced to the two-dimensional scalar problem.

The transmitted field expressed in the (x,y,z) cartesian co-ordinate system, whose origin is on the axis of the cylinder, as shown in Fig. 1, is given with $\exp(-j\omega t)$ time-dependence by

$$\underline{E}_t = E_0(\sin \delta \hat{y}_0 + \cos \delta \hat{z}_0) \exp(jkR) \quad (2.2.1)$$

$$\underline{H}_t = \sqrt{\frac{\epsilon_0}{\mu_0}} \underline{E}_t \times \hat{x}_0 \quad (2.2.2)$$

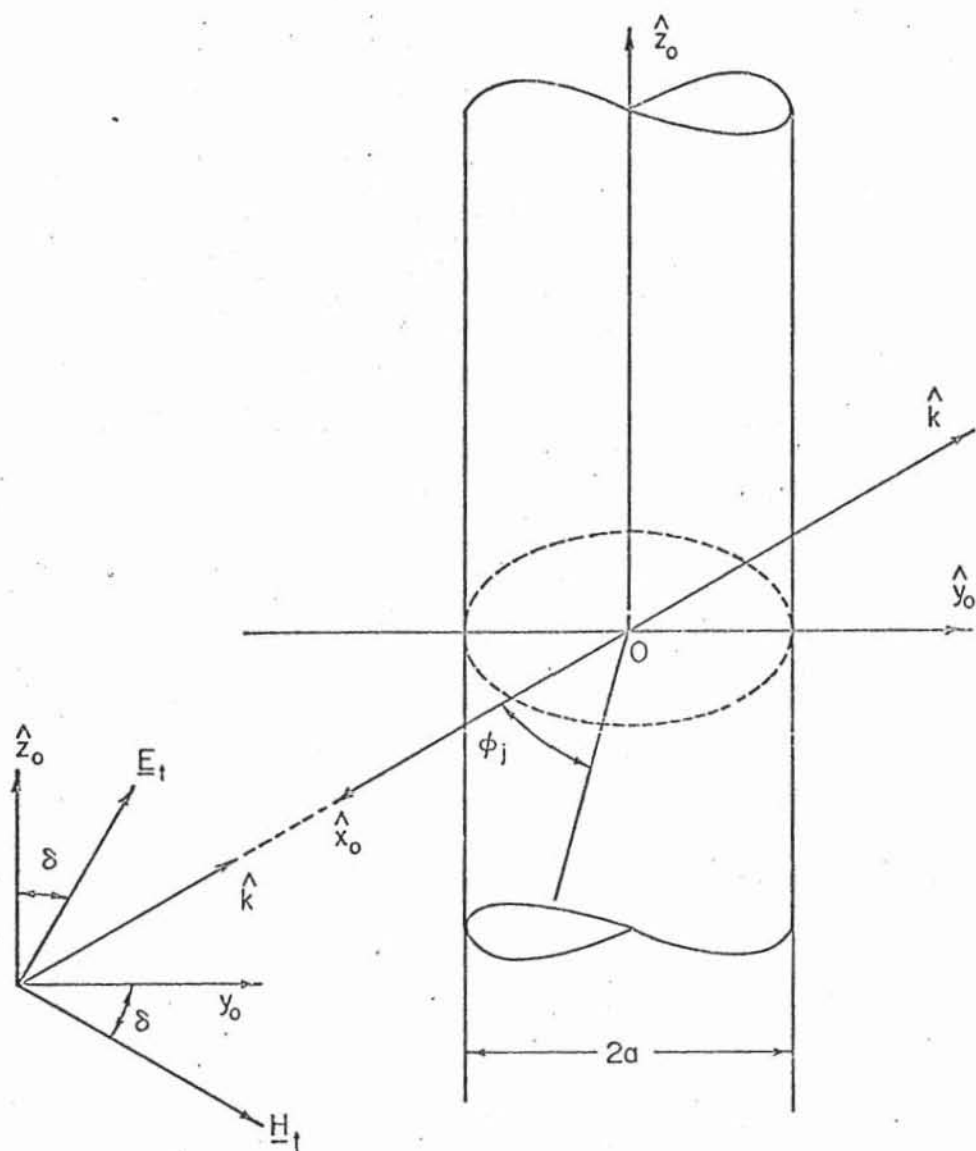


Fig. 1 Geometry for Plane Wave Incidence

where δ is the polarization angle, R the range, and (ϵ_0, μ_0) the characteristics of the propagation medium.

For the perfectly conducting circular cylinder, the scattered field components $(\underline{E}_s, \underline{H}_s)$ can be expressed in terms of circular cylindrical wave functions using the (R, ϕ) polar co-ordinate system⁽⁴⁶⁾. The scattered field may be considered as the superposition of a TM and a TE field which are proportional to $\cos \delta$ and $\sin \delta$, respectively. The transverse electrical field components are given by Einarsson, Kleinman, Laurin, and Uslenghi⁽¹¹⁾.

$$E_{s_z}^{\text{TM}} \approx \cos \delta E_0 \sum_{n=0}^{\infty} \epsilon_n a_n'' \cos(n\phi) \quad (2.2.3)$$

$$E_{s_z}^{\text{TE}} \approx \sin \delta E_0 \sum_{n=0}^{\infty} \epsilon_n b_n'' \cos(n\phi) \quad (2.2.4)$$

where

$$\epsilon_n = \begin{cases} 1, & n = 0 \\ 2, & n \geq 1 \end{cases}$$

$$a_n'' = j^n a_n H_n^{(1)}(kR) \quad (2.2.5a)$$

$$a_n = -\frac{J_n(ka)}{H_n^{(1)}(ka)} \quad (2.2.5b)$$

$$b_n'' = j^n b_n H_n^{(1)'}(kR) \quad (2.2.6a)$$

$$b_n = -\frac{J_n'(ka)}{H_n^{(1)'}(ka)} \quad (2.2.6b)$$

where $J_n(ka)$ represents the Bessel function of the first kind, $H_n^{(1)}(ka)$ the Hankel function of the first kind. In equations (2.2) the derivatives are with respect to the argument (kR) or (ka) . The polarization

angle δ , assumed as known, is removed by normalizing E_s and H_s , although it will be shown in Appendix A.1, how δ can be theoretically recovered.

Therefore, the normalized field components are expressed as:

$$e_z^{\text{TM}} = \sum_{n=0}^{\infty} \epsilon_n a_n'' \cos(n\phi) \quad (2.2.7)$$

$$e_\phi^{\text{TM}} = \sum_{n=0}^{\infty} \epsilon_n b_n'' \cos(n\phi) \quad (2.2.8)$$

These infinite series can be truncated to the order M , whose lower bound depends directly on "ka" as given in Einarsson, Kleinman, Laurin, Uslenghi, 1966⁽¹¹⁾ by the relation

$$M > 2ka; \quad ka \geq 4 \quad (2.2.9)$$

This problem of truncation is reviewed in detail in section (2.6.2).

In order that equations (2.2.7) and (2.2.8) may be expressed in the matrix form

$$[e] = [\phi(N)] \cdot [X] \quad (2.2.10)$$

$N = M + 1$ values of e_z^{TM} or of e_ϕ^{TE} must at least be known for nonidentical aspect angles (ϕ_r ; $r = 0, 1, \dots, N-1$)

The transpose, $[e]^T$, of the column vector $[e]$ is expressed as

$$[e]^T = [e_0, e_1, \dots, e_{N-1}]$$

and the column vector $[X]$ representing either the unknown a_n'' or b_n'' coefficients is written as⁽⁷⁾

$$[X]^T = [X_0, X_1, \dots, X_{N-1}]$$

which determines the arrangement of the matrix elements as

$$[\phi(N)] = \begin{bmatrix} 1 & 2\cos \phi_0 & 2 \cos 2\phi_0 & \dots & 2 \cos (N-1)\phi_0 \\ 1 & 2\cos \phi_1 & 2 \cos 2\phi_1 & \dots & 2 \cos (N-1)\phi_1 \\ \vdots & \vdots & \vdots & \ddots & \vdots \\ 1 & 2\cos \phi_{N-1} & 2 \cos 2\phi_{N-1} & \dots & 2 \cos (N-1)\phi_{N-1} \end{bmatrix} \quad (2.2.11)$$

To recover the unknown X_V , the matrix must be inverted. The upper limit on N is determined by stability criteria inherent in the matrix inversion procedure⁽⁵³⁾ and is investigated in section (2.6.2), in connection with the problem of accuracy.

2.3 CLOSED-FORM SOLUTION AND OPTIMIZATION OF THE DETERMINANT ASSOCIATED WITH THE MATRIX $|\phi(N)|$

2.3.1 CLOSED FORM SOLUTION OF THE DETERMINANT $|\phi(N)|$

Employing the Tchebyscheff expansion of $\cos n\phi$ for $n > 1$

$$\begin{aligned} \cos n\phi &= \sum_{k=0}^n \binom{n}{2k} \cos^{n-2k}\phi \sin^{2k}\phi = 2^{n-1} \cos^n\phi - \frac{n}{1} 2^{n-3} \cos^{n-2}\phi \\ &+ \frac{n}{2} \binom{n-3}{1} 2^{n-5} \cos^{n-4}\phi - \frac{n}{3} \binom{n-4}{2} 2^{n-7} \cos^{n-6}\phi \pm \dots \end{aligned} \quad (2.3.1)$$

the determinant $|\phi(N)|$ associated with (2.2.11) is evaluated in closed form. Using general properties of the Vandermonde determinant as reported in Appendix A.2, $|\phi(N)|$ reduces to⁽⁷⁾

$$\begin{aligned} |\phi(N)| &= \begin{vmatrix} 1 & 2x_0 & 2^2x_0^2 & \dots & 2^{N-1}x_0^{N-1} \\ 1 & 2x_1 & 2^2x_1^2 & \dots & 2^{N-1}x_1^{N-1} \\ \vdots & \vdots & \vdots & \ddots & \vdots \\ 1 & 2x_{N-1} & 2^2x_{N-1}^2 & \dots & 2^{N-1}x_{N-1}^{N-1} \end{vmatrix} & (2.3.2) \\ &= 2^{\frac{N(N-1)}{2}} \prod_{\substack{N-1 > r > s > 0}} (x_r - x_s) \end{aligned}$$

where $x_r = \cos \phi_r$.

2.3.2 OPTIMIZATION PROCEDURE

To ensure most stable inversion, it is necessary⁽⁷⁾ to optimize the closed-form solution of (2.3.2) which in turn affects the practical design of measurement techniques. Namely, the optimal distribution of aspect angles spread over some limited measurement wedge of half-angle ϕ_a , as shown in Fig. 2, is sought for which $|\phi(N)|$ becomes maximum. In addition to the mirror symmetry about $\phi = 0$ resulting from the cylindrical scattering geometry, it is observed that the value of the associated determinant increases for larger half-angle $|\phi_a| \leq \pi/2$. Since the two wedge-limiting aspect angles α and β may be fixed *a priori*, the number of unknown aspect angles ϕ_r , which must be optimized, is reduced to $(N-2)$. To obtain the closed form solution of the optimal distribution of aspect angles, it is necessary to introduce ϕ_r' in such a way that

$$\cos \phi_r' = \cos \phi_r - \cos \phi_0 \quad (2.3.3a)$$

where

$$\cos \phi_0 = \frac{\cos \alpha + \cos \beta}{2} \quad (2.3.3b)$$

The associated quantity $u_r' = \cos \phi_r'$ is normalized with respect to its maximum value, namely $|u_r'|_{\max} = \left| \cos \alpha - \left(\frac{\cos \alpha + \cos \beta}{2} \right) \right| = \left| \cos \beta - \left(\frac{\cos \alpha + \cos \beta}{2} \right) \right| = \left| \frac{\cos \alpha - \cos \beta}{2} \right|$ so that

$$u_r = \frac{u_r'}{\left| \frac{\cos \alpha - \cos \beta}{2} \right|}; \quad (-1 \leq u_r \leq 1) \quad (2.3.3c)$$

This leads to:

$$x_r = \cos \phi_r = u_r \left| \frac{\cos \alpha - \cos \beta}{2} \right| + \frac{(\cos \alpha + \cos \beta)}{2} \quad (2.3.3d)$$

Therefore, with the cosines u_r symmetrical about $\cos \phi_0$, equation (2.3.2) results in

$$|\phi(N)| = (\cos\alpha - \cos\beta) \frac{N(N-1)}{2} \prod_{N-1 > r > s > 0} (u_r - u_s) \quad (2.3.4)$$

In Part B, it is shown that the roots of

$$(1 - u_r^2)^{1/2} P_{n+1}^1(u_r) = 0 \quad (2.3.5)$$

represent the optimum distribution of the normalized cosines u_r , where $P_{n+1}^1(u_r)$ represents, with $N = n + 2$, the associated Legendre function of the first kind and first degree and order $n + 1$ as defined in Jahnke (16). Hence, assuming that the measurements are compiled within an arbitrary polar wedge over the unit circle of directions, as shown in Fig. 2, the optimization procedure is:

a) Choose the measurement wedge to lie within the ranges of either $0 \leq \phi \leq \pi$ or $\pi \leq \phi \leq 2\pi$ to ensure maximum retrieval of information from the scattered field data.

b) Normalize all non-identical aspect angles ϕ_r with respect to the wedge-limiting aspect angles α and β shown in Fig. 3, so that with (2.3.3d)

$$u_r = \frac{2 \cos \phi_r - (\cos\alpha + \cos\beta)}{|\cos\alpha - \cos\beta|}$$

c) Then the zeros of $(1 - u_r^2)^{1/2} P_{n+1}^1(u_r)$ are the desired normalized cosines of the determinant $|\Phi(N)|$ which, for a given half angle $\phi_a = \frac{\beta - \alpha}{2}$, is maximum if the centre wedge angle $\phi_w = \frac{\alpha + \beta}{2}$ in Fig. 2 is $\pi/2$ or $3\pi/2$, since in these cases $(\cos\alpha - \cos\beta)$ in (2.3.4) is maximum for a given ϕ_a .

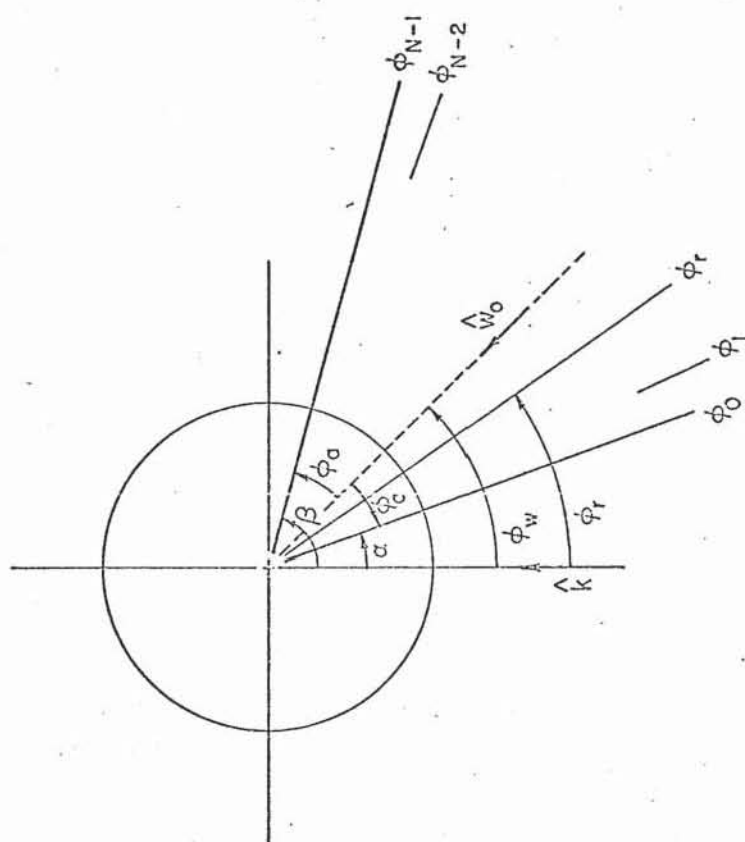


Fig. 2 Measurement aspect angles

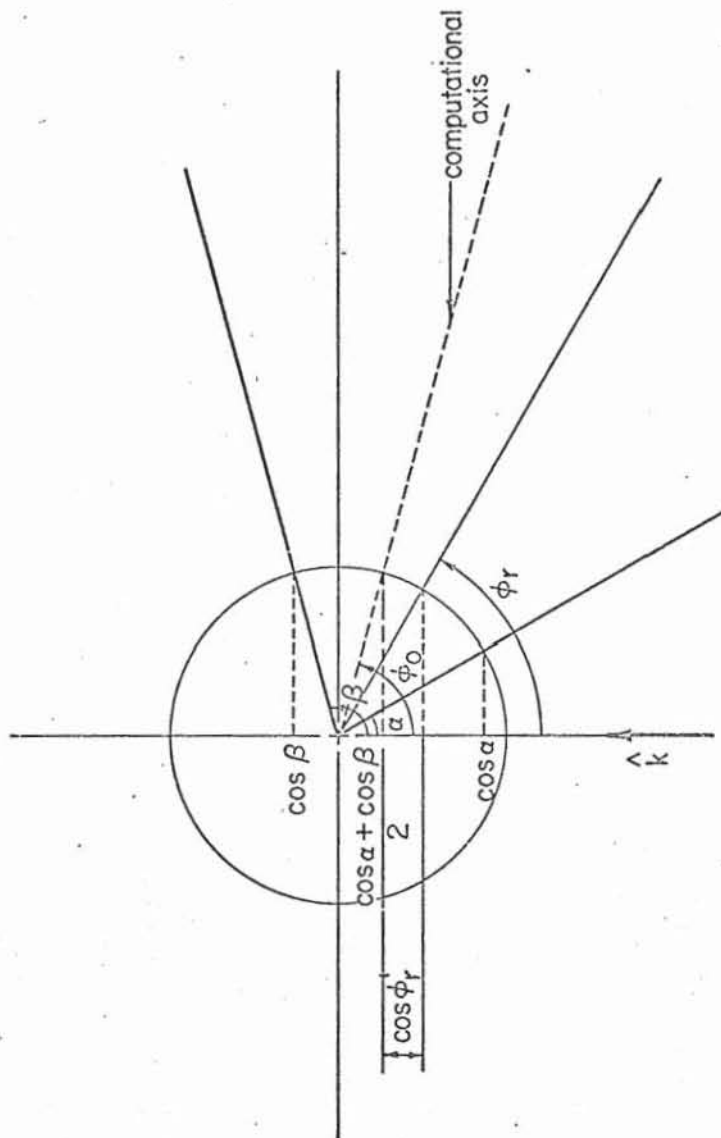


Fig. 3 Coordinates for the Optimization Procedure



2.3.3 COMPUTATIONAL RESULTS

Computational results are given in Table 1, proving that an optimum distribution can be found for any ϕ_w and ϕ_a . These results are presented in relation to uniform distribution of angles ϕ_r as well as their $\cos \phi_r$ and $\sin \phi_r$ distribution. Comparing these distributions, it is observed that in all cases the optimum distribution satisfying (2.3.5) is the best choice, although the uniform aspect angle distribution (column [4]) for large N, approximates the optimum distribution (column [1]) most closely for α and β symmetrical about 90° . However, if good accuracy is desired from the values of the coefficients, the large values of N are disregarded since in that case, the matrix inversion would be exceedingly difficult to perform. This is the object of study of a subsequent paragraph (2.6.2) related to truncation accuracy problems.

2.4 DERIVATION OF THE ELECTRICAL RADIUS "ka"

2.4.1 INTRODUCTION

Up to the present, inverse scattering boundary conditions⁽⁵⁴⁾, or methods of analytical continuation^(54, 32), were employed to recover the shape of the unknown, perfectly conducting, scatterer. However, in the case of a circular cylindrical scatterer, all information required to retrieve "ka" is explicitly contained in the set of expansion

TABLE 1: VERIFICATION OF THE OPTIMIZATION PROCEDURE

$$|\phi(N)| = (\cos\alpha - \cos\beta) \frac{N(N-1)}{2} \prod_{N-1 \geq r > s \geq 0} (u_r - u_s)$$

Optimization Procedure: Column [1]; uniform cosine distribution $\cos\phi_r$: column [2]; uniform sine distribution $\sin\phi_r$: column [3]; uniform aspect angle distribution: column [4].

$$\alpha = 180^\circ, \beta = 0^\circ, |\cos\alpha - \cos\beta| = 2$$

N	[1]	[2]	[3]	[4]
3	0.1600×10^2	0.1600×10^2	0.0000	0.1600×10^2
4	0.7327×10^2	0.6742×10^2	0.0000	0.7199×10^2
5	0.3752×10^3	0.2880×10^3	0.0000	0.3620×10^3
6	0.2108×10^4	0.1215×10^4	0.0000	0.2000×10^4
7	0.1281×10^5	0.4988×10^4	0.0000	0.1197×10^5
8	0.8339×10^5	0.1964×10^5	0.0000	0.7863×10^5
9	0.5762×10^6	0.7358×10^5	0.0000	0.5242×10^6
10	0.4201×10^7	0.2602×10^6	0.0000	0.3779×10^7
11	0.3216×10^8	0.8643×10^6	0.0000	0.2862×10^8
12	0.2572×10^9	0.2682×10^7	0.0000	0.2267×10^9
13	0.2143×10^{10}	0.7751×10^7	0.0000	0.1872×10^{10}
14	0.1854×10^{11}	0.2078×10^8	0.0000	0.1606×10^{11}

TABLE 1: (continued)

$$\alpha = 90^0, \beta = 0^0, |\cos\alpha - \cos\beta| = 1$$

N	[1]	[2]	[3]	[4]
3	0.2499	0.2499	0.1160	0.2071
4	0.1788×10^{-1}	0.1646×10^{-1}	0.2020×10^{-2}	0.1061×10^{-1}
5	0.3578×10^{-3}	0.2746×10^{-3}	0.5125×10^{-5}	0.1309×10^{-3}
6	0.1963×10^{-5}	0.1132×10^{-5}	0.1853×10^{-8}	0.3800×10^{-6}
7	0.2913×10^{-8}	0.1134×10^{-8}	0.9418×10^{-13}	0.2555×10^{-9}
8	0.1157×10^{-11}	0.2726×10^{-12}	0.6651×10^{-18}	0.3932×10^{-13}
9	0.1220×10^{-15}	0.1557×10^{-16}	0.6475×10^{-24}	0.1373×10^{-17}
10	0.3393×10^{-20}	0.2101×10^{-21}	0.8653×10^{-31}	0.1081×10^{-22}
11	0.2476×10^{-25}	0.6656×10^{-27}	0.1569×10^{-38}	0.1907×10^{-28}
12	0.4724×10^{-31}	0.4925×10^{-33}	0.3869×10^{-47}	0.7507×10^{-35}
13	0.2346×10^{-37}	0.8483×10^{-40}	0.1290×10^{-56}	0.6568×10^{-42}
14	0.3024×10^{-44}	0.3389×10^{-47}	0.5798×10^{-67}	0.1273×10^{-49}
15	0.1009×10^{-51}	0.3132×10^{-55}	0.0000	0.5451×10^{-58}

coefficients $\{a_n'', b_n''; 0 \leq n \leq N\}$ for either polarization case. This cognizance is the foundation of the method presented here. This method will be later applied to other geometries as well.

For the problem at hand, the expansion coefficients a_n'' and b_n'' are first obtained from the non-singular matrix inversion procedure previously mentioned. Furthermore, since measurements are made on a circular arc of known radius, the radial functions in (2.2.5a) and (2.2.6a) are computed for each mode n and the corresponding values of a_n and b_n calculated. To show how the procedure leads to the retrieval of "ka", we consider the three polarization cases in detail.

2.4.2 TM CASE: $\delta = 0$

Let (2.2.5b) be rewritten in the alternative form $J_n = -a_n H_n^{(1)}$ where the arguments are omitted and $\rho = ka$. Employing the recurrence relations of cylindrical radial functions

$$Z_\nu = \frac{\rho}{2\nu} (Z_{\nu-1} + Z_{\nu+1}) \quad (2.4.1)$$

for $\nu = n$ and $\nu = n + 1$, the square of the electrical radius may⁽⁷⁾ then be expressed as

$$\rho^2 = \frac{4n(n+1) \frac{Z_{n+1}}{Z_{n-1}}}{\left[1 + \frac{Z_{n+1}}{Z_{n-1}}\right] \left[1 + \frac{Z_{n+2}}{Z_n}\right]} \quad (2.4.2)$$

An expression for $(Z_{\nu+1} / Z_{\nu-1})$ in terms of the expansion coefficients a_n is obtained from (2.2.5b) and (2.4.1) where for $Z_\nu = H_\nu^{(1)}$ in (2.4.1)

$$+ a_{\nu} H_{\nu}^{(1)} = + a_{\nu} \frac{\rho}{2\nu} (H_{\nu-1}^{(1)} + H_{\nu+1}^{(1)})$$

and for $Z_{\nu} = J_{\nu}$ in (2.4.1) and with (2.2.5b)

$$- a_{\nu} H_{\nu}^{(1)} = - \frac{\rho}{2\nu} (a_{\nu-1} H_{\nu-1}^{(1)} + a_{\nu+1} H_{\nu+1}^{(1)})$$

which, when combined, result for general ν in

$$\frac{H_{\nu+1}^{(1)}}{H_{\nu-1}^{(1)}} = \frac{a_{\nu-1} - a_{\nu}}{a_{\nu} - a_{\nu+1}} \quad \text{or} \quad \frac{J_{\nu+1}}{J_{\nu-1}} = \frac{a_{\nu+1} (a_{\nu-1} - a_{\nu})}{a_{\nu-1} (a_{\nu} - a_{\nu+1})} \quad (2.4.3)$$

Substituting either expression for the chosen $\nu = n$, $\nu = n + 1$ into (2.4.2) yields the desired recurrence relationship for the TM case

$$(ka)^2 = 4n(n+1) \frac{(a_{n-1} - a_n) (a_{n+1} - a_{n+2})}{(a_{n-1} - a_{n+1}) (a_n - a_{n+2})} \quad (2.4.4)$$

requiring only four contiguous expansion coefficients; a_{n-1} , a_n , a_{n+1} and a_{n+2} for any $n \geq 1$.

2.4.3 MIXED TM-TE CASE: $0 < \delta < \pi/2$

Assuming that $\delta = \delta_0$ and both the a_n and the b_n coefficients are available, the recurrence relationship for ρ is obtained from the definition of a_n given by (2.2.5b) and that of b_n given by (2.2.6b) rewritten as $J_n' = -b_n H_n^{(1)'}$. Employing the recurrence relationship

$$Z_{\nu}' = \frac{1}{2} [Z_{\nu-1} - Z_{\nu+1}] \quad (2.4.5)$$

together with (2.2.5b) and (2.2.6b), another relationship for $\left(\frac{Z_{\nu+1}}{Z_{\nu-1}}\right)$ results in the following⁽⁷⁾:

$$\begin{aligned}
 J'_v &= \frac{1}{2} (J_{v-1} - J_{v+1}) \\
 &= -\frac{1}{2} (a_{v-1} H_{v-1}^{(1)} - a_v H_{v+1}^{(1)}) \quad (2.4.6a)
 \end{aligned}$$

$$\begin{aligned}
 &= -b_v H_v^{(1)} \\
 &= -\frac{1}{2} b_v (H_{v-1}^{(1)} - H_{v+1}^{(1)}) \quad (2.4.6b)
 \end{aligned}$$

Comparing (2.4.6a) and (2.4.6b) leads to

$$\frac{H_{v+1}^{(1)}}{H_{v-1}^{(1)}} = \frac{b_v - a_{v-1}}{b_v - a_{v+1}} \quad \text{or} \quad \frac{J_{v+1}}{J_{v-1}} = \frac{a_{v+1}}{a_{v-1}} \cdot \frac{b_v - a_{v-1}}{b_v - a_{v+1}} \quad (2.4.7)$$

Since (2.4.3) and (2.4.7) hold in general, a nonlinear relationship⁽⁷⁾ is obtained between one b_v and three contiguous a_v coefficients,

$$b_v = \frac{a_v (a_{v-1} + a_{v+1}) - 2a_{v-1} a_{v+1}}{2a_v - (a_{v-1} + a_{v+1})} \quad (2.4.8)$$

which indicates that an inverse relationship between one a_v and a finite number of contiguous b_v coefficients, similar to (2.4.8), does not exist for general v .

Employing (2.2.5b), (2.2.6b), (2.4.5) and

$$z'_v = z_{v-1} - \frac{v}{\rho} z_v \quad (2.4.9a)$$

or

$$z'_v = \frac{v}{\rho} z_v - z_{v+1} \quad (2.4.9b)$$

yields for general v

$$\rho = \frac{v z_v}{z_{v-1} - z'_v} = \frac{v z_v}{z_{v-1}} \left[\frac{2}{1 + \frac{z_{v+1}}{z_{v-1}}} \right] \quad (2.4.10a)$$

or

$$\rho = \frac{vZ_v}{Z_{v-1} - Z'_v} = \frac{vZ_v}{Z_{v+1}} \cdot \left[\frac{2}{1 + \frac{Z_{v-1}}{Z_{v+1}}} \right] \quad (2.4.10b)$$

Substitution of $\left(\frac{Z_{v+1}}{Z_{v-1}}\right)$ in (2.4.10a) by its value as given in (2.4.3) or (2.4.7) results in

$$\rho = \frac{v H_v^{(1)}}{H_{v-1}^{(1)}} \cdot \left[\frac{2(b_v - a_{v+1})}{2b_v - a_{v+1} - a_{v-1}} \right] \quad (2.4.11a)$$

or

$$\rho = \frac{v H_v^{(1)}}{H_{v-1}^{(1)}} \cdot \left[\frac{2(a_v - a_{v+1})}{a_{v-1} - a_{v+1}} \right] \quad (2.4.11b)$$

Equating (2.4.11a) with (2.4.11b) leads to

$$\frac{2(b_v - a_{v+1})}{2b_v - a_{v+1} - a_{v-1}} = \frac{2(a_v - a_{v+1})}{a_{v-1} - a_{v+1}} = \frac{b_v - a_v}{b_v - a_{v-1}} \quad (2.4.12)$$

which gives

$$\rho = v \cdot \frac{H_v^{(1)} \cdot (b_v - a_v)}{H_{v-1}^{(1)} \cdot (b_v - a_{v-1})} \quad (2.4.13a)$$

Similarly, if (2.4.10b) is employed with (2.4.3) or (2.4.7), another formulation is obtained, namely

$$\rho = v \cdot \frac{H_v^{(1)} \cdot (b_v - a_v)}{H_{v+1}^{(1)} \cdot (b_v - a_{v+1})} \quad (2.4.13b)$$

Multiplying (2.4.13a) for $v = n + 1$ by the same expression for $v = n$, or similarly (2.4.13b) for $v = n - 1$ and $v = n$, yields

$$\rho^2 = n(n+1) \frac{H_{n+1}^{(1)} (b_n - a_n) (b_{n+1} - a_{n+1})}{H_{n-1}^{(1)} (b_n - a_{n-1}) (b_{n+1} - a_n)} \quad \text{or} \quad \rho^2 = (n-1)n \frac{H_{n-1}^{(1)} (b_n - a_n) (b_{n-1} - a_{n-1})}{H_{n+1}^{(1)} (b_n - a_{n+1}) (b_{n-1} - a_n)}$$

which together with (2.4.7) becomes

$$(ka)^2 = n(n+1) \frac{(b_n - a_n)(b_{n+1} - a_{n+1})}{(b_n - a_{n+1})(b_{n+1} - a_n)} \quad (2.4.14a)$$

or

$$(ka)^2 = (n-1)n \frac{(b_{n-1} - a_{n-1})(b_n - a_n)}{(b_{n-1} - a_n)(b_n - a_{n-1})}, \quad (2.4.14b)$$

respectively. Here (2.4.14b) can be directly obtained from (2.4.14a) by changing $\nu = n$ into $\nu = n - 1$, which again requires only four contiguous expansion coefficients for $n \geq 1$ in (2.4.14) --- which reduces to (2.4.4) if (2.4.8) is properly substituted.

2.4.4 TE CASE: $\delta = \pi/2$

We wish to recover "ka" solely from the given set of $\{b_\nu\}$ coefficients. Since no recurrence relationship between three contiguous derivatives of cylindrical functions exists⁽⁷⁾, no expression can result for $Z'_{\nu+1}/Z'_{\nu-1}$ in terms of only three contiguous b_ν coefficients, similar to (2.4.3) or (2.4.7). This can be observed from the recurrence relationship between four derivatives of cylindrical functions

$$(\nu+2) Z'_{\nu+1} - (\nu-2) Z'_{\nu-1} = \rho/2(Z'_{\nu+2} - Z'_{\nu-2}) \quad (2.4.15)$$

which involves non-contiguous Bessel functions and results, for $\nu = n$ and $\nu = n + 1$, in

$$\rho^2 = 4(n-2)(n+3) \frac{\left[\left(\frac{n+2}{n-2} \right) \frac{Z'_{n+1}}{Z'_{n-1}} - 1 \right] \left[\left(\frac{n-1}{n+3} \right) \frac{Z'_n}{Z'_{n+2}} - 1 \right]}{\left[\left(\frac{n+3}{n-1} \right) \left(\frac{Z'_{n+1}}{Z'_{n+1}} \right) - 1 \right] \left[\left(\frac{n-2}{n} \right) \left(\frac{Z'_n}{Z'_{n+2}} \right) - 1 \right]} \quad (2.4.16)$$

with either $Z_V^{(1)'} = H_V^{(1)'}$ or $Z_V' = -b_V H_V^{(1)'}$. Equation (2.4.16) cannot be expressed, similar to (2.4.4) and (2.4.14), explicitly in terms of a limited number of contiguous b_V coefficients for any n , since from (2.4.5), (2.4.3) and (2.4.7) it follows that⁽⁷⁾

$$\begin{aligned} \frac{H_{n+1}^{(1)'}}{H_{n-1}^{(1)'}} &= \frac{1 - \frac{H_{n+2}^{(1)}}{H_n^{(1)}}}{\frac{H_{n-2}^{(1)}}{H_n^{(1)}} - 1} = \frac{(2a_{n+1} - a_n - a_{n+2})(a_{n-2} - a_{n-1})}{(2a_{n-1} - a_n - a_{n-2})(a_{n+1} - a_{n+2})} \\ &= \frac{(b_{n-1} - a_{n-2})(a_{n+2} - a_n)}{(b_{n+1} - a_{n+2})(a_n - a_{n-2})} \end{aligned} \quad (2.4.17)$$

which is not expressible in terms of the b_n coefficients. From (2.4.3) and (2.4.7),

$$\frac{a_V - a_{V-1}}{a_V - a_{V+1}} = -\frac{b_V - a_{V-1}}{b_V - a_{V+1}} \text{ or } a_{V+1} = \frac{2b_V a_V - a_{V-1}(b_V + a_V)}{(a_V + b_V) - 2a_{V-1}} \quad (2.4.18)$$

results which demonstrates that no relation exists giving the a_n coefficients in terms of three b_n contiguous coefficients, in contrast with (2.4.8). It may now be argued that if the complete set $\{b_V, N\}$ is given, an expression for "ka", explicit in b_V , must exist as well as for the other two polarizations. To attain this, two contiguous a_V coefficients must be determined in terms of a finite number of b_V coefficients. This is shown in *Appendix A.3* where a_0 and a_2 are formulated in terms of only 5 contiguous coefficients as given by the equations (A.3.16) and (A.3.17). All higher order a_V coefficients required in either (2.4.4), (2.4.14) or (A.3.17) for the retrieval of

"ka" in the TE-case are then obtained using (A.3.16) and (A.3.17) and iteration of (2.4.8). Nevertheless, in contrast to the other two polarization cases, where any four contiguous expansion coefficients are necessary and sufficient to recover "ka", in the TE-case the first five TE coefficients are necessary and sufficient only for $n = 1$, and $n = 2$ in (2.4.4), $n = 1, 2$ and 3 in (2.4.14), and $n = 3$ in (2.4.16). For any higher order n in (2.4.4), (2.4.14) or (2.4.16) the entire set of $\{b_\nu\}$ coefficients is required.

In the high frequency TE-case (i.e. for $ka > 5$) it is valuable to note that the zero-order TM coefficients a_0 may be approximated by

$$a_0 \approx - (1 + a_1) \approx - (1 + b_0) \quad (2.4.19)$$

This result together with the identity $a_1 \equiv b_0$ are important in as much as they may be employed favourably instead of the lengthy sophisticated equations derived in *Appendix A.3* to shorten the computation time of the retrieval. In *chapter five*, it will be demonstrated that this approximation becomes a true identity for the case of the coefficients associated with the spherical Bessel functions. Equation (2.4.19) results from the comparison of the numerical values of J_0 , Y_1 , J_1 , and Y_0 . In particular, it is shown^(16, 1) that for argument $\rho > 3$

$$J_0(\rho) \approx - Y_1(\rho) \quad (2.4.20)$$

$$J_1(\rho) \approx Y_0(\rho)$$

which implies that

$$\begin{aligned}
 a_0 &= - \frac{J_0(\rho)}{J_0(\rho) + jY_0(\rho)} \approx \frac{Y_1(\rho)}{-Y_1(\rho) + jJ_1(\rho)} \\
 &\approx -1 - \frac{J_1(\rho)}{J_1(\rho) + jY_1(\rho)} \quad (2.4.21)
 \end{aligned}$$

which is identical with the relation (2.4.19).

2.5 COMPUTATION OF ka FROM THE EXACT VALUES OF THE a_n AND b_n COEFFICIENTS

To verify and interpret the theoretical results already obtained, computations are presented in Tables 2 to 5 for the three particular values $ka = 1.0, 5.0, 10.0$, representing the resonance and higher frequency cases. The coefficients a_n and b_n are presented in Table 2. The values of a_2 , computed for (A.3.17) in terms of the required set of coefficients $\{b_n\}$, is identical with the value resulting from (2.2.5b) and presented in Table 3. It is shown in Table 4 that "ka" can be recovered for all three polarization cases, where ρ_{TM} corresponds to the TM-case as given by (2.4.4), ρ_{TM-TE} to the mixed TM-TE case as given by (2.4.14) and ρ_{TE} to the TE-case computed from (2.4.14), (2.4.18) and (A.3.17). The accuracy of the results based on (2.4.4), (2.4.14) and (A.3.17) depends exclusively on the accuracy of the expansion coefficients a_n and b_n , which have been calculated with 6 digit accuracy. In practice, the overall accuracy would also be dictated by the resolution of any suitable measurement technique for compiling amplitude, phase and polarization of the scattered field. The computed results in Table 3 for the high-frequency TE-case, $ka = 10$, demonstrate that

TABLE 2: TABULATION OF a_n AND b_n COEFFICIENTS

ka = 1.000

AN(0)	-0.986913E 00	0.113829E 00	BN(0)	-0.240880E 00	-0.427630E 00
AN(1)	-0.240880E 00	-0.427630E 00	BN(1)	-0.122694E 00	0.328094E 00
AN(2)	-0.482235E-02	-0.692770E-01	BN(2)	-0.691193E-02	0.828519E-01
AN(3)	-0.112935E-04	-0.336064E-02	BN(3)	-0.126362E-04	0.355480E-02
AN(4)	-0.553886E-08	-0.744250E-04	BN(4)	-0.575551E-08	0.758667E-04
AN(5)	-0.919887E-12	-0.959103E-06	BN(5)	-0.936609E-12	0.967806E-06
AN(6)	-0.663354E-16	-0.814455E-08	BN(6)	-0.670027E-16	0.818548E-08
AN(7)	-0.241210E-20	-0.491127E-10	BN(7)	-0.242697E-20	0.492636E-10
AN(8)	-0.489961E-25	-0.221350E-12	BN(8)	-0.491955E-25	0.221799E-12
AN(9)	-0.599390E-30	-0.774200E-15	BN(9)	-0.601089E-30	0.775295E-15
AN(10)	-0.467864E-35	-0.216301E-17	BN(10)	-0.468825E-35	0.216523E-17
AN(11)	-0.243944E-40	-0.493907E-20	BN(11)	-0.244317E-40	0.494284E-20
AN(12)	-0.881861E-46	-0.939075E-23	BN(12)	-0.882904E-46	0.939629E-23
AN(13)	-0.227971E-51	-0.150985E-25	BN(13)	-0.228181E-51	0.151057E-25
AN(14)	-0.432561E-57	-0.207981E-28	BN(14)	-0.432882E-57	0.208058E-28
AN(15)	-0.616015E-63	-0.248196E-31	BN(15)	-0.616384E-63	0.248271E-31
AN(16)	-0.671254E-69	-0.259086E-34	BN(16)	-0.671581E-69	0.259149E-34
AN(17)	-0.569174E-75	-0.238573E-37	BN(17)	-0.569410E-75	0.238623E-37
AN(18)	0.0	-0.195235E-40	BN(18)	0.0	0.195269E-40
AN(19)	0.0	-0.142927E-43	BN(19)	0.0	0.142948E-43
AN(20)	0.0	-0.941561E-47	BN(20)	0.0	0.941677E-47

TABLE 2: (continued)

ka = 5.000

AN(0)	-0.248892E 00	0.432371E 00	BN(0)	-0.830741E 00	-0.374981E 00
AN(1)	-0.830741E 00	-0.374981E 00	BN(1)	-0.990171E-01	0.298685E 00
AN(2)	-0.157870E-01	0.124650E 00	BN(2)	-0.999995E 00	-0.230529E-02
AN(3)	-0.861524E 00	0.345400E 00	BN(3)	-0.274878E 00	-0.446453E 00
AN(4)	-0.805672E 00	-0.395682E 00	BN(4)	-0.290032E-01	0.167815E 00
AN(5)	-0.248855E 00	-0.432350E 00	BN(5)	-0.198326E 00	0.398739E 00
AN(6)	-0.324799E-01	-0.177271E 00	BN(6)	-0.618447E-01	0.240874E 00
AN(7)	-0.178316E-02	-0.421898E-01	BN(7)	-0.285374E-02	0.533442E-01
AN(8)	-0.425699E-04	-0.652442E-02	BN(8)	-0.541874E-04	0.736101E-02
AN(9)	-0.505556E-06	-0.711025E-03	BN(9)	-0.576459E-06	0.759249E-03
AN(10)	-0.341183E-08	-0.584108E-04	BN(10)	-0.369961E-08	0.608244E-04
AN(11)	-0.143149E-10	-0.378350E-05	BN(11)	-0.151210E-10	0.388857E-05
AN(12)	-0.396690E-13	-0.199171E-06	BN(12)	-0.412587E-13	0.203122E-06
AN(13)	-0.759029E-16	-0.871222E-08	BN(13)	-0.781640E-16	0.884104E-08
AN(14)	-0.103823E-18	-0.322215E-09	BN(14)	-0.106197E-18	0.325878E-09
AN(15)	-0.104424E-21	-0.102187E-10	BN(15)	-0.106304E-21	0.103104E-10
AN(16)	-0.790682E-25	-0.281189E-12	BN(16)	-0.802100E-25	0.283211E-12
AN(17)	-0.459783E-28	-0.678070E-14	BN(17)	-0.465204E-28	0.682054E-14
AN(18)	-0.208892E-31	-0.144531E-15	BN(18)	-0.210932E-31	0.145234E-15
AN(19)	-0.752699E-35	-0.274353E-17	BN(19)	-0.758859E-35	0.275473E-17
AN(20)	-0.217964E-38	-0.466867E-19	BN(20)	-0.219476E-38	0.468482E-19

TABLE 2: (continued)

ka = 10.000

AN(0)	-0.951574E 00	-0.215403E 00	BN(0)	-0.295855E-01	0.169470E 00
AN(1)	-0.295855E-01	0.169470E 00	BN(1)	-0.985440E 00	-0.121149E 00
AN(2)	-0.999804E 00	-0.230413E-01	BN(2)	-0.887116E-03	-0.297763E-01
AN(3)	-0.511981E-01	-0.220440E 00	BN(3)	-0.921109E 00	0.270139E 00
AN(4)	-0.696771E 00	0.459906E 00	BN(4)	-0.363875E 00	-0.481240E 00
AN(5)	-0.749508E 00	-0.433585E 00	BN(5)	-0.188809E 00	0.391437E 00
AN(6)	-0.265382E-02	-0.514554E-01	BN(6)	-0.979578E 00	0.142592E 00
AN(7)	-0.537689E 00	-0.498758E 00	BN(7)	-0.586266E 00	-0.492701E 00
AN(8)	-0.100032E 01	0.338324E-02	BN(8)	-0.340482E-01	-0.181384E 00
AN(9)	-0.682211E 00	-0.465861E 00	BN(9)	-0.855564E-01	0.279759E 00
AN(10)	-0.249627E 00	-0.432894E 00	BN(10)	-0.216543E 00	0.411976E 00
AN(11)	-0.530354E-01	-0.224143E 00	BN(11)	-0.103121E 00	0.304174E 00
AN(12)	-0.647825E-02	-0.802399E-01	BN(12)	-0.123189E-01	0.110323E 00
AN(13)	-0.451472E-03	-0.212466E-01	BN(13)	-0.677331E-03	0.260211E-01
AN(14)	-0.187737E-04	-0.433350E-02	BN(14)	-0.239356E-04	0.489321E-02
AN(15)	-0.501759E-06	-0.708421E-03	BN(15)	-0.586153E-06	0.765747E-03
AN(16)	-0.920020E-08	-0.959153E-04	BN(16)	-0.102486E-07	0.101247E-03
AN(17)	-0.121334E-09	-0.110151E-04	BN(17)	-0.131340E-09	0.114601E-04
AN(18)	-0.119004E-11	-0.109087E-05	BN(18)	-0.126471E-11	0.112458E-05
AN(19)	-0.890730E-14	-0.943777E-07	BN(19)	-0.934630E-14	0.966749E-07
AN(20)	-0.519445E-16	-0.720722E-08	BN(20)	-0.540054E-16	0.734877E-08

TABLE 3: EXPANSION COEFFICIENT a_2 AS GIVEN BY (2.2.5b) AND BY (A.3.17)

$$a_2 = -\frac{J_2(ka)}{H_2^{(1)}(ka)} = \frac{b_0 b_{13} L - b_1 b_{03} M}{b_{13} L - b_{03} M}$$

ka	a_2 {Real}	a_2 {Im.}
1.0	-0.004822	-0.06921
5.0	-0.01578	-0.12465
10.0	-0.99980	-0.02304

TABLE 4: DETERMINATION OF ka FOR THE TM, TM-TE AND TE CASES

$$\rho_{TM} = 4n(n+1) \frac{(a_{n-1} - a_n)}{(a_{n-1} - a_{n+1})} \cdot \frac{(a_{n+1} - a_{n+2})}{(a_n - a_{n+2})} ;$$

$$\rho_{TM-TE} = n(n+1) \frac{(b_n - a_n)}{(b_n - a_{n+1})} \cdot \frac{(b_{n+1} - a_{n+1})}{(b_{n+1} - a_{n+2})}$$

$\rho_{TE} = \rho_{TM-TE}$ where a_n is computed from (2.4.18) and Table 1.

	n	ρ_{TM}		ρ_{TM-TE}		ρ_{TE}	
		Real	Im	Real	Im	Real	Im
ka = 1.	2	1.000	-0.14×10^{-6}	1.000	0.88×10^{-7}	0.999	0.11×10^{-6}
	3	1.000	0.0	0.999	-0.29×10^{-7}	0.999	0.47×10^{-6}
	4	0.999	0.23×10^{-9}	0.999	-0.35×10^{-9}	0.999	0.13×10^{-4}
	5	0.999	0.29×10^{-10}	1.000	-0.35×10^{-10}	0.982	0.56×10^{-3}
ka = 5.	4	5.000	0.0	5.000	-0.56×10^{-6}	5.000	-0.47×10^{-6}
	5	4.999	-0.20×10^{-5}	5.000	-0.44×10^{-5}	5.000	0.0
	6	5.000	0.16×10^{-5}	5.000	0.81×10^{-6}	5.000	0.66×10^{-6}
	7	5.000	0.18×10^{-6}	5.000	-0.47×10^{-6}	5.000	0.26×10^{-5}
	8	5.000	0.95×10^{-7}	5.000	0.35×10^{-7}	5.000	0.19×10^{-4}
ka = 10.	7	10.000	-0.73×10^{-6}	10.000	-0.12×10^{-7}	10.000	-0.72×10^{-6}
	8	10.000	0.0	10.000	0.26×10^{-5}	10.000	-0.57×10^{-5}
	9	10.000	0.22×10^{-5}	10.000	-0.11×10^{-5}	10.000	-0.34×10^{-5}
	10	10.000	-0.21×10^{-5}	10.000	-0.76×10^{-5}	10.000	0.21×10^{-5}
	11	10.000	0.87×10^{-6}	10.000	-0.69×10^{-6}	10.000	0.12×10^{-4}
	12	10.000	-0.27×10^{-5}	10.000	-0.94×10^{-6}	10.000	0.55×10^{-4}
	13	10.000	0.0	9.999	0.95×10^{-7}	10.000	0.25×10^{-3}

TABLE 5: DETERMINATION OF ka FOR THE TE-CASE EMPLOYING THE APPROX-IMATION $a_0 \approx -(1 + b_0)$

$$[\rho_{TE}] \text{ approximate} = n(n+1) \frac{(b_n - a_n)}{(b_n - a_{n+1})} \cdot \frac{(b_{n+1} - a_{n+1})}{(b_{n+1} - a_n)}, \quad a_1 = b_0,$$

$$a_0 \approx -(1 + b_0)$$

n	[ρ_{TE}] approximate		[ρ_{TE}] approximate with selection routine		
	Real	Im	Real	Im	
ka = 5.	3	4.850	-0.35×10^{-5}	0.0	0.0
	4	4.803	0.71×10^{-6}	0.0	0.0
	5	4.958	0.30×10^{-6}	5.004	0.87×10^{-5}
	6	5.036	0.93×10^{-7}	5.003	0.10×10^{-6}
	7	5.286	-0.14×10^{-5}	0.0	0.0
	8	6.239	-0.53×10^{-5}	0.0	0.0
ka = 10.	7	10.070	-0.46×10^{-3}	0.0	0.0
	8	9.895	0.65×10^{-3}	0.0	0.0
	9	9.992	0.46×10^{-3}	10.018	-0.34×10^{-5}
	10	9.980	0.11×10^{-3}	10.001	-0.49×10^{-5}
	11	10.018	-0.11×10^{-3}	10.000	0.58×10^{-4}
	12	10.112	-0.66×10^{-3}	0.0	0.0
	13	10.469	-0.24×10^{-2}	0.0	0.0

the approximation (2.4.19) may be applied with reasonable confidence, provided a selective subroutine is employed. This subroutine uses the a_n coefficients obtained from (2.4.8) and (2.4.9) and the known set $\{b_n\}$ to recover "ka" from (2.4.14). Employing the obtained value of "ka" in (2.2.6b), the resulting b_n coefficients are then compared with the original ones, and if a difference in the third digit of b_n is found, they are rejected.

2.6 COMPUTATION OF ka FROM THE COEFFICIENTS VALUES OBTAINED AFTER INVERSION OF $[\phi(N)]$

2.6.1 INTRODUCTION

Results in Table 4 and 5 clearly illustrate that the electrical radius of curvature of a perfectly conducting cylinder can be recovered according to the scattering model technique developed in section (2.4), whenever the coefficients a_n and b_n are known accurately up to the 6th digit. However, in practice, the accuracy and the resolution of any measurement technique used to compile the amplitude, phase and polarization information about the scattered field is not likely to be of this magnitude. Finally, whenever the electrical radius of curvature is relatively high, the order of truncation M increases, the size of the matrix $[\phi(N)]$ increases, and the results of its inversion are bound to be partially erroneous. This situation deteriorates further in the case where the bistatic angles are confined within a relatively small

domain of observation, even when the optimizational method presented in Part B is employed. Though this whole accuracy problem may seem alien to those unfamiliar with practical calculations, it is to our concern, an essential part of this investigation. The aim of the following sections is hence to analyse the parameters involved in the determination of the final accuracy. In the light of the previous remarks, there are two main parameters: the order of truncation M and the available domain of observation. The first is connected with the size of the circular cylinder and the second with the importance of the recording station.

2.6.2 ACCURACY DEPENDENCE UPON THE ORDER OF TRUNCATION M

The infinite series representing the far scattered field components are truncated to the order M , whose lower bound depends on ka , as recalled in section (2.2), namely $M \approx 2ka$; $ka > 4$. This order of truncation corresponds to a difference between $a_M(ka)$ and $b_M(ka)$ less than 10^{-4} and to the ratio

$$\frac{a_M(ka)}{a_0(ka)} \quad \text{or} \quad \frac{b_M(ka)}{b_0(ka)}$$

less than 10^{-4} which insures sufficient convergence. For $ka < 4$, M must be greater than $2ka$, to accurately represent the far scattered field components.

In a situation where $ka > 4$, the inversion of the matrix becomes labor-

ious and very little accuracy can be expected, since the system of equations formulated in the concise form (2.2.10) is to some extent overdetermined. To gain insight into this matter, one must only recall that, theoretically, the electrical radius can be recovered from 4 to 5 contiguous expansion coefficients. Therefore, the other coefficients expressed as a function of "ka" depend implicitly upon the first four, and consequently; the system of $N > 4$ equations is overdetermined. Hence, the first objective is to implement the formulation of these coefficients a_n, b_n in terms of the first four.

2.6.3 FORMULATION OF ($a_n; n \geq 4$) IN TERMS OF a_0, a_1, a_2 , AND a_3

Only the case of the a_n coefficients is carried out, since the conclusion of this section does not justify another lengthy derivation of limited interest. It is also conjectured that the conclusions drawn from the $\{a_n\}$ set are also valid for the $\{b_n\}$ set.

Employing equation (2.4.4) for $v = n + 1$ and $v = n + 2$, the coefficient a_{n+4} for $n \geq 0$ will be expressed as

$$a_{n+4} = \frac{a_{n+3} T_{n+4} - a_{n+2} U_{n+4}}{T_{n+4} - U_{n+4}} \quad (2.6.1)$$

with

$$T_{n+4} = (n+3) \cdot (a_{n+2, n+1}) \cdot (a_{n+2, n}) \quad (2.6.2)$$

and

$$U_{n+4} = (n+1) \cdot (a_{n+3, n+2}) \cdot (a_{n+1, n})$$

where the notation $a_{\mu\nu} = a_\mu - a_\nu$ is used.

Equations (2.6.1) and (2.6.2) as applied to the case $n = 0$, gives

$$a_4 = \frac{a_3 T_4 - a_2 U_4}{T_4 - U_4} \quad (2.6.3)$$

with

$$\begin{aligned} T_4 &= 3a_{21}a_{20} \\ U_4 &= a_{32}a_{10} \end{aligned} \quad (2.6.4)$$

In *Appendix A.4*, an expression for the higher coefficients a_{n+4} ; $n \geq 0$ is derived in terms of (a_0, a_1, a_2, a_3) . It is demonstrated that for any n

$$a_{n+4} = \frac{a_3 A_{n+4} - a_2 B_{n+4}}{A_{n+4} - B_{n+4}} \quad (2.6.5)$$

with

$$\left. \begin{aligned} A_{n+4} &= \frac{(n+3)}{2} a_{31} A_{n+3} - A_{n+2} B_4 \\ B_{n+4} &= \frac{(n+3)}{2} a_{31} B_{n+3} - B_{n+2} B_4 \end{aligned} \right\} ; n \text{ odd } \geq 1 \quad (2.6.6)$$

and

$$\left. \begin{aligned} A_{n+4} &= (n+3)a_{20}A_{n+3} - A_{n+2}B_4 \\ B_{n+4} &= (n+3)a_0B_{n+3} - B_{n+2}B_4 \end{aligned} \right\} ; n \text{ even } \geq 0 \quad (2.6.7)$$

together with the following definitions, namely

$$\begin{aligned} A_2 &= 0; A_3 = a_{21} \\ B_2 &= -1; B_3 = 0 \\ B_4 &= U_4 = a_{32}a_{10} \end{aligned} \quad (2.6.8)$$

Equations (2.6.5) to (2.6.8) represent a closed-form solution of the

coefficients a_{n+4} , $n \geq 0$ in terms of the set $\{a_0, a_1, a_2, a_3\}$. The dependency of a_{n+4} in terms of this set is highly nonlinear and there is no possible reduction of the system (2.2.10) into a system of four unknown variables. However, for $ka \approx 4$, the values of a_4 to a_8 , as calculated from (2.6.5), can be used as additional constraints to the 9 simultaneous equations system, to gain higher accuracy. For a larger electrical radius, $(M+1-4)$ additional constraints can be theoretically employed, but the relations involving $\{a_0, a_1, a_2, a_3\}$ are so complex that they cannot improve the final accuracy. Hence, some other means must be developed to circumvent this handicap in the retrieval of the coefficients.

2.6.4 ACCURACY DEPENDENCE UPON THE DOMAIN OF OBSERVATION

Although the formulation of the far field components as given by (2.2.7) and (2.2.8) is correct for any bistatic angle ϕ_r , the cylindrical wave functions used in the expansion are orthogonal within the interval $(\phi = 0, \pi)$. The highest level of accuracy in the recovery of the a_n or b_n coefficients thus occurs when data is available within this interval. In other cases, results must be approximative. This is amplified by the fact that, when the domain of observation is limited to a small wedge angle, the bistatic angles are extremely closely-packed, and the matrix $[\phi(N)]$ becomes quasi-singular. The worst eventuality occurs under the simultaneous presence of a large electrical radius ($ka > 4$), which requires many terms in the formulation of the

scattered field components, and a finite small domain of observation whose center wedge angle ϕ_{ω} is far from $\pi/2$ or $3\pi/2$. In this case, the cumulative error is so great that the calculated coefficients are meaningless.

In conclusion to these remarks, the theory developed in section (2.4) must be appreciably modified for practical use, though remaining of tantamount importance to its theoretical results. All the pertinent information regarding the circular cylinder is included in (2.2.5b), (2.2.6b); however, a method is lacking for the actual precise retrieval of its electrical radius. The following section provides a practical means to portray various rotationally symmetric bodies, when it is conjectured that all information concerning their shape is indeed included in the far scattered field components.

2.7. ITERATIVE AVERAGING METHOD DEVELOPED TO RETRIEVE THE ELECTRICAL RADIUS OF CURVATURE OF THE CYLINDER

2.7.1 INTRODUCTION

The lack of accuracy inherent in the theoretical method derived in the previous section results from

- i) the truncation order M of the far scattered field matrix
- ii) the restricted domain of observation
- iii) the matrix inversion procedure.

In connection with the practical aspects of the "inverse scattering problem", an alternative technique is presented which can accurately recover the shape of the circular cylinder. In practical situations, as it is well-known^(22, 32), determination of average characteristics in the form of cross-sections proved to be valuable in the study of the general problem of scattering. Such quantities relating the magnitude of the back-scattered field to the illuminated area of the scatterer should also be of practical interest in the case of the inverse problem, inasmuch as they could provide means to describe the obstacle fairly accurately. Although not analytically satisfying, this aspect is examined in this section.

The fact that scattering geometries of identical curvature when illuminated by the same wave incidence, give rise on the average to back-scattered fields of identical magnitudes has been acknowledged for many years. This forms the foundation of the following method since a knowledge of the field's magnitude necessarily reflects some information on the curvature of the obstacle. Although there are no analytical formulae relating these two quantities, the larger the radius of curvature the larger the magnitude of the back-scattered field is. Notwithstanding this general overall behaviour small amplitude oscillations occasionally arise; for example, a slight decrease in the magnitude of the back-scattered field may occur due to a small increase in the body radius of curvature and vice versa. This, however, is not the case for larger variations and in the following analysis, these oscil-

lations are ignored at first. They will be reconsidered later in a refinement procedure.

It is also valuable to note that the phase information contained in the far scattered field has been disregarded since it consists usually of a fast varying function of the overall configuration of the obstacle and is therefore not representative of the illuminated area of the scatterer.

The aforementioned dependency being valid on an average statistical basis, any method based on this concept implies the measurement of the back-scattered field at various aspect angles. Since these angles can be arbitrarily chosen within a given domain of observation, the distribution obtained via the optimization procedure is selected as a typical set of measurement locations.

Obviously then, any alternative attempt to retrieve the local radius of curvature of the obstacle requires an iterative method. To illustrate the operating mechanism of this method, "the inverse scattering problem" is reviewed in an entirely different light. The association of the unknown remote scatterer with the back-scattered field for a given incident plane wave can be considered as a system. From this perspective, the objective of the "inverse scattering problem" is then reduced to a synthesis of this system, in other words, the recovery of the radius of curvature of the body around the illuminated area. The basic steps

involved in a system synthesis are then briefly described in order to introduce and explain the function of the iterative averaging method.

In order, they are:

- i) the identification of the parameters which are significant to the system.
- ii) the attribution of particular numerical values to these parameters.
- iii) the evaluation of the system performance corresponding to that particular choice of parameters.

These operations are then repeated if the desired results are not obtained. As this iteration is proceeding, the quality of the selection of the parameters is estimated by comparing the actual results with the desired performance of the system. This quality is usually evaluated by a merit factor or quality function which must be optimized. That particular method of optimization chosen generally is conditioned by the time allotted to the synthesis; however, it does not affect the quality of the system.

2.7.2 ITERATIVE AVERAGING METHOD

In following operational sequence usually adopted in system synthesis as described in (2.7.1), the system relative to the "inverse scattering problem" is first presented and the influent parameters identified.

Since no measurements were carried out, the far scattered fields for a given plane wave incidence are first calculated at "n" aspect angles

via an integral equation for the numerical solution of two dimensional diffraction problems as reported in (43). The sum of the magnitudes of the fields at these aspects is then computed and denoted as S_n^e where "e" stands for exact values. This summation depends upon the curvature of the inobservable body; therefore, the electrical radius "ka" of the impact area is selected as the important parameter in this synthesis; i.e. the recovery of the obstacle.

The transfer function "T" calculates the far field scattered by a circular cylinder whose electrical radius is given by a particular value of the parameter.

The initialization " ka_1 " is obtained employing equations (2.4.4) or (2.4.14) which are relative to the theoretical method developed throughout this chapter. To avoid instabilities and inaccuracy in the inversion procedure, only five terms are considered in the expansion of the far scattered field components. This particular choice results from the compromise between the two alternatives of

- i) a good representation of the field components resulting in poor accuracy in the recovery of the associated coefficients.
- ii) a misrepresentation of the field components with no inversion accuracy problem.

For the particular case of a circular cylinder another method may also be considered employing the additional constraints as defined in (2.6.5).

This option can be of interest only if $2 \leq ka \leq 4$. Nevertheless, even for $ka \leq 4$, " ka_1 " will be approximate because we assume the data to be available only within a small domain of observation. Consequently, even in the case of the circular cylinder a more general technique must be implemented.

In this technique, the far scattered field originating from a hypothetical cylinder of electrical radius " ka_1 " is first calculated using "T". The magnitudes of the fields at the "n" aspects considered earlier are added and the result is denoted by $S_n^{\text{appr.}}$, where "appr." stands for approximate. A merit factor "F" is then defined as $S_n^e - S_n^{\text{appr.}}$. From its value and according to its sign, " ka_1 " is modified to " ka_2 " and the process repeats itself.

This process is best visualized by considering the symbolic block-diagram of the system as shown in Fig. 4 and the associated flow-chart as shown in Fig. 5.

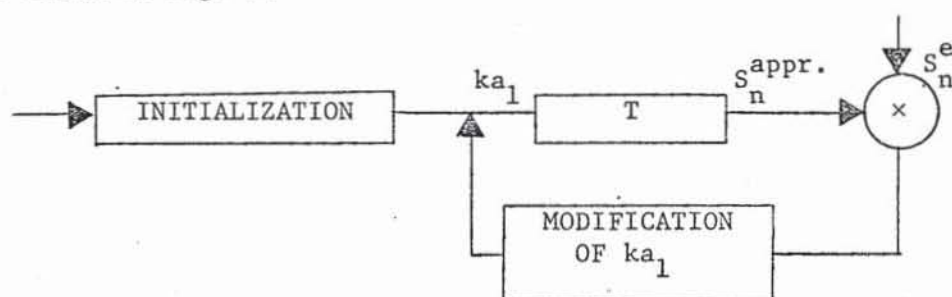


FIG. 4 BLOCK-DIAGRAM OF THE ITERATIVE AVERAGING METHOD

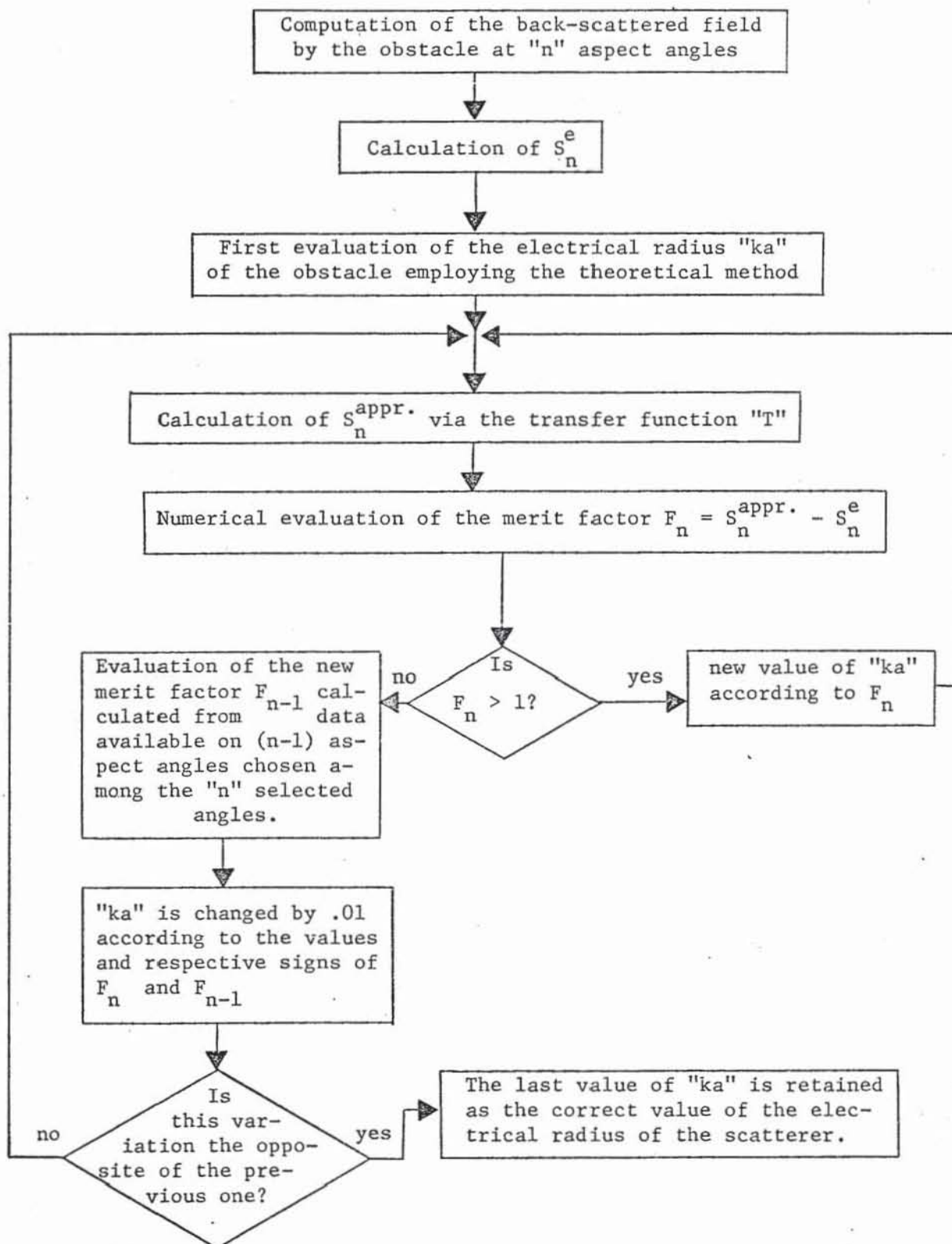


FIG. 5 FLOW-CHART OF THE ITERATIVE AVERAGING METHOD

2.7.3 FLOW-CHART AND COMPUTATIONAL RESULTS

The flow-chart as it is shown in Fig. 5 is self-explanatory except for the refinement branch which leaves the logical statement (is F_n greater than 1?) when the decision is "no". At this junction a new merit factor F_{n-1} is introduced. Although this branch may seem redundant at first, it has the purpose to refine the proposed method by taking into account the small oscillations which exist in connection with the magnitude of the back-scattered field and the curvature of the obstacle at hand. Since the magnitude of the back-scattered field is only calculated at five aspect angles, the refinement branch consists in comparing at least one of the values of that magnitude of a field which would then be given off by a hypothetical circular cylinder. If the sum of the magnitudes of the scattered field over five aspects and that of any one particular aspect almost coincide with the similar quantities evaluated for the hypothetical circular cylinder, the electrical radius of curvature of that cylinder gives the electrical radius of curvature of the illuminated area of the obstacle with a high degree of confidence. A careful examination of the merit factors F_n and F_{n-1} is directed towards this goal. The final value of this electrical radius is selected when the change in "ka" initiated by F_{n-1} is equal to the negative value of the last change ordered by F_{n-1} .

This method has been applied to the recovery of the electrical radius of the circular cylinder ranging from 0.5 to 15 when the observation

wedge angle varies from π to a limited value chosen arbitrarily to be $\pi/36$. The results correspond with the original values and are illustrated in Table 6.

2.8 CONCLUSIONS

An electromagnetic inverse scattering model technique has been presented for the perfectly conducting cylinder. Although the approach is not the most general, as compared to those of Lewis⁽²⁸⁾; Weston, Bowman and Ergun Ar⁽⁵⁷⁾; Weston and Boerner⁽⁵⁴⁾; Millar⁽³⁰⁾; or Mittra and Imbriale⁽³¹⁾, some rather fundamental relations have been derived and shown to be relevant to the problem of inverse scattering.

In order to employ this technique, the transverse field components must be obtained in amplitude, phase and polarization using relative phase measurement techniques with the incident field as phase reference. Such measurement techniques are not discussed here nor are measurement results given. However, with the resulting closed-form solution of the determinant (2.3.4) associated with the scattered field matrix (2.2.10) and the novel optimization procedure described in Part B, one may reliably predict the proper distribution of the measurement aspect angles for most stable inversion procedures. In particular, it is observed from (2.3.4) and (2.3.5) that the determinant $|\Phi(N)|$ is symmetric about $\phi = 0$ and therefore measurements must be compiled only within the range $0 \leq \phi \leq \pi$ or $\pi \leq \phi \leq 2\pi$.

TABLE 6: RETRIEVAL OF THE ELECTRICAL RADIUS OF THE CYLINDER FROM
THE ITERATIVE AVERAGING METHOD

Domain of Observation: $\frac{\pi}{12}$

Original Value	1	5	10
Resulting Value	0.980	4.998	10.40

Domain of Observation: $\frac{\pi}{36}$

Original Value	1	5	10
Resulting Value	0.963	4.96	10.37

Optimum results are obtained if the measurement domain is centered about the 90° bistatic angle, which is consistent with the mono-bistatic equivalence theorem⁽²²⁾. The optimization procedure is verified by computational results given in Table 1. If the measurement aspect angles are such that the optimization constraints of (2.3.5) are satisfied, the unknown coefficients $\{a_n''\}$ and $\{b_n''\}$ are obtained from standard precision matrix inversion techniques to the degree of accuracy dictated only by the employed measurement technique⁽⁵⁴⁾.

Since the ultimate aim is to recover the electrical radius of the cylinder, it is evident from (2.4.4), (2.4.14) and (A.3.17) that " ka " may be retrieved directly for all three polarizations using a_n and b_n but without any recourse to inverse scattering boundary conditions or methods of analytical continuation. The results are valid for any value of " kR ", although measurement data are usually obtained in the far field (i.e. $kR \rightarrow \infty$). Furthermore, the relations (2.4.8), (A.3.2), (A.3.16) and (A.3.17) may be used to recover the unknown polarization angle as shown in *Appendix A.1*.

It is also valuable to note that a relationship exists between the sets of coefficients $\{a_n\}_{TM}$ and $\{b_n\}_{TE}$ which could indicate a similar relation between the two associated types of vector wave functions. If such a relation could be found, the problem of electromagnetic inverse scattering would be resolved in terms of one unique set of vector wave functions.

The theoretical study presented here lacks accurate results whenever the order of the far scattered field matrix is higher than five or whenever the finite domain of observation is small and centers far from the bistatic angle $\pi/2$ or $3\pi/2$. This accuracy problem remains of prime importance in any practical approach and imposes a modification on this study in order to include this exigency.

In order to reduce the size of the far scattered field matrix higher order associated expansion coefficients have been expressed in terms of the first coefficients. A general formulation has been developed for the TM case; nevertheless, the iterative formulae obtained are too sophisticated to be of interest for any circular geometry.

A new iterative averaging method has been next presented which is based on a different concept. In this alternative, the "inverse scattering problem" has been re-examined as the synthesis of a system which includes the remote scatterer and the back-scattered field at various aspects. The synthesis of this system (i.e. the recovery of the electrical radius of curvature of the circular cylinder) has been completed and computational results are in agreement with the desired performance of the system. This alternative method proved to be invaluable in objectifying the obstacle and its applicability has not yet been completely explored although it will be successfully employed in the next chapter.

*chapter three*THE ELLIPTIC CYLINDER3.1 INTRODUCTION

The analysis of the elliptic cylinder in light of the inverse scattering problem follows logically from the previous examination of the circular cylinder in *chapter two*. This particular geometry is interesting in many respects: its boundary surface is a level surface in the elliptic co-ordinate system (η, ξ, z) in which the separation of the scalar wave equation related to the direct problem of scattering is possible; secondly, computer subroutines already exist for the calculation of the far scattered field components when a plane wave impinges on its surface. Finally, by changing the eccentricity value, we are able to cover an entire range of shapes from the circular cylinder to the strip.

The method used in this investigation is that developed for the circular cylinder, when we assume that the scattered field components contain all information pertaining to the shape of the body. The far scattered field components are first expanded in terms of Mathieu wave functions. The associated expansion coefficients are expressed here as an infinite series of these functions. This is in direct contrast to the circular cylinder case, where their formulation was reduced to a one term series involving cylindrical Bessel functions.

Due to this increased complexity, it is impossible to extricate any tangible information relative to the geometry of the scatterer from the analytical expression of these coefficients.

For large values of ξ_0 which defines the generating ellipse of the cylinder, these coefficients are expressed in terms of the Bessel functions. This could then lead to a simplified solution. However, these expansions are very difficult to obtain in practice, since the employment of the Watson transform is necessary as a preliminary step to replace the series into a contour integral. Assuming that such a derivation would be carried out, the elliptic cylinder would then be viewed as a circular cylinder of large radius of curvature, and no information would be gained as the relative magnitudes of the principle axes of the cylinder. Such a solution is therefore not pursued here.

The iterative averaging method examined in section (2.7) is then successfully applied to recover the electrical radii of the generating ellipse. This method was first developed for the analysis of this problem and was to constitute the core of this particular chapter; however, it has been included in *chapter two* for the sake of convenience.

3.2 FORMULATION OF THE FAR FIELD

Consider a perfectly conducting elliptic cylinder of major and minor axes a and b , with its invariant axis along the \hat{z} -direction of an

(x, y, z) rectangular co-ordinate system. Its interfocal distance will be equal to d (Fig, 6). If k is the wave propagation constant, the scattering problem for vertical propagation is two-dimensional and consists in finding a solution to the Helmholtz equation

$$(\nabla^2 + k^2) u = 0 \quad (3.2.1)$$

which satisfies the Sommerfeld radiation condition at ∞ and the prescribed boundary condition $u = 0$ on the cylinder.

Let us now introduce the elliptical co-ordinates ξ and η on the plane (x, y) according to the transformation

$$\begin{aligned} x &= \frac{d}{2} \cdot \cosh\xi \\ y &= \frac{d}{2} \cdot \sinh\xi \end{aligned} \quad (3.2.2)$$

The wave equation (3.2.1) in the co-ordinate system (ξ, η, z) is decomposed into

$$\begin{aligned} \frac{\partial^2 \Phi}{\partial \eta^2} + 2h^2 (\ell^2 - \cos 2\eta) \Phi &= 0 \\ \frac{\partial^2 \Psi}{\partial \xi^2} - 2h^2 (\ell^2 - \cosh 2\xi) \Psi &= 0 \end{aligned} \quad (3.2.3)$$

where $u(\xi, \eta) = \Phi(\eta) \cdot \Psi(\xi)$, $4h$ equals kd and ℓ is an arbitrary constant.

If ξ_0 defines the generating ellipse of the cylinder, the $\psi(\xi)$ function must satisfy the boundary condition

$$\psi(\xi_0) = 0 \quad (3.2.4)$$

The system of equations, as expressed in (3.2.2) and (3.2.3), has been extensively studied and the solutions are known^(26, 50, 17, 29). For a \hat{z} polarized incident plane wave,

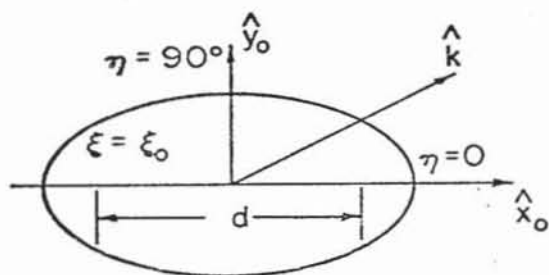


Fig. 6 Coordinates used for the Elliptic Cylinder

$$\underline{E}_z^i = \underline{E}_0 e^{jk \cdot \underline{R}} = \underline{E}_0 e^{jk(x \cos \theta + y \sin \theta)} \quad (3.2.5)$$

$$= 2\underline{E}_0 \sum_{n=0}^{\infty} \left\{ \left[\frac{1}{p_{2n}} \cdot Ce_{2n}(\xi) \cdot ce_{2n}(\eta) \cdot ce_{2n}(\theta) + \frac{1}{s_{2n+2}} \cdot Se_{2n+2}(\xi) \cdot se_{2n+2}(\eta) \cdot se_{2n+2}(\theta) \right] + j \left[\frac{1}{p_{2n+1}} \cdot Ce_{2n+1}(\xi) \cdot ce_{2n+1}(\eta) \cdot ce_{2n+1}(\theta) + \frac{1}{s_{2n+1}} \cdot Se_{2n+1}(\xi) \cdot se_{2n+1}(\eta) \cdot se_{2n+1}(\theta) \right] \right\} \quad (3.2.6)$$

where θ gives the direction of the plane wave as shown in Fig. 6, the scattered field \underline{E}_z^s for large values of ξ is expressed as

$$\underline{E}_z^s = \sqrt{\frac{8}{\pi k R}} \underline{E}_0 e^{j(kR + 3\frac{\pi}{4})} \sum_{n=0}^{\infty} \left\{ \alpha_{2n}(\xi_0) \cdot ce_{2n}(\eta) \cdot ce_{2n}(\theta) + \delta_{2n+1}(\xi_0) \cdot se_{2n+1}(\eta) \cdot se_{2n+1}(\theta) + \gamma_{2n+1}(\xi_0) \cdot ce_{2n+1}(\eta) \cdot ce_{2n+1}(\theta) + \beta_{2n+2}(\xi_0) \cdot se_{2n+2}(\eta) \cdot se_{2n+2}(\theta) \right\} \quad (3.2.7)$$

This is derived in *Appendix A.5*, where the notations are explicitly defined. They are not reported here for the sake of brevity. As it was asserted earlier, all pertinent information regarding the generating ellipse of the scatterer is contained in the coefficients α_{2n} , β_{2n+2} , γ_{2n+1} , δ_{2n+1} appearing in equation (3.2.7). However, it is virtually impossible to analytically extract ξ_0 from (A.5.8), due to the complexity of the Mathieu functions involved in describing the far scattered field. The problem is hence presented for the reduced cases $\theta = 0$ (i.e. propagation along the \hat{x} direction) and $\theta = \frac{\pi}{2}$ (i.e. propagation in the \hat{y} direction), for which (3.2.7) can be simplified.

Plane wave incident along $\theta = 0$

In this case, it is shown in (29) that

$$se_{2n+1}^{(0)} = se_{2n+2}^{(0)} = 0 \quad (3.2.8)$$

Dividing (3.2.7) by the normalization constant defined as

$$- E_0 \sqrt{\frac{2}{\pi kR}} e^{j(kR + \frac{\pi}{4})} \quad (3.2.9)$$

the normalized far scattered field results in

$$e_{(0)}^{(\eta)} = -2 \cdot \sum_{n=0}^{\infty} \begin{bmatrix} ce_{2n}(\eta) \cdot ce_{2n}^{(0)} & 0 \\ 0 & ce_{2n+1}(\eta) \cdot ce_{2n+1}^{(0)} \end{bmatrix} \begin{bmatrix} \alpha_{2n}(\xi_0) \\ \gamma_{2n+1}(\xi_0) \end{bmatrix} \quad (3.2.10)$$

where the subscript (0) refers to the case $\theta = 0$.

Plane wave incident along $\theta = \frac{\pi}{2}$

Since for $\theta = \frac{\pi}{2}$

$$ce_{2n+1}^{(\frac{\pi}{2})} = se_{2n+2}^{(\frac{\pi}{2})} = 0 \quad (3.2.11)$$

the normalized far scattered field is written in this case as

$$e_{(\frac{\pi}{2})}^{(\eta)} = -2 \sum_{n=0}^{\infty} \begin{bmatrix} ce_{2n}(\eta) \cdot ce_{2n}^{(\frac{\pi}{2})} & 0 \\ 0 & se_{2n+1}(\eta) \cdot se_{2n+1}^{(\frac{\pi}{2})} \end{bmatrix} \begin{bmatrix} \alpha_{2n}(\xi_0) \\ \delta_{2n+1}(\xi_0) \end{bmatrix} \quad (3.2.12)$$

where the subscript $(\frac{\pi}{2})$ refers to the case $\theta = \frac{\pi}{2}$.

3.3 INVERSION PROCEDURE

Equations (3.2.10) and (3.2.12) express the far scattered field, in terms of the Fourier coefficients $\alpha_{2n}(\xi_0)$, $\gamma_{2n+1}(\xi_0)$, and $\delta_{2n+1}(\xi_0)$ associated with the elliptic wave functions for the two cases $\theta = 0$ and $\theta = \frac{\pi}{2}$. The procedure developed in *chapter two* to retrieve the Fourier coefficients consists in inverting those matrices implicitly defined in (3.2.10) and (3.2.12). However, in contrast with the case of the circular cylinder, the elliptic wave functions depend critically on the interfocal distance d , which is not *a priori* known, and cannot be generally formulated. Therefore, we must take recourse to further approximations to mitigate these extra complications. The following sections will be devoted to this analysis.

3.4 REDUCTIONS OF EQUATION (3.2.10) AND (3.2.12)

3.4.1 REVIEW OF THE NOTATIONS

In order to proceed, the notations are reviewed for the sake of clarity. The direction of the bistatic receiver is assumed to be in the vicinity of that of the transmitter and located at an angle ϕ with respect to the \hat{x} axis. Since we are in the far field region, the angle ϕ is equivalent to the angle η . The parameter q , used in the Mathieu functions as introduced in (A.5.4) and (A.5.5), is equal to

$$q = h^2 = \frac{k^2 d^2}{16} \quad (3.4.1)$$

The electric major and minor axes of the generating ellipse are equal to

$$ka = (kd/2) \cdot \cosh \xi_0 = 2\sqrt{q} \cosh \xi_0 \quad (3.4.2)$$

$$kb = (kd/2) \cdot \sinh \xi_0 = 2\sqrt{q} \sinh \xi_0 \quad (3.4.3)$$

3.4.2 REDUCTION OF EQUATION (3.2.12)

Equation (3.2.12) can be reduced if the far field quantities are known in the directions ϕ and $(-\phi)$ with respect to the \hat{x} axis as shown in Fig. 7, namely,

$$\begin{aligned} D(\phi) &= \frac{e_{\left(\frac{\pi}{2}\right)}(\phi) - e_{\left(\frac{\pi}{2}\right)}(-\phi)}{2} = - \sum_{n=0}^{\infty} \{ ce_{2n}\left(\frac{\pi}{2}\right) \cdot \alpha_{2n}(\xi_0) \cdot [A_0^{2n} + A_2^{2n} \cos 2\phi + \dots] \\ &+ se_{2n+1}\left(\frac{\pi}{2}\right) \cdot \delta_{2n+1}(\xi_0) \cdot [B_1^{2n+1} \sin \phi + \dots] \} - \sum_{n=0}^{\infty} \{ ce_{2n}\left(\frac{\pi}{2}\right) \cdot \\ &\alpha_{2n}(\xi_0) \cdot [-A_0^{2n} - A_2^{2n} \cos 2\phi + \dots] + se_{2n+1}\left(\frac{\pi}{2}\right) \cdot \delta_{2n+1}(\xi_0) \cdot \\ &[B_1^{2n+1} \sin \phi + B_3^{2n+1} \sin 3\phi + \dots] \} \quad (3.4.4) \\ &= - 2 \sum_{n=0}^{\infty} se_{2n+1}\left(\frac{\pi}{2}\right) \cdot \delta_{2n+1}(\xi_0) \cdot se_{2n+1}(\phi) \end{aligned}$$

Substituting $se_{2n+1}(\phi)$ by its expression as given in (A.5.12) leads to

$$\begin{aligned} D(\phi) &= - 2 \sin \phi \sum_{n=0}^{\infty} B_1^{2n+1} se_{2n+1}\left(\frac{\pi}{2}\right) \cdot \delta_{2n+1}(\xi_0) - 2 \sin 3\phi \sum_{n=0}^{\infty} B_3^{2n+1} \cdot \\ &se_{2n+1}\left(\frac{\pi}{2}\right) \cdot \delta_{2n+1}(\xi_0) - \dots - 2 \sin(2n+1)\phi \sum_{n=0}^{\infty} B_{2n+1}^{2n+1} \cdot \\ &se_{2n+1}\left(\frac{\pi}{2}\right) \cdot \delta_{2n+1}(\xi_0) \quad (3.4.5) \end{aligned}$$

which can be written in matrix form as

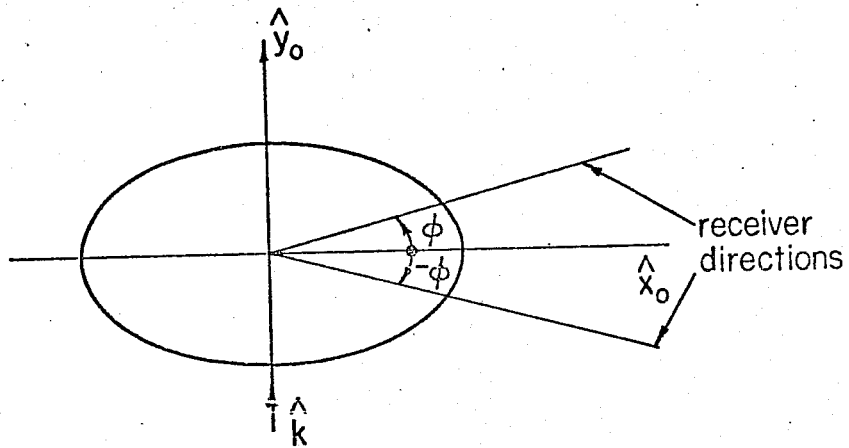


Fig. 7 Receiver Directions for the Reduction of Equation [3.2.12]

$$\begin{bmatrix} D(\phi_1) \\ D(\phi_2) \\ \vdots \end{bmatrix} = \begin{bmatrix} 2\sin\phi_1 & 2\sin 3\phi_1 & 2\sin 5\phi_1 & \dots \\ 2\sin\phi_2 & 2\sin 3\phi_2 & 2\sin 5\phi_2 & \dots \\ \vdots & \vdots & \vdots & \vdots \end{bmatrix} \begin{bmatrix} - \sum_{n=0}^{\infty} B_1^{2n+1} \cdot \text{se}_{2n+1}(\frac{\pi}{2}) \cdot \delta_{2n+1}(\xi_0) \\ - \sum_{n=0}^{\infty} B_3^{2n+1} \cdot \text{se}_{2n+1}(\frac{\pi}{2}) \cdot \delta_{2n+1}(\xi_0) \\ \dots \end{bmatrix} \quad (3.4.6)$$

Similarly, the sum of the far scattered field in the direction ϕ and $(-\phi)$ can be taken instead, which results in:

$$S(\phi) = \frac{e_{\frac{\pi}{2}}(\phi) + e_{\frac{\pi}{2}}(-\phi)}{2} = -2 \sum_{n=0}^{\infty} c e_{2n}(\frac{\pi}{2}) \cdot \alpha_{2n}(\xi_0) \cdot c e_{2n}(\phi) \quad (3.4.7)$$

and in matrix formulation

$$\begin{bmatrix} S(\phi_1) \\ S(\phi_2) \\ \vdots \end{bmatrix} = \begin{bmatrix} 2 & 2\cos 2\phi_1 & 2\cos 4\phi_1 & 2\cos 6\phi_1 & \dots \\ 2 & 2\cos 2\phi_2 & 2\cos 4\phi_2 & 2\cos 6\phi_2 & \dots \\ \vdots & \vdots & \vdots & \vdots & \vdots \end{bmatrix} \begin{bmatrix} - \sum_{n=0}^{\infty} A_0^{2n} \cdot c e_{2n}(\frac{\pi}{2}) \cdot \alpha_{2n}(\xi_0) \\ - \sum_{n=0}^{\infty} A_2^{2n} \cdot c e_{2n}(\frac{\pi}{2}) \cdot \alpha_{2n}(\xi_0) \\ \vdots \end{bmatrix} \quad (3.4.8)$$

3.4.3 REDUCTION OF EQUATION (3.2.10)

There is a formulation similar to equations (3.4.6) and (3.4.8) in this case, namely:

$$\begin{bmatrix} e_0(\phi_1) \\ e_0(\phi_2) \\ \vdots \end{bmatrix} = \begin{bmatrix} 2 & 2\cos\phi_1 & 2\cos 2\phi_1 & \dots \\ 2 & 2\cos\phi_2 & 2\cos 2\phi_2 & \dots \\ \vdots & \vdots & \vdots & \vdots \end{bmatrix} \begin{bmatrix} - \sum_{n=0}^{\infty} A_0^{2n} \cdot c e_{2n}(0) \cdot \alpha_{2n}(\xi_0) \\ - \sum_{n=0}^{\infty} A_1^{2n+1} \cdot c e_{2n+1}(0) \cdot \gamma_{2n+1}(\xi_0) \\ \vdots \end{bmatrix} \quad (3.4.9)$$

3.4.4 PRELIMINARY CONCLUSIONS

In both cases, $\theta = 0$ and $\theta = \frac{\pi}{2}$, the formulation of the far scattered field is expressed in a matrix form similar to equation (2.2.10), relative to the circular case. However, in contrast with the latter, it is still not possible to extract ξ_0 when the last members of the equations (3.4.6), (3.4.8) and (3.4.9) are known. This arises essentially because of the complexity of the coefficients A_n^m and B_n^m introduced in the expansion of the Mathieu functions. One of the terms appearing in the second member of (3.4.9) is analysed in detail; it is demonstrated that (3.4.9) is identical to (2.2.11) in the limiting case, where the eccentricity of the generating ellipse goes to zero.

3.4.5 ANALYSIS OF $-\sum_{n=0}^{\infty} A_1^{2n+1} \cdot ce_{2n+1}(0) \cdot \gamma_{2n+1}(\xi_0)$

The only way to make ξ_0 accessible is to extract $\gamma_{2n+1}(\xi_0)$ from the summation sign in (3.4.9). This is best achieved by considering the high frequency case, when $\gamma_{2n+1}(\xi_0)$ is independent of $(2n+1)$. The expansion of $\gamma_{2n+1}(\xi_0)$ in terms of the Bessel functions is thus appropriate. However, proceeding with this high frequency hypothesis, ka and kb must take large values and very little information is then gained as to their relative values, since the elliptic cylinder is hence viewed as a circular cylinder with a radius of curvature approximately equal to ka and kb . In order to bring more insight in this analysis, the coefficients $\gamma_{2n+1}(\xi_0)$ are expressed in terms of Bessel and Hankel functions as:

$$\gamma_{2n+1}(\xi_0) = \frac{ce_{2n+1}(\xi_0, q)}{Me_{2n+1}^{(1)}(\xi_0, q)} = \frac{-\frac{ce'_{2n+1}(\frac{\pi}{2}, q)}{\sqrt{qA_1^{2n+1}}} \sum_{r=0}^{\infty} (-1)^r A_{2r+1}^{2n+1} \cdot J_{2r+1}(ka)}{-\frac{ce'_{2n+1}(\frac{\pi}{2}, q)}{\sqrt{qA_1^{2n+1}}} \sum_{r=0}^{\infty} (-1)^r A_{2r+1}^{2n+1} \cdot H_{2r+1}^{(1)}(ka)} \quad (3.4.10)$$

where the derivative of ce_{2n+1} is taken with respect to the argument. However, another expression also exists for $\gamma_{2n+1}(\xi_0)$ if ce_{2n+1} and $Me_{2n+1}^{(1)}$ are expanded differently, namely

$$\gamma_{2n+1}(\xi_0) = \frac{\frac{ce_{2n+1}(0, q)}{\sqrt{qA_1^{2n+1}}} \cdot \coth \xi_0 \cdot \sum_{r=0}^{\infty} (2r+1) \cdot A_{2r+1}^{2n+1} \cdot J_{2r+1}(kb)}{\frac{ce_{2n+1}(0, q)}{\sqrt{qA_1^{2n+1}}} \cdot \coth \xi_0 \cdot \sum_{r=0}^{\infty} (2r+1) \cdot A_{2r+1}^{2n+1} \cdot H_{2r+1}^{(1)}(kb)} \quad (3.4.12)$$

For the large argument, which corresponds to the high frequency case, $ka \approx kb \approx x$, and

$$J_{2r+1}(x) \approx \sqrt{\frac{2}{\pi x}} (-1)^r \sin(x - \frac{\pi}{4}) \quad (3.4.13)$$

$$H_{2r+1}^{(1)}(x) \approx j^{-\frac{3}{2}} \sqrt{\frac{2}{\pi x}} (-1)^r e^{-jx} \quad (3.4.14)$$

Substituting (3.4.13) and (3.4.14) in (3.4.10) results in

$$\gamma_{2n+1}(\xi_0) \approx \frac{\sqrt{\frac{2}{\pi ka}} \sum_{r=0}^{\infty} (-1)^{2r} A_{2r+1}^{2n+1} \cdot \sin(ka - \frac{\pi}{4})}{j^{-3/2} \sqrt{\frac{2}{\pi ka}} \sum_{r=0}^{\infty} (-1)^{2r} A_{2r+1}^{2n+1} \cdot e^{-jka}} \quad (3.4.15)$$

$$\approx -e^{-j(ka + \frac{\pi}{4})} \sin(ka - \frac{\pi}{4}) \quad (3.4.16)$$

Similarly, substituting (3.4.13) and (3.4.14) in (3.4.12) leads to

$$\gamma_{2n+1}(\xi_0) \approx -e^{-j(kb + \frac{\pi}{4})} \sin(kb - \frac{\pi}{4}) \quad (3.4.17)$$

In proceeding with this analysis, it has been assumed that the infinite series appearing in the numerator and the denominator of equations (3.4.10) and (3.4.12) could be rigorously calculated. However, in order to do this, the asymptotic behaviour of the coefficients A_{2r+1}^{2n+1} would have to be known, which is not the case. The procedure commonly adopted in order to obtain rigorous asymptotic expansions of (3.4.10) and (3.4.12) consists in the employment of the Watson transform to replace these infinite series into contour integrals, which may then be evaluated asymptotically. Such an analysis is not pursued here, as it exceeds the scope of our goal. Nevertheless, some conclusions can be noted as regards the validity of the results (3.4.16) and (3.5.17). For example, if the values of $\gamma_{2n+1}(\xi_0)$ as given by (3.4.16) and the analogous result for $\alpha_{2n}(\xi_0)$ are substituted in (3.4.10), the far scattered normalized field can be written as

$$e_{\left(\frac{\pi}{2}\right)}(\phi) = 2e^{-j(ka + \pi/4)} \sin(ka - \pi/4) \cdot \sum_{n=0}^{\infty} \{ce_{2n}(\phi) \cdot ce_{2n}(\pi/2) + se_{2n+1}(\phi) \cdot se_{2n+1}(\pi/2)\} \quad (3.4.18)$$

In this formulation, the phase term corresponding to the backscattering direction $\phi = \pi/2$, is equal to ka , which is in direct contradiction with the known result $2ka$, obtained from physical optics for the circular cylinder⁽¹¹⁾. This is the best example of the asymptotic results given by (3.4.16) and (3.4.17) being in general questionable, and of their incompatibility with the study of the inverse problem of scattering. Therefore, only the technique presented in section (2.7), and based on average properties related to the far scattered field, seems to be suitable for this elliptic cylinder problem. However, before applying this iterative averaging method, the limiting case of the circular cylinder is rederived for the sake of completeness.

3.4.6 LIMITING CASE OF THE CIRCULAR CYLINDER

When the eccentricity of the generating ellipse goes to zero, $q = h^2$ goes to zero and the following holds:

$$A_r^m(q) \begin{cases} 1, & r = m \\ 0, & r \neq m \end{cases} \quad m \geq 1 \quad (3.4.19)$$

$$B_r^m(q) \begin{cases} 1, & r = m \\ 0, & r \neq m \end{cases} \quad m \geq 1$$

With (3.4.10), the coefficient $\gamma_{2n+1}(\xi_0)$ results in

$$\gamma_{2n+1}(\xi_0) = \frac{J_{2n+1}(ka)}{H_{2n+1}^{(1)}(ka)} \quad (3.4.20)$$

and $-\sum_{n=0}^{\infty} A_1^{2n+1} ce_{2n+1}(0) \cdot \gamma_{2n+1}(\xi_0)$ in

$$- A_1^1 ce_1(0) \cdot \gamma_1(\xi_0) = - \frac{\cos(0) J_1(ka)}{H_1^{(1)}(ka)}$$

$$= - \frac{J_1(ka)}{H_1^{(1)}(ka)} \quad (3.4.21)$$

which are identical to the coefficient a_1 shown for the circular cylinder.

For $r = 0$,

$$A_0^0 ce_0(0) = A_0^0 \cdot A_0^0 = \frac{1}{\sqrt{2}} \cdot \frac{1}{\sqrt{2}} = \frac{1}{2} \quad (3.4.22)$$

and

$$- A_0^0 ce_0(0) \alpha_0(\xi_0) = - \frac{1}{2} \frac{J_0(ka)}{H_0^{(1)}(ka)} \quad (3.4.23)$$

which is identical to the coefficient a_0 for the circular cylinder, since the $\frac{1}{2}$ in (3.4.23) cancels the 2 in the first column of the matrix defined in (3.4.9).

3.5 RETRIEVAL OF THE AXES OF THE CYLINDER BY EMPLOYING AN ITERATIVE AVERAGING METHOD

In contrast with the case of the circular cylinder, there is no direct technique available to retrieve the axes of the elliptic cylinder. A method, duplicated from that demonstrated in section (2.7), and essentially based on average properties of the backscattered field is presented here to enable us to recover the local radius of curvature of the illuminated area. This technique consists in imagining a hypothetical cylinder, which if illuminated by a plane wave, would originate a backscattered field, whose magnitude in a small wedge angle of observation would be identical to that given off by the obstacle at hand. We then conjecture that the local radius of curvature within this region of impact is that of the hypothetical cylinder. This technique is essentially of practical value and based on statistical average properties of the magnitude of the backscattered field, rather than on calculations shown to be inextricable.

The far scattered field, for a given plane wave incidence, is calculated at various aspect angles, via an integral equation, for the numerical solution of two dimensional diffraction problems, as reported in (43). In Fig. 8a, 8b, 8c and 8d, the magnitude of this field, and that obtained from a circular cylinder of identical curvature, are plotted versus the bistatic angle ϕ . One may notice that within a wedge angle less than $\pi/12$ from the specular point, $\phi = 180^\circ$, both curves coalesce; thus demonstrating the validity of our hypothesis.

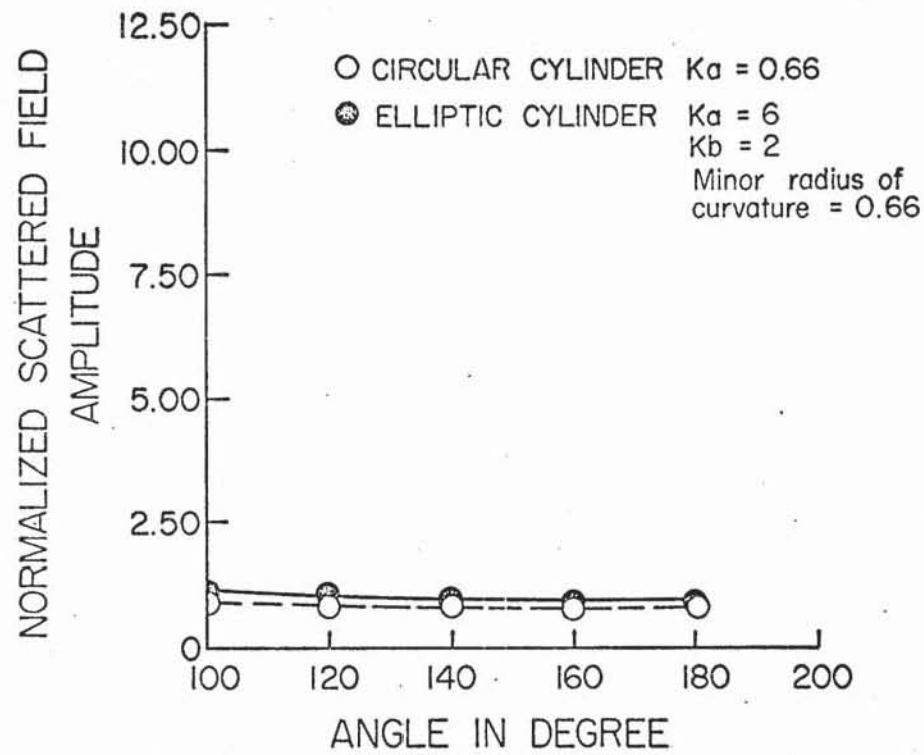


Fig. 8a Comparison of the Backscattered Field from an Elliptic Cylinder and a Circular Cylinder of Identical Radius of Curvature.

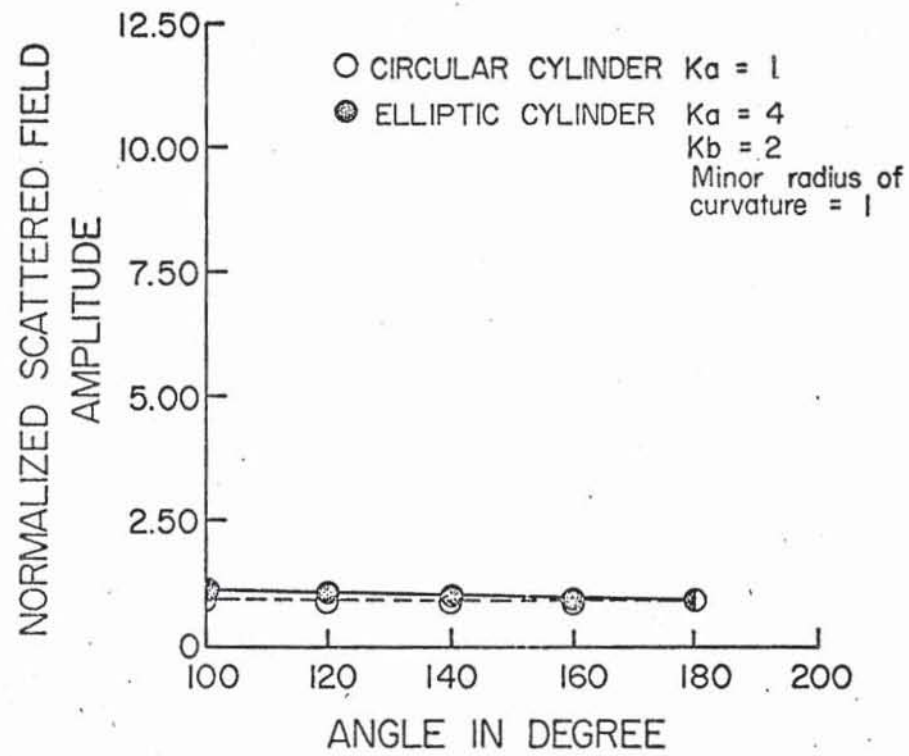


Fig. 8b Comparison of the Backscattered Field from an Elliptic Cylinder and a Circular Cylinder of Identical Radius of Curvature.

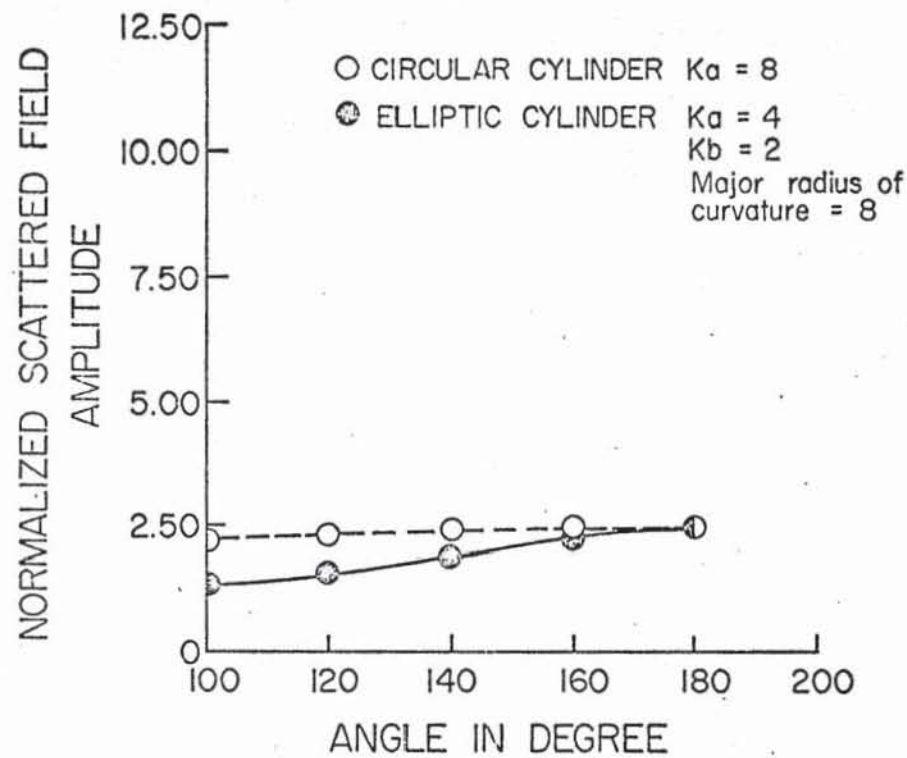


Fig. 8c · Comparison of the Backscattered Field from an Elliptic Cylinder and a Circular Cylinder of Identical Radius of Curvature.

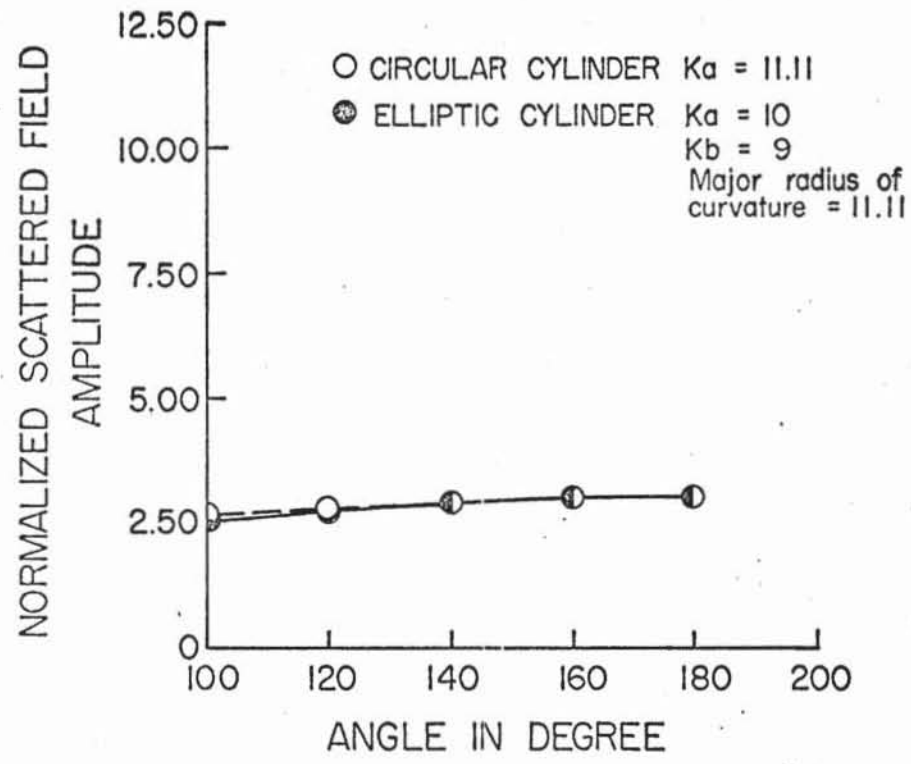


Fig. 8d Comparison of the Backscattered Field from an Elliptic Cylinder and a Circular Cylinder of Identical Radius of Curvature.

The technique consists, then, of selecting, at random, points within that domain of observation, and to compare the magnitude of the known scattered field, given off by the elliptic cylinder, and that of a hypothetical circular cylinder. This technique is described in detail in *chapter two*, section (2.7.2), where it is shown to be one of system analysis, where the system is constituted of the incident field, the scattered field and the scatterer. A merit factor has been defined as the difference between the sum of the magnitudes of the scattered field, evaluated at 'n' aspect angles, and the sum of the magnitudes of the scattered fields, given off by the circular cylinder at the same aspects. Although the set of 'n' aspect angles can be chosen at random, it has been though most convenient to use those obtained via the optimization procedure, as applied to a circular geometry. It is to be noted that only five aspect angles have been retained during this analysis, in order to have a number of points small enough to make the comparison and large enough to avoid the cancellation process in the averaging technique. With the knowledge of the merit factor, we can now proceed to use a refined subroutine in order to approximate more precisely the exact value of the radius of curvature (see section (2.7.2)).

This technique has been applied to retrieve the radius of curvature of elliptic cylinders of various sizes, whose electric axes ranged from 4 to 11. The results are presented in Table 7, where the first row gives the values of the larger radius of curvature of the generating ellipse as $(ka)^2/kb$ and the second row gives the values obtained with the iterative averaging technique. For this complete range, the exact values and our results are fairly consistent. It is also interesting to note that our values are always smaller than the exact values, and that this discrepancy seems to vary in the same way as does the eccentricity. This may be purely coincidental due to the technique employed in calculating the magnitudes of the various fields. However, the following point could be put forward as well: Since we have made use of a knowledge of the scattered field amplitude at various aspects about the specular point, at aspects where the radii of curvature are smaller, their contributions may slightly decrease the radius of curvature at the specular point. If such is the case, this discrepancy would be due to the scheme of the averaging technique. It is anticipated that this practical approach would then be adequate in order to recover the shape of smooth-curved bodies of revolution.

3.6 CONCLUSIONS

The inverse scattering model developed in *chapter two* is applied to the perfectly conducting elliptic cylinder whenever the scattered field components are known in amplitude, phase and polarization. However,

The technique consists, then, of selecting, at random, points within that domain of observation, and to compare the magnitude of the known scattered field, given off by the elliptic cylinder, and that of a hypothetical circular cylinder. This technique is described in detail in *chapter two*, section (2.7.2), where it is shown to be one of system analysis, where the system is constituted of the incident field, the scattered field and the scatterer. A merit factor has been defined as the difference between the sum of the magnitudes of the scattered field, evaluated at 'n' aspect angles, and the sum of the magnitudes of the scattered fields, given off by the circular cylinder at the same aspects. Although the set of 'n' aspect angles can be chosen at random, it has been though most convenient to use those obtained via the optimization procedure, as applied to a circular geometry. It is to be noted that only five aspect angles have been retained during this analysis, in order to have a number of points small enough to make the comparison and large enough to avoid the cancellation process in the averaging technique. With the knowledge of the merit factor, we can now proceed to use a refined subroutine in order to approximate more precisely the exact value of the radius of curvature (see section (2.7.2)).

TABLE 7: DETERMINATION OF THE ELECTRICAL AXES OF AN ELLIPTIC CYLINDER EMPLOYING THE ITERATIVE AVERAGING METHOD

Domain of Observation: $\frac{\pi}{6}$

	ka=3, kb=2	ka=4, kb=2	ka=5, kb=2	ka=6, kb=5	ka=10, kb=9
Larger Radius of Curvature	$\frac{9}{2} = 4.5$	$\frac{16}{2} = 8$	$\frac{25}{2} = 12.5$	$\frac{36}{5} = 7.5$	$\frac{100}{9} = 11.1$
Result	4.1	6.9	10.3	7.054	11.33

in contrast with the case of the perfectly conducting circular cylinder, it has not been possible to extract the parameters determining the geometrical features of the cylinder, due to the extreme sophistication of the Mathieu functions. The case of the circular cylinder has been rederived as a limiting case of the elliptic cylinder, when the eccentricity tends to zero, and found to be identical with the equation (2.2.10).

The analysis is then undertaken when the electrical axes ka and kb take large values. However, in this case, it is emphasized that the expansions of the associated expansion coefficients α_{2n} , γ_{2n+1} , etc., in terms of the Bessel functions, necessary to simplify the problem are extremely difficult to obtain. Even in the perspective where these asymptotic expansions were known, no information would be gained as regards the relative values of the electrical axes of the cylinder, because of the high frequency hypothesis. Therefore, such a derivative is not presented here, as it exceeds the scope of this dissertation.

Finally, the iterative averaging method, based on the dependence of the magnitude of the far scattered field upon the geometry of the local illuminated region of the scatterer, is employed. It gives excellent results for eccentricities varying from 0.08 to 0.98. This alternative method, independent of the phase information is anticipated to be well adapted for the retrieval of geometries of smooth convex shapes.

*chapter four*THE SPHERE4.1 INTRODUCTION

The sphere comes second only to the circular cylinder insofar as the simplicity of the relationship of the co-ordinate system to its boundary conditions is concerned. It is hence natural to study the "inverse scattering problem" of a sphere in a similar manner taken for the circular cylinder. Therefore, the principal method of attack for the mathematical solution of this inverse problem is a duplication of that developed at length for the cylinder. It is assumed, for instance, that all information relative to the salient features of the sphere is included in the associated expansion coefficients when the scattered field is formulated in terms of a series expansion in spherical wave functions. The only major difference between the study of the sphere and that of the circular cylinder results in the fact that the former is three-dimensional in nature while the latter is of the two-dimensional type. As for the circular cylinder, the prime objective of this chapter lies in the recovery of the electrical radius of the sphere, from bi-static measurement data for a given incidence plane wave.

This is carried out by calculating the associated expansion coefficients via the scattered field matrix inversion procedure. The instabilities inherent in this calculation are analysed in detail from the properties

of the determinant associated with the scattered field matrix⁽⁸⁾. An optimization procedure, similar to that derived for the circular cylinder, is employed to avoid these singularities and to determine the direction of the bistatic angles for which the accuracy of the retrieval of the associated coefficients is optimum.

4.2 MATRIX FORMULATION OF THE SCATTERED FIELD

It is assumed that for a given transmitted field, the measured far scattered field can be accurately obtained in amplitude, phase, and polarization for a sufficiently large number N of properly distributed bistatic angles $(\theta_c, \phi_c; c = 1, 2, \dots, N)$. The incident wave \underline{E} (of amplitude E_0 , and phase δ) is chosen to propagate in the direction of the negative \hat{z} -axis of a spherical co-ordinate system, whose origin is located at the center of the unknown scatterer. The polarization vector \hat{e}_t of the transmitted wave is parallel to the positive \hat{x} -axis. (Fig. 9) Eliminating the time dependence $\exp(-j\omega t)$,

$$\underline{E}_t = E_0 [\sin\theta \cos\theta \hat{R} + \cos\theta \cos\phi \hat{\theta} - \sin\phi \hat{\phi}] \exp j(\delta - kR\cos\theta) \quad (4.2.1)$$

For $E_0 = 1$ and $\delta = 0$, the scattered field of the c th receiver located at (R_c, θ_c, ϕ_c) may be represented by a series expansion in spherical vector wave functions

$$\begin{aligned} \underline{E}_c^S(R_c, \theta_c, \phi_c) = & \sum_{n=1}^{\infty} \sum_{m=0}^n \{ (j)^{n+1} a_{e_{mn}} \frac{M_{e_{mn}}}{o_{mn}}(R_c, \theta_c, \phi_c) \\ & + (j)^n b_{e_{mn}} \frac{N_{e_{mn}}}{o_{mn}}(R_c, \theta_c, \phi_c) \} \end{aligned} \quad (4.2.2a)$$

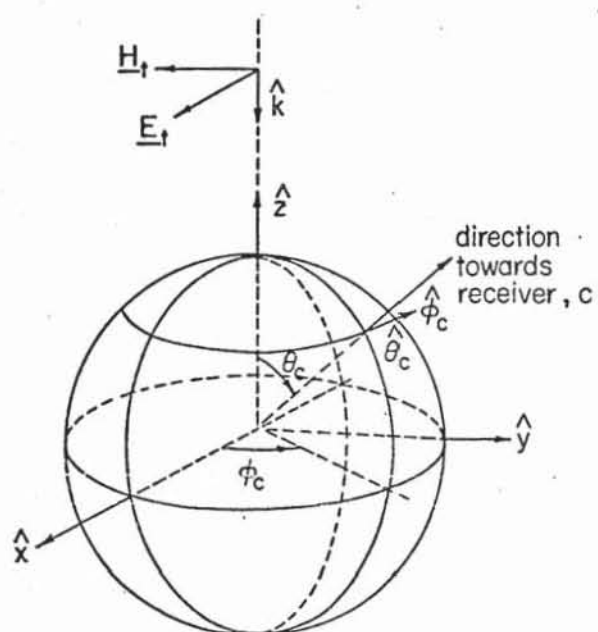


Fig. 9 Scattering Geometry for the Sphere.

The subscripts e and o respectively designate the even (cosine) and odd (sine) dependence on ϕ of the Mie series. Hansen's spherical vector wave functions as derived from the Mie series ⁽³⁴⁾ are defined by

$$\begin{aligned} \frac{M}{o} e_{mn} (R, \theta, \phi) = & \mp \{h_n^{(1)}(kR) {}^1G_n^m(\cos\theta) \frac{\sin(m\phi)}{\cos(m\phi)}\} \hat{\theta} \\ & - \{h_n^{(1)}(kR) {}^2G_n^m(\cos\theta) \frac{\cos(m\phi)}{\sin(m\phi)}\} \hat{\phi} \end{aligned} \quad (4.2.2b)$$

$$\begin{aligned} \frac{N}{o} e_{mn} (R, \theta, \phi) = & \left\{ \frac{n(n+1)}{(kR)} h_n^{(1)}(kR) P_n^m(\cos\theta) \frac{\cos(m\phi)}{\sin(m\phi)} \right\} \hat{R} \\ & + \{k_n^{(1)}(kR) {}^2G_n^m(\cos\theta) \frac{\cos(m\phi)}{\sin(m\phi)}\} \hat{\theta} \\ & \mp \{k_n^{(1)}(kR) {}^1G_n^m(\cos\theta) \frac{\sin(m\phi)}{\cos(m\phi)}\} \hat{\phi} \end{aligned} \quad (4.2.2c)$$

$$\begin{aligned} P_n^m(\cos\theta) = & (-1)^m \frac{\Gamma(n+m+1)}{\Gamma(n-m+1)} P_n^{-m}(\cos\theta) = (1 - \cos^2\theta)^{m/2} \\ & \cdot \left\{ \frac{d^m P_n(\cos\theta)}{d(\cos\theta)^m} \right\} \end{aligned} \quad (4.2.3a)$$

represent the associated Legendre's functions of the first kind and of degree m and order n , while $P_n(\cos\theta) = P_n^0(\cos\theta)$ are the ordinary Legendre's polynomials of order n given by

$$P_n(\cos\theta) = \frac{1}{2^n n!} \frac{d^n (\cos^2\theta - 1)^n}{d(\cos\theta)^n} \quad (4.2.3b)$$

${}^1G_n^m(\cos\theta)$ and ${}^2G_n^m(\cos\theta)$ are abbreviations for

$$\begin{aligned} {}^1G_n^m(\cos\theta) = & \frac{m}{\sin\theta} P_n^m(\cos\theta) = \{1/2 \cos\theta [(n-m+1)(n+m) P_n^{m-1}(\cos\theta) \\ & + P_n^{m+1}(\cos\theta)] + m \sin\theta P_n^m(\cos\theta)\} \end{aligned} \quad (4.2.3c)$$

$$Z_{G_n}^m(\cos\theta) = \frac{\partial \{P_n^m(\cos\theta)\}}{\partial \theta} = 1/2 \{(n-m+1)(n+m) P_n^{m-1}(\cos\theta) - P_n^{m+1}(\cos\theta)\} \quad (4.2.3d)$$

$h_n^{(1)}(kR)$ denotes the spherical Hankel function of the first kind given in terms of the cylindrical Hankel function by

$$h_n^{(1)}(kR) = \left(\frac{\pi}{2kR}\right)^{1/2} H_{n+1/2}^{(1)}(kR) \quad (4.2.4a)$$

and $k_n^{(1)}$ in (4.2.2c) is given by

$$k_n^{(1)}(kR) = \frac{1}{(kR)} - \frac{d}{dR} \{R h_n^{(1)}(kR)\} \quad (4.2.4b)$$

For a rotationally symmetric scattering body, the expansion coefficients

$a_{o_{mn}}^e$, $b_{o_{mn}}^e$ bear the following relationship with the expansion coefficients a_n^r , b_n^r given by Stratton for the special case of end-on incidence on a perfectly conducting sphere for which $m = 1$:

$$a_{o_{1n}}^e = j(-1)^{n+1} \frac{(2n+1)}{n(n+1)} a_n^r \quad a_n^r = -\frac{j_n(ka)}{h_n^{(1)}(ka)} \quad (4.2.5a)$$

$$b_{e_{1n}}^e = j(-1)^n \frac{(2n+1)}{n(n+1)} b_n^r \quad b_n^r = -\frac{[ka j_n(ka)]}{[ka h_n^{(1)}(ka)]} \quad (4.2.5b)$$

The ultimate aim is to recover a truncated number of the unknown expansion coefficients $a_{o_{mn}}^e$ and $b_{o_{mn}}^e$ employing matrix inversion techniques. This is accomplished by considering only the transverse electric field components of the scattered field, where the quantities $E_{\theta_c}^s(R_c, \theta_c, \phi_c)$ and $E_{\theta_c}^s(R_c, \theta_c, \phi_c)$, in practice, are obtained from far field measurements. Therefore, the radial dependence in (4.2.2b) and (4.2.2c) could be extracted by employing the asymptotic approximations

of the spherical Hankel functions

$$\lim_{(kR) \rightarrow \infty} \{h_n^{(1)}(kR)\} \approx (-j)^{n+1} \frac{\exp(jkR)}{(kR)}$$

and

$$\lim_{(kR) \rightarrow \infty} \{k_n^{(1)}(kR)\} \approx (-j)^n \frac{\exp(jkR)}{(kR)} \quad (4.2.6a)$$

resulting in

$$E_{\theta_c}^s(\theta_c, \phi_c) \approx \frac{\exp(jkR)}{(kR)} \sum_{n=1}^M \sum_{m=0}^n \{a_{e_{0mn}} {}^1G_{e_{0mn}}(\theta_c, \phi_c) + b_{e_{0mn}} {}^2G_{e_{0mn}}(\theta_c, \phi_c)\} \cdot \quad (4.2.6b)$$

$$E_{\phi_c}^s(\theta_c, \phi_c) \approx \frac{\exp(jkR)}{(kR)} \sum_{n=1}^M \sum_{m=0}^n \{-a_{e_{0mn}} {}^2G_{e_{0mn}}(\theta_c, \phi_c) + b_{e_{0mn}} {}^1G_{e_{0mn}}(\theta_c, \phi_c)\} \cdot \quad (4.2.6c)$$

where the spherical vector surface harmonics ${}^2G_{e_{0mn}}(\theta, \phi)$ and ${}^1G_{e_{0mn}}(\theta, \phi)$ are defined by

$${}^1G_{e_{0mn}}(\theta_c, \phi_c) = + {}^{-1}G_n^m(\cos\theta_c) \frac{\sin(m\phi_c)}{\cos(m\phi_c)} \quad (4.2.7a)$$

$${}^2G_{e_{0mn}}(\theta_c, \phi_c) = {}^2G_n^m(\cos\theta_c) \frac{\cos(m\phi_c)}{\sin(m\phi_c)} \quad (4.2.7b)$$

The order of truncation M is approximately determined by the electrical radius ka of the minimum sphere of radius a , enclosing the equivalent sources⁽⁶⁰⁾ of the scatterer in question. In particular, it was found⁽⁵⁴⁾ that for $m = 1$

$$n = M \approx (ka) + (ka)^{1/3} \quad (4.2.8)$$

Although the commonly employed far field approximation yields rather accurate results in practice, its application is not required to formulate the scattered field matrix, which is expressed only in terms of

the vector surface harmonics. Namely, instead of employing (4.2.6a), the radial dependence of the vector wave functions of (4.4.2b) and (4.4.2c) is combined with the expansion coefficients, where

$$a_{e_{mn}} = (j)^{n+1} h_n^{(1)}(kR) a_{e_{mn}} \quad (4.2.9a)$$

$$b'_{e_{mn}} = (j)^n k_n^{(1)}(kR) b_{e_{mn}} \quad (4.2.9b)$$

The accuracy of the transverse scattered field components will thus be limited only by the accuracy of measurement and truncation and not by having neglected terms of relative order $(kR)^{-1}$. Employing (4.2.9a) and (4.2.9b), the transverse scattered field is

$$\underline{E}_c^S(\theta_c, \phi_c) \approx \hat{\theta} E_{\theta_c}^S(\theta_c, \phi_c) + \hat{\phi} E_{\phi_c}^S(\theta_c, \phi_c) \quad (4.2.9c)$$

with

$$E_{\theta_c}^S(\theta_c, \phi_c) \approx \sum_{n=1}^M \sum_{m=0}^n \{ a'_{e_{mn}} {}^1G_{e_{mn}}(\theta_c, \phi_c) + b'_{e_{mn}} G_{e_{mn}}(\theta_c, \phi_c) \} \quad (4.2.9d)$$

$$E_{\phi_c}^S(\theta_c, \phi_c) \approx \sum_{n=1}^M \sum_{m=0}^n \{ -a'_{e_{mn}} {}^1G_{e_{mn}}(\theta_c, \phi_c) + b'_{e_{mn}} G_{e_{mn}}(\theta_c, \phi_c) \} \quad (4.2.9e)$$

These equations can be expressed in matrix form

$$[E] = [F] \cdot [X] \quad (4.2.10a)$$

where the transpose $[E]^T$ of the column matrix $[E]$ is given by

$$[E]^T = [E_{\theta_1}(\theta_1, \phi_1), E_{\theta_2}(\theta_2, \phi_2) \dots E_{\theta_N}(\theta_N, \phi_N), E_{\phi_1}(\theta_1, \phi_1), E_{\phi_2}(\theta_2, \phi_2), \dots E_{\phi_N}(\theta_N, \phi_N)] \quad (4.2.10b)$$

which consists of $2N$ complex elements, and so does the transpose $[X]^T$

of the column matrix $[X]$ which represents the unknown expansion coefficients. Since both $\{^1G_{on}(\theta, \phi)\} = 0$ and $\{^2G_{on}(\theta, \phi)\} = 0$, the corresponding expansion coefficients a_{on} and b_{on} must be eliminated, thus

$$[X]^T = [a_{e_{01}}, a_{e_{11}}, a_{o_{11}}, a_{e_{02}}, a_{e_{12}}, a_{o_{12}}, a_{e_{22}}, a_{o_{22}}, \dots, a_{e_{MM}}, a_{o_{MM}}, b_{e_{01}}, b_{o_{11}}, b_{e_{02}}, b_{o_{12}}, b_{e_{22}}, b_{o_{22}}, b_{e_{03}}, \dots, b_{e_{0M}}, b_{e_{1M}}, \dots, b_{e_{MM}}, b_{o_{MM}}] \quad (4.2.10c)$$

The relationship between N , the total number of non-identical aspect angles, and M , the order of truncation ($n = M$), therefore, is given for general m by

$$N = (M + 1)^2 - 1 = M(M + 2) \quad (4.2.10d)$$

Equation (4.2.10d) states that if all N existing expansion coefficients of the electric type $a_{e_{mn}}$ and all N existing expansion coefficients of the magnetic type $b_{o_{mn}}$ up to the order of truncation $n = M$ are to be determined, then N aspect angles are required with the associated set of N scattered field vectors $\underline{E}_c^S(\theta_c, \phi_c, c = 1, 2, \dots, N)$. With the chosen arrangements of the elements of column matrices $[E]$ and $[X]$, the arrangement of the elements of the scattered field matrix is determined as well. From inspection of (4.2.9d) and (4.2.9c), the scattered field matrix is represented by

$$[F] = \begin{bmatrix} [1_G] & [2_G] \\ [2_G] & [1_G] \end{bmatrix} \quad (4.2.11a)$$

$[F]$ is a matrix of order $2N = 2M(M + 2)$, whose submatrices $[^1G]$ and

2G are of order $N = M(M + 2)$ with elements defined by

$${}^1g_{\mu\nu} = {}^1G_{\underbrace{(e_{mn})}_v}(\theta_\mu, \phi_\mu) \quad \mu = c = 1, 2, \dots, N \quad (4.2.11b)$$

$${}^2g_{\mu\nu} = {}^2G_{\underbrace{(e_{mn})}_v}(\theta_\mu, \phi_\mu) \quad \mu = c = 1, 2, \dots, N \quad (4.2.11c)$$

and $v = (e_{mn})$ as determined by (4.2.10c).

Furthermore, since the spherical vector surface harmonics ${}^1G_{e_{mn}}(\theta, \phi)$ and ${}^2G_{e_{mn}}(\theta, \phi)$ are purely real quantities for real aspect angles, so is $[F]$ a purely real matrix for real aspect angles. Since for computational purposes the objective was to formulate a real matrix $[F]$, the expansion coefficients $a_{e_{mn}}$ and $b_{e_{mn}}$ are re-normalized in accordance with the definition of Stratton⁽⁴⁶⁾, which was shown by (4.2.5a) and (4.2.5b).

4.3 CLOSED FORM SOLUTION AND OPTIMIZATION OF THE DETERMINANT ASSOCIATED WITH THE MATRIX $[F_m]$

4.3.1 DECOMPOSITION OF THE DETERMINANT ASSOCIATED WITH $[F_m]$ INTO ITS POLAR AND AZIMUTHAL PARTS

The scattered field matrix $[F]$ for $m = \text{constant}$ and with $\hat{e}_t = \hat{x}_o$ is given by the equation:

$$[F_m] = \begin{bmatrix} [{}^1G_{om}] & [{}^2G_{em}] \\ [{}^2G_{om}] & [{}^1G_{em}] \end{bmatrix} \quad (4.3.1)$$

where the elements of the various submatrices are defined together with equations (4.2.7) and (4.2.10) by

$${}^1g_{\mu\nu}^{om} = {}^1G_{omn}(\theta_c, \phi_c) \Big|_{\substack{c = \mu \\ n = \nu+m-1}} = {}^1G_{m\nu}(\theta_\mu) \cos m\phi_\mu \quad (4.3.2)$$

$${}^1g_{\mu\nu}^{em} = {}^2G_{emn}(\theta_c, \phi_c) \Big|_{\substack{c = \mu \\ n = \nu+m-1}} = -{}^1G_{m\nu}(\theta_\mu) \sin m\phi_\mu \quad (4.3.3)$$

$${}^2g_{\mu\nu}^{em} = {}^2G_{emn}(\theta_c, \phi_c) \Big|_{\substack{c = \mu \\ n = \nu+m-1}} = {}^2G_{m\nu}(\theta_\mu) \cos m\phi_\mu \quad (4.3.4)$$

$${}^2g_{\mu\nu}^{om} = {}^2G_{omn}(\theta_c, \phi_c) \Big|_{\substack{c = \mu \\ n = \nu+m-1}} = {}^2G_{m\nu}(\theta_\mu) \sin m\phi_\mu \quad (4.3.5)$$

Inspection of (4.3.2) to (4.3.5) shows that the far scattered field matrix can be decomposed into the product of two matrices

$$[F_m] = [\phi_m(\phi_\mu)] \cdot [\Theta_m(\theta_\mu, \nu)] \quad (4.3.6)$$

where the premultiplied matrix $[\phi_m(\phi_\mu)]$ incorporates solely the azimuthal ϕ -dependence, and the post-multiplied matrix $[\Theta_m(\theta_\mu, \nu)]$ the polar θ -dependence expressed in terms of associated Legendre's functions.

$$4.3.2 \quad \underline{\text{DET } [\phi_m(\phi_\mu)]} = |\phi_m(\phi_\mu)|$$

It is demonstrated in Boerner and Vandenberghe⁽⁸⁾ that the determinant of $[\phi_m(\phi_\mu)]$ is given by:

$$|\phi_m(\phi_\mu)| = \frac{(-)^N}{2^N} \prod_{\mu=1}^N \sin 2m\phi_\mu \quad (4.3.7)$$

$$4.3.3 \quad \underline{\text{DET } [\Theta_m(\theta_{\mu, \nu})]} = |\Theta_m(\theta_{\mu, \nu})|$$

The derivation of a closed-form solution for the determinant $|\Theta_m(\theta_{\mu, \nu})|$ representing the polar dependence of the various multipole cases ($m = \text{constant} \geq 1$) is also derived in Boerner and Vandenberghe⁽⁸⁾. It is given by:

$$|\Theta_m(\theta_{\mu, \nu})| = \left[(-1)^{\frac{N(N-1)}{2}} \prod_{\nu=m+1}^{N+m-1} \frac{(\nu(2\nu-1)!!)}{(\nu-m)!} \right]^2 \cdot \prod_{\mu=1}^N \sin^{2m} \theta_{\mu} \cdot \prod_{\substack{N > r > s > 1}} (\cos \theta_r - \cos \theta_s)^2 \quad (4.3.8)$$

4.3.4 SUMMARY AND INTERPRETATION OF THE CLOSED-FORM SOLUTION OF THE DETERMINANT $|\underline{F_m(\theta_{\mu}, \phi_{\mu})}|$

The singular behaviour of these determinants can be formulated according to the following theorem.

THEOREM 1

The determinant $|F_m|$ of the far scattered field matrix $[F_m]$ associated with a vector scattering geometry representing the m th degree multipole case becomes singular for

$$i) \quad \phi_{\text{sing}} \frac{p\pi}{2m} : p = 0, \underline{+1}, \underline{+2}; m \geq 1$$

and attain its maximum value for

$$ii) \quad \phi_{\text{max}} \frac{(2p+1)}{4m} \pi : p = 0, \underline{+1}, \underline{+2}; m \geq 1$$

Furthermore, increasing pseudo-singular behaviour is encountered for multipole degree m if the aspect angles lie closely packed within narrow cones about the \hat{z} -axis, whose relative half angle θ_{MC} increases with increasing degree $m \geq 1$.

In general, the optimum distribution of the aspect angles (θ_c, ϕ_c) depends on the given number N of receiver locations, where the distribution of the polar dependence must be determined by employing optimization techniques for each separate case ($N = \text{constant}$, $M = \text{constant}$). Employing a novel optimization procedure for determinants of the type (4.3.8), the optimum distribution of aspect angles for general N and m will be derived and proved in the following section.

4.4 OPTIMIZATION PROCEDURE

The objective is to optimize the distribution of measurement angles, to ensure maximum value of the determinant $|F_m(\theta_\mu, \phi_\mu; N)|$, thus assuring the most stable inversion of the associated scattered field matrix $[F_m(\theta_\mu, \phi_\mu; N)]$ given by (4.2.11a). From inspection of (4.3.2), it is found that, for any of the m th degree multipole cases, the azimuthal ϕ and the polar θ dependence are independent of one another, thus greatly simplifying the optimization procedure. Whereas the optimization of the azimuthal ϕ dependence follows directly from inspection of (4.3.2) as $\phi_{\text{opt}} = \frac{2p+1}{4m} \pi$, the optimization of the polar θ dependence requires further detailed analysis.

Neglecting multiplicative constants in (4.3.8), the polar part of the determinant which needs to be optimized may then be formulated as:

$$|\Theta_m(N)| = \prod_{t=1}^N (1 - x_t^2)^m \prod_{\substack{N > r > s > 1}} (x_r - x_s)^2 = \left[\prod_{t=1}^N (1 - x_t^2)^{\frac{m}{2}} \prod_{\substack{N > r > s > 1}} (x_r - x_s) \right]^2 \quad (4.4.1)$$

with $x_r = \cos \phi_r$.

It suffices to optimize the expression in square brackets which is mirror symmetric about $x = 0$, and may, therefore, be reduced to

$$|\Theta_m(q = \frac{N}{2}, N \text{ even})| = \left[\prod_{t=1}^q (1 - x_t^2)^{\frac{m}{2}} x_t^{1/2} \prod_{\substack{q > r > s > 1}} (x_r^2 - x_s^2) \right]^4 \quad (4.4.2a)$$

$$|\Theta_m(q = \frac{N-1}{2}, N \text{ odd})| = \left[\prod_{t=1}^q (1 - x_t^2)^{\frac{m}{2}} x_t^{1/2} \prod_{\substack{q > r > s > 1}} (x_r^2 - x_s^2) \right]^4 \quad (4.4.2b)$$

Since in practice measurements may have to be compiled within a finite polar sector of limiting aspect angles θ_{m_a} , and $\theta_{m_b} > \theta_{m_a}$, as shown in Fig. 10, $|\Theta_m(q)|$ must be normalized if the optimal distribution of aspect angles within this range is sought. However, in contrast with the cylindrical case treated in *chapter two*, the two limiting measurement aspect angles θ_{m_a} and θ_{m_b} do not represent the limiting computational aspect angles θ_a and θ_b , since for $\theta_{m_a} = 0$ and $\theta_{m_b} = \pi$, $|\Theta_m(q)|$ is singular. This results from the fact that the weighting factor $\prod_{t=1}^N (1 - x_t^2)^m$ is encountered in (4.4.1) which was not the case for the cylindrical scattering geometry. However, to make optimal use of the given polar sector of measurement aspect angles, a computational co-ordinate system must now be introduced. This is achieved by en-

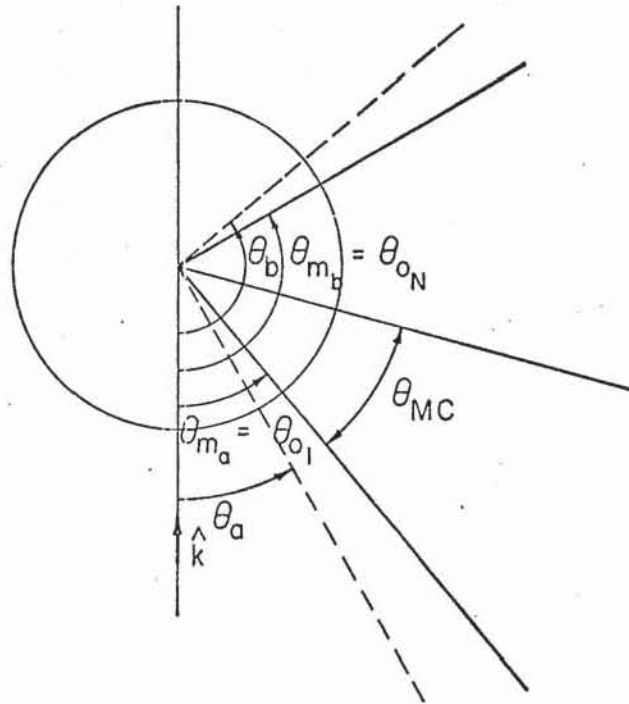


Fig. 10 Measurement Polar Angle used for the Geometries Representing the m th Degree Multipole Cases

larging the measurement polar sector to the limiting computational aspect angles α and β , where by introducing the optimization angles θ_{0_r} (θ_{0_r} ; $r = 1, 2, 3, \dots, N$) such that

$$\alpha < \theta_{m_a} = \theta_{0_1} < \theta_{0_2} < \dots < \theta_{0_r} < \dots < \theta_{0_N} = \theta_{m_b} < \beta \quad (4.4.3a)$$

and neither α nor β belong to the set of N optimization angles

(θ_{0_r} ; $r = 1, 2, 3, \dots, N$). The two exterior optimization angles θ_{0_1} and θ_{0_N} may then be associated with the two limiting measurement aspect angles θ_{m_a} and θ_{m_b} as:

$$\theta_{m_a} = \theta_{0_1} > \alpha \qquad \theta_{m_b} = \theta_{0_N} < \beta \quad (4.4.3b)$$

which is shown in Fig. 10, illustrating the computational co-ordinate system. This co-ordinate system is the same as that employed for the cylindrical case, where the limiting computational cosines are defined by:

$$\cos\alpha > \cos\theta_{m_a}, \qquad \cos\beta < \cos\theta_{m_b} \quad (4.4.3c)$$

The given cosines $x_r = \cos\theta_r$ of (4.4.2) are then normalized so that

$$u_r = \frac{x_r - \frac{(\cos\alpha + \cos\beta)}{2}}{\left| \frac{\cos\alpha - \cos\beta}{2} \right|} \quad \text{or} \quad x_r = u_r \left| \frac{\cos\alpha - \cos\beta}{2} \right| + \frac{(\cos\alpha + \cos\beta)}{2} \quad (4.4.3d)$$

which results in a symmetrical set of computational aspect angles.

Therefore,

$$\left| \theta_m \left(q = \frac{N}{2}, N \text{ even} \right) \right| = \left| \prod_{t=1}^q (1 - u_t^2)^{\frac{m}{2}} u_t^{1/2} \prod_{\substack{q>r>s>1 \\ s=1}} (u_r^2 - u_s^2) \right|^4 \quad (4.4.4a)$$

$$|\theta_m (q = \frac{N-1}{2}, N \text{ odd})| = \left| \prod_{t=1}^q (1 - u_t^2)^{\frac{m}{2}} u_t^{3/2} \cdot \underbrace{\prod_{q>r>s>1} (u_r^2 - u_s^2)} \right|^4 \quad (4.4.4b)$$

where $u_0(x_0 = \cos\alpha) = +1$ and $u_{N+1}(x_{N+1} = \cos\beta) = -1$. The u_r are arranged so that $u_r > u_{s_1} > u_{s_2} > \dots > u_{s_{q-1}}$, where the relationship between $\cos\alpha$, $\cos\beta$, $\cos\theta_{m_a}$, $\cos\theta_{m_b}$, u_{m_a} and u_{m_b} is derived from interpretation of the solution.

In Part B, it is demonstrated that the roots of

$$O_N^m(u_r) = \frac{1}{(1 - u_r^2)^{\frac{m-1}{2}}} P_{N+m-1}^{m-1}(u_r) \quad (4.4.5)$$

represent the optimum distribution of u_r , where P_{N+m-1}^{m-1} represents the associated Legendre function of the first kind and $(m-1)$ degree and order $(N+m-1)$ as defined in Jahnke and Emde⁽¹⁶⁾. It is to be noted that for $m=2$, equation (4.4.5) is identical with the expression obtained for the circular case (see equation (2.3.5)). Furthermore, it is observed that for the higher order multipole case, i.e. $m \geq 2$, the optimization cosines $u_r = \pm 1$ are removed in (4.4.5) which complies with (4.4.3a). Although the two limiting computational cosines $\cos\alpha > \cos\theta_{m_a} = \cos\theta_{0_1}$ and $\cos\beta < \cos\theta_{m_b} = \cos\theta_{0_N}$ were not known *a priori*, it is possible to specify those for the given limiting measurement aspect angles θ_{m_a} and θ_{m_b} . Namely, assuming that m and N , the total number of measurement aspect angles θ_{m_p} , is given, then the two exterior optimization cosines, u_{0_1} and $u_{0_N} = -u_{0_1}$ can be obtained from (4.4.5). Since by definition of (4.4.3c), the associated measurement aspect angles of u_{0_1} and u_{0_N} are the limiting measurement aspect angles $\theta_{m_a} =$

θ_{0_1} and $\theta_{m_b} = \theta_{0_N}$, the unknown normalization factors can be defined as

$$\left| \frac{\cos\alpha - \cos\beta}{2} \right| = \frac{x_{m_a} - x_{m_b}}{2u_{0_1}}, \quad \begin{cases} x_{m_a} = \cos\theta_{m_a} \\ x_{m_b} = \cos\theta_{m_b} \end{cases} \quad (4.4.6a)$$

and

$$\left| \frac{\cos\alpha + \cos\beta}{2} \right| = \frac{x_{m_a} + x_{m_b}}{2u_{0_1}} \quad (4.4.6b)$$

It is to be noted that $\left| \frac{\cos\alpha - \cos\beta}{2} \right|$ must always be less than or equal to unity and therefore (4.4.6a) cannot be satisfied in all cases, i.e. for example if $x_{m_a} = +1$ and $x_{m_b} = -1$, which indicates that the optimum distribution of aspect angles within a limited polar sector of measurement may not employ the total range given. The optimization procedure is summarized in the following theorem:

THEOREM 2

The optimum distribution for the polar θ dependence of the N measurement aspect angles involved in the formulation (4.3.8) of the determinant $|F_m(N)|$ is given by the N zeros of the optimization function

$$O_N^m(u_r) = \frac{1}{(1 - u_r^2)^{\frac{m-1}{2}}} P_{N+m-1}^{m-1}(u_r) \quad (4.4.5)$$

$$u_r = \frac{x_r - \frac{(\cos\alpha + \cos\beta)}{2}}{\left| \frac{\cos\alpha - \cos\beta}{2} \right|}, \quad x_r = \cos\theta_r$$

If measurements are confined to a finite range of the polar θ -dependence, the limiting computational aspect angles θ_a and θ_b are defined by (4.4.6).

These properties are illustrated in Figs. 11 and 12, representing a vector scattering geometry associated with the first multipole case, for transmitter-receiver configurations which may occur in practice most frequently. For both considered cases, the N receiver aspect angles are assumed to be distributed within a narrow cone whose invariant axis \hat{a} is oriented in Fig. 11 along and in the same direction as the positive \hat{z} -axis and in Fig. 12 perpendicular to the back scattering direction. For simplicity, it is assumed that $\phi_r = (2p + 1)\frac{\pi}{4}$; $p = \underline{+1}, \underline{+2}$ and main attention will be concentrated on the polar θ -dependence.

The determinant associated with the configuration of Fig. 11 tends to become pseudo-singular if a large number of aspect angles are involved; whereas, the second configuration constitutes the optimum choice as regards the orientation of the invariant axis \hat{a} . Computational results employing (4.4.5) are not given here since detailed analysis is presented for the similar cylindrical case in *chapter two*.

Therefore, it is anticipated that the unknown expansion coefficients a_n and b_n can be obtained with standard double precision matrix inversion techniques, if the half angle θ_{MC} of the measurement cone is sufficiently large and the distribution of aspect angles satisfies the conditions of Theorems 1 and 2.

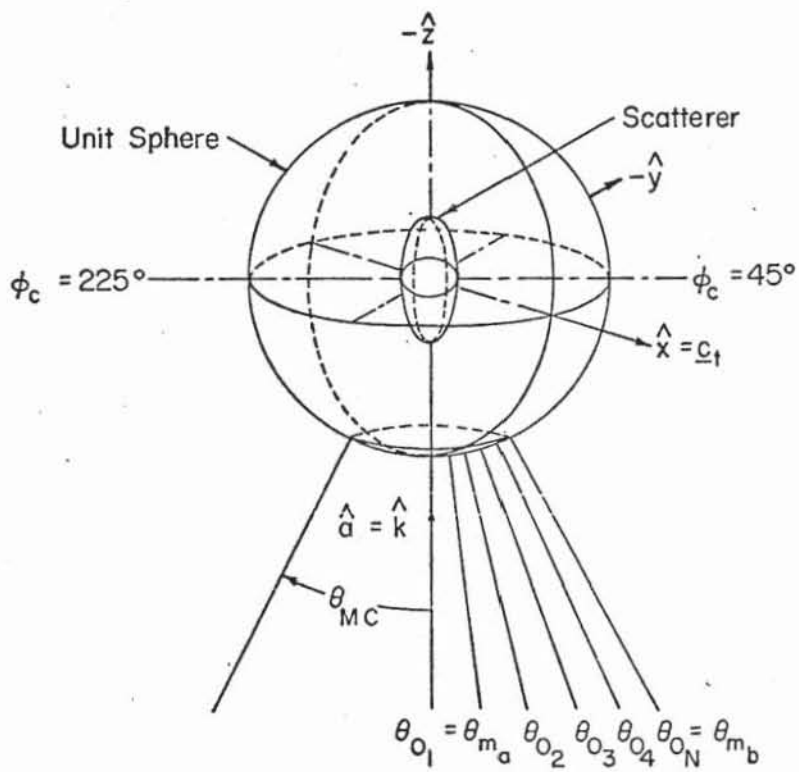


Fig. 11 "Pseudo-Singular" Distribution of Aspect Angles

4.5 DETERMINATION OF THE EQUIVALENT RADIUS OF CURVATURE OF THE SPHERE

4.5.1 INTRODUCTION

In the previous sections, it has been shown how the sufficient sets of expansion coefficients a_n and b_n are recovered via a matrix inversion procedure from the optimal measured set of far scattered field data. If these sets are sufficient to express the far scattered field, they should regenerate the near field to some approximation if the initial expansions of (4.2.2) are employed⁽⁵⁵⁾. We could then proceed to recover the shape of the unknown, perfectly conducting, scatterer by employing inverse scattering boundary conditions⁽⁵⁵⁾ or methods of analytical continuation^(55, 32, 30, 31). However, it may be argued that all the information required for the retrieval of "ka" is explicitly contained in the set of expansion coefficients for $m = \text{const} = 1$ $\{a_n, b_n; 0 \leq n \leq N\}$, implying that "ka" could be directly recovered from $\{a_n, b_n; 0 \leq n \leq N\}$ without requiring any other information. This follows from the definition of a_n and b_n and from the recurrence relationships between three contiguous radial functions. Since such recurrence expressions for the determination of ka are derived in detail in *chapter two* for the cylindrical case, relationships for the spherical case will now be presented in a comprehensive manner.

4.5.2 DERIVATION

Instead of employing the definitions of $a_{0_{1n}}$ and $b_{0_{1n}}$ given in (4.2.5), we will use those of Stratton⁽⁴⁶⁾, for convenience

$$a_n = - \frac{j_n}{h_n^{(1)}} \quad (4.5.1a)$$

$$b_n = - \frac{[\rho j_n]'}{[\rho h_n^{(1)}]'} = - \frac{[\rho j_{n-1} - n j_n]}{[\rho h_{n-1}^{(1)} - n h_n^{(1)}]} = - \frac{[(n+1) j_n - \rho j_{n+1}]}{[(n+1) h_n^{(1)} - \rho h_{n+1}^{(1)}]} \quad (4.5.1b)$$

where arguments are omitted and $\rho = ka$ is the electrical radius of the sphere. The two alternative representations of (4.5.1b) are then obtained from the existing recurrence relations of spherical radial functions⁽¹⁾.

$$z_n = \frac{\rho}{2n+1} (z_{n-1} + z_{n+1}) \quad (4.5.2a)$$

$$z_n' = \frac{1}{2n+1} [n z_{n-1} - (n+1) z_{n+1}] \quad (4.5.2b)$$

$$[\rho z_n]' = (n+1) z_n - \rho z_{n+1} = \rho z_{n-1} - n z_n \quad (4.5.2c)$$

An expression is obtained for the determination of "ka" employing both a_n and b_n by substituting (4.5.1a) into (4.5.1b), where

$$\rho = \frac{n(b_n - a_n) h_n^{(1)}}{(b_n - a_{n-1}) h_{n-1}^{(1)}} \quad (4.5.3a)$$

$$\text{or} \quad \rho = \frac{(n+1) (b_n - a_n) h_n^{(1)}}{(b_n - a_{n+1}) h_{n+1}^{(1)}} \quad (4.5.3b)$$

and therefore

$$\frac{h_{n+1}^{(1)}}{h_{n-1}^{(1)}} = \frac{(n+1)}{n} \frac{(b_n - a_{n-1})}{(b_n - a_{n+1})} \quad (4.5.4a)$$

$$\text{or } \frac{j_{n+1}}{j_{n-1}} = \frac{a_{n+1}}{a_{n-1}} \frac{(b_n - a_{n-1})}{(b_n - a_{n+1})} \frac{(n+1)}{n} \quad (4.5.4b)$$

Multiplying the expression of (4.5.3a) for $n = \nu$ with that of (4.5.3b) for $n = \nu - 1$ yields

$$\rho^2 = \nu^2 \frac{(b_\nu - a_\nu)(b_{\nu-1} - a_{\nu-1})}{(b_\nu - a_{\nu-1})(b_{\nu-1} - a_\nu)} \quad (4.5.5)$$

which, except for the multiplier ν^2 , is identical in form to the determinate expression obtained for the cylindrical mixed TE-TM case, which requires only two contiguous expansion coefficients of each kind and of the same order.

Similarly to the cylindrical case, it is also possible to recover "ka" exclusively from the a_n and/or the b_n coefficients in the spherical case. The expression associated with the a_n coefficients results from (4.5.2a) and (4.5.1a), since

$$j_n = -a_n h_n^{(1)} = -\frac{a_n \rho}{2n+1} (h_{n+1}^{(1)} + h_{n-1}^{(1)}) = -\frac{\rho}{2n+1} (a_{n+1} h_{n+1}^{(1)} + a_{n-1} h_{n-1}^{(1)}) \quad (4.5.6a)$$

thus

$$\frac{h_{n+1}^{(1)}}{h_{n-1}^{(1)}} = \frac{a_{n-1} - a_n}{a_n - a_{n+1}} \quad (4.5.6b)$$

and

$$\rho = (2n + 1) \frac{(a_n - a_{n-1}) h_n^{(1)}}{(a_{n+1} - a_{n-1}) h_{n+1}^{(1)}} \quad (4.5.6c)$$

Multiplying the expression of (4.5.6c), which results for $n = \nu$, $n = \nu - 1$, and substituting (4.5.6b) yields

$$\rho^2 = (2\nu - 1)(2\nu + 1) \frac{(a_{\nu+1} - a_\nu)(a_{\nu-1} - a_{\nu-2})}{(a_{\nu+1} - a_{\nu-1})(a_\nu - a_{\nu-2})} \quad (4.5.7)$$

which, except for the multiplier $(2\nu - 1)(2\nu + 1)$, is again identical in form to the expression obtained for the cylindrical TM case, requiring only four contiguous expansion coefficients $\nu \geq 2$ in (4.5.7).

However, as in the cylindrical case, no expression similar to (4.5.5) and (4.5.7) exists for expressing $\rho = ka$ in terms of a limited number of contiguous coefficients b_n . This results from the fact that no recurrence relationship between three contiguous derivatives of the form $|\rho z_n(\rho)|'$ exists. This can be verified by equating (4.5.4b) and (4.5.6b) leading to

$$b_n = \frac{n a_{n+1} (a_n - a_{n-1}) - (n+1) a_{n-1} (a_{n+1} - a_n)}{n (a_n - a_{n-1}) - (n+1) (a_{n+1} - a_n)} \quad (4.5.8a)$$

or

$$a_{n+1} = \frac{n b_n (a_n - a_{n-1}) + (n+1) a_n (b_n - a_{n-1})}{(n+1) (b_n - a_{n-1}) + n (a_n - a_{n-1})} \quad (4.5.8b)$$

In other words, one b_n coefficient can be expressed in terms of three contiguous a_ν coefficients for any order of n , whereas a similar inverse relationship of one coefficient a_n cannot possibly be expressed in terms of a limited number of contiguous b_ν for any n . Thus, to

determine exclusively "ka" from (4.5.5) or (4.5.7) in terms of b_ν coefficients, at least two contiguous a_ν coefficients, i.e. a_0 and a_1 , must be independently related to a finite number of b_ν employing degenerate relations of spherical radial functions not used up until this point. The first relationship is given for the degenerate case $n = 0$ which follows from the definitions⁽¹⁾ of

$$j_0(\rho) = \frac{\sin \rho}{\rho}, \quad y_0(\rho) = -\frac{\cos \rho}{\rho}, \quad j_1(\rho) = \frac{\sin \rho}{\rho^2} - \frac{\cos \rho}{\rho},$$

$$Y_1(\rho) = -\frac{\cos \rho}{\rho^2} - \frac{\sin \rho}{\rho}$$

where

$$a_0 = -\frac{j_0}{h_0^{(1)}} = \frac{1}{j \cot \rho - 1} \quad \text{and} \quad b_0 = -\frac{j_0 - \rho j_1}{h_0^{(1)} - \rho h_1^{(1)}} = -\frac{1}{1 + j \tan \rho}$$

and therefore

$$a_0 = -(1 + b_0) \quad (4.5.9)$$

It is to be noted that it was shown in *chapter two* that this expression can be employed, in terms of cylindrical functions in the cylindrical case as an approximation if $\rho > 3$, whereas in the spherical case, it is an exact relationship. The second degenerate relationship, required for a_1 , involves the resolution of two quadratic equations in a_1 which can be obtained simply from (4.5.5). The first equation is obtained by equating (4.5.5) for $\nu = 1$ and $\nu = 2$.

$$\frac{(b_1 - a_1)(b_0 - a_0)}{(b_1 - a_0)(b_0 - a_1)} = 4 \frac{(b_2 - a_2)(b_1 - a_1)}{(b_2 - a_1)(b_1 - a_2)} \quad (4.5.10)$$

Adopting the notation $b_{\mu\nu} = b_\mu - b_\nu$ which satisfies the transformation identity

$$b_{rs} b_{uv} = b_{ru} b_{sv} + b_{rv} b_{us} \quad (4.5.11)$$

and employing (4.5.8b) and (4.5.9), (4.5.10a) can be arranged as

$$\begin{aligned} & \{(b_1 - a_1)^2 [2b_{21} - b_{10} + 3(b_1 + b_0 + 1)] + \\ & (b_1 - a_1) [4b_{10} - 5b_{21} - 3b_{21}b_{10}] + 6(b_1 + b_0 + 1) [b_{21}b_{10}]\} = \\ & (b_1 - a_1)^2 L_1 + (b_1 - a_1) M_1 + N_1 = 0 \end{aligned} \quad (4.5.10b)$$

The second expression results from equating (4.5.5) for $v = 2$ and $v = 3$

$$4 \frac{(b_2 - a_2)(b_1 - a_1)}{(b_2 - a_1)(b_1 - a_2)} = 9 \frac{(b_3 - a_3)(b_2 - a_2)}{(b_3 - a_2)(b_2 - a_3)} \quad (4.5.12a)$$

which with successive application of (4.5.8a), (4.5.9) and (4.5.11)

reduces to

$$\begin{aligned} & \{(b_1 - a_1)^2 [10(b_1 + b_0 + 1)^2 - (b_1 + b_0 + 1)(10b_{32} + b_{31}) - 2b_{31}b_{21}] \\ & + (b_1 - a_1) b_{31} (b_1 + b_0 + 1) [21(b_1 + b_0 + 1) + 3b_{21}] + \\ & 9(b_1 + b_0 + 1)^2 b_{21} b_{31}\} = 0 \\ & = (b_1 - a_1)^2 L_2 + (b_1 - a_1) M_2 + N_2 = 0 \end{aligned} \quad (4.5.12b)$$

The system of two quadratic equations (4.5.10b) and (4.5.12b) in a_1 has the unique solution

$$a_1 = b_1 + \frac{L_1 N_2 - N_1 L_2}{L_1 M_2 - M_1 L_2} \quad (4.5.13)$$

where the constant multipliers in b_v of (4.5.10b) and (4.5.12b) are abbreviated for the sake of convenient representation.

Thus, it is found that the electrical radius can be determined from either a mixed set of four contiguous coefficients a_n and b_n with (4.5.5); exclusively from any four contiguous coefficients a_n with (4.5.9), or with (4.5.8b) and (4.5.13) from the entire set of coeffi-

icients b_n required for the particular order of n used in either (4.5.5) or (4.5.9).

4.5.3 COMPUTATION OF ka FROM THE EXACT VALUES OF THE a_n AND b_n COEFFICIENTS

In Table 9, computed results are presented for the determination of the electrical radius in the particular spherical cases $ka = 1.00$, 5.00 and 10.00 employing the relationships for either the mixed a_n/b_n , the a_n and the b_n cases. The accuracy of the results based on (4.5.9), (4.5.13) and (4.5.8b) depends exclusively on the accuracy of the expansion coefficients a_n and b_n which have been calculated with six digit accuracy. In Table 8, the coefficients a_0 and a_1 are calculated from the required set of b_n coefficients as given by (4.5.9) and (4.5.13).

4.6 CONCLUSIONS

An electromagnetic inverse scattering model technique has been presented for the case of perfectly conducting spherical scatterers employing an expansion of the scattered field in spherical vector wave functions. Although the approach is not as generally applicable as compared to those of Weston, Bowman and Ar⁽⁵⁷⁾, or Mittra and Imbriale⁽³¹⁾, some quite fundamental relations have been derived.

The determinant associated with the scattered field matrix, which relates a finite set of transverse scattered field components to the

TABLE 8: EXPANSION COEFFICIENT a_0 AND a_1 AS GIVEN BY (4.5.9)
AND BY (4.5.13)

$$a_0 \equiv - [1 + b_0] = - \frac{j_0(ka)}{h_0^{(1)}(ka)} ; \quad a_1 \equiv b_1 + \frac{L_1 N_2 - N_1 L_2}{L_1 M_2 - M_1 L_2} = - \frac{j_1(ka)}{h_1^{(1)}(ka)}$$

ka	a_0 [Real]	a_0 [Imag.]	a_1 [Real]	a_1 [Imag.]
1.0	-0.708073	-0.454649	-0.453516	-0.208074
5.0	-0.919536	-0.272011	-0.217355	-0.412446
10.0	-0.295959	-0.456473	-0.609610	-0.487838

TABLE 9: DETERMINATION OF ka FOR THE TM, TM-TE AND TE CASES

$$\rho_{TM} = (2_n - 1) (2_n + 1) \frac{(a_{n+1} - a_n) (a_{n-1} - a_{n-2})}{(a_{n+1} - a_{n-1}) (a_n - a_{n-2})} ;$$

$$\rho_{TM-TE} = n^2 \frac{(b_n - a_n) (b_{n-1} - a_{n-1})}{(b_n - a_{n-1}) (b_{n-1} - a_n)}$$

$\rho_{TE} = \rho_{TM-TE}$ where a_n is computed from (4.5.9), (4.5.13) and (4.5.8b).

	n	ρ_{TM}		ρ_{TM-TE}		ρ_{TE}	
$ka = 1.0$	2	1.000	-0.84×10^{-7}	1.000	0.18×10^{-6}	1.000	0.18×10^{-6}
	3	1.000	-0.11×10^{-7}	1.000	0.18×10^{-8}	1.000	0.18×10^{-8}
	4	1.000	-0.34×10^{-9}	1.000	0.36×10^{-10}	1.000	-0.36×10^{-10}
	5	1.000	0.0	1.000	0.0	1.000	0.0
	$ka = 5$	4	5.000	-0.31×10^{-6}	5.000	0.91×10^{-7}	5.000
5		5.000	0.67×10^{-6}	5.000	-0.25×10^{-6}	5.000	-0.25×10^{-6}
6		5.000	-0.62×10^{-6}	5.000	0.96×10^{-6}	5.000	0.96×10^{-6}
7		5.000	-0.94×10^{-7}	5.000	0.94×10^{-7}	5.000	0.94×10^{-7}
8		5.000	-0.11×10^{-7}	5.000	-0.59×10^{-8}	5.000	-0.59×10^{-8}
$ka = 10$	7	10.000	0.66×10^{-6}	10.000	0.32×10^{-5}	10.000	0.32×10^{-5}
	8	10.000	-0.62×10^{-6}	10.000	-0.13×10^{-5}	10.000	-0.13×10^{-5}
	9	10.000	0.47×10^{-7}	10.000	-0.13×10^{-5}	10.000	-0.13×10^{-5}
	10	10.000	-0.13×10^{-5}	10.000	0.19×10^{-6}	10.000	0.19×10^{-6}
	11	10.000	0.11×10^{-5}	10.000	0.14×10^{-5}	10.000	0.14×10^{-5}
	12	10.000	0.73×10^{-6}	10.000	0.37×10^{-6}	10.000	0.37×10^{-6}
	13	10.000	-0.95×10^{-7}	10.000	-0.14×10^{-6}	10.000	-0.14×10^{-6}

truncated set of unknown expansion coefficients has been analysed in terms of its singularities. The analysis then proceeds in employing the optimization procedure as derived at length in *chapter six*. In particular, the proper distribution of the aspect angles is derived for which the degree of accuracy on the recovery of the expansion coefficients is only dictated by the order of truncation of the scattered field series expansion and the employed measurement technique. This is summarized in Theorems 1 and 2 which establish basic measurement requirements. For example, in order to obtain optimum accuracy in the recovered expansion coefficients, the scattered field must be measured in a finite equatorial belt over the unit sphere of direction as regards the computational co-ordinate system. This is illustrated in Fig. 12. This also agrees with the mono-bistatic equivalence theorem⁽²²⁾. An expansion of the scattered field in vector spherical wave functions is then justified within this belt. This is not true, however, if the measurement aspect angles lie within a narrow cone of the unit sphere of directions which centers around the \hat{z} -axis as shown in Fig. 11.

Finally, the electrical radius " ka " of the sphere has been directly recovered from either the magnetic and/or the electric type expansion coefficients. The results presented here are valid for any region of space although measurement data are usually obtained in the far field.

This retrieval does not apply inverse boundary conditions⁽⁵⁵⁾ or methods of analytical continuation⁽³⁰⁾ and should be valuable to anyone interested in this area.

*chapter five*THE PROLATE SPHEROID5.1 INTRODUCTION

The problem of recovering the salient features of a perfectly conducting prolate spheroid illuminated by a plane wave is considered to illustrate the inverse scattering model theory as previously developed for the circular cylinder and the sphere. In this model theory, the transverse scattered field is expressed in terms of a truncated series expansion of the associated wave functions. Then the unknown expansion coefficients are recovered from the bistatic scattered field data by employing a matrix inversion procedure.

Although the direct problem has received rigorous treatment by classical methods^(41, 18, 27), there is, to our understanding, no numerical data on the total scattered field (amplitude, phase and polarization) because of a shortage of tables of spheroidal functions. Therefore, for this geometry, the following analysis is purely theoretical and no computation is carried out.

Instead of directly employing an expansion in spheroidal wave functions, the following development is based upon an alternative expansion of the scattered field as given by Senior⁽⁴²⁾. That representation was first introduced by Stevenson⁽⁴⁵⁾, who expanded the scattered field

as a power series in the propagation constant k using a formulation in vector spherical wave functions. Employing these results, it is shown that the characteristic features of the prolate spheroid can be recovered from Senior's coefficients providing the leading term in a low-frequency expansion of the scattered field. These coefficients are related to the transverse far scattered field via a matrix which is identical to that encountered in *chapter four* for the non-symmetrical spherical cases. Using the same optimization and matrix inversion procedures, these coefficients are recovered from the far scattered field to an accuracy only dictated by any suitable measurement technique. Expressions for the interfocal distance d and the eccentricity $\epsilon = 1/\epsilon_0$ of the ellipse, generating the prolate spheroid, are then derived from these coefficients employing properties of the associated Legendre's functions of the first and the second kind.

5.2 MATRIX FORMULATION OF THE SCATTERED FIELD

In the course of examining Senior's results⁽⁴²⁾ for a prolate spheroid, a form of presentation was discovered which relates the far scattered field with the associated expansion coefficients, which depend implicitly on the principal axes of the prolate spheroid. In order to formulate the scattered field matrix, Senior's solution is briefly reviewed. He considered plane wave incidence, given by

$$\underline{E}_i = (\ell_1, m_1, n_1) \cdot \exp[jk(\ell x + m y + n z)] \quad (5.2.1a)$$

$$\text{and } \underline{H}_i = \sqrt{\frac{\epsilon_0}{\mu_0}} \cdot (\ell_2, m_2, n_2) \cdot \exp[jk(\ell x + m y + n z)] \quad (5.2.1b)$$

where the three orthogonal set of direction cosines (l_1, m_1, n_1) , (l_2, m_2, n_2) and (l, m, n) express the directions of the incident electric and magnetic fields and the propagation vector \underline{k} , respectively.

The perfectly conducting prolate spheroid is defined by the equation

$$\frac{x^2}{\xi_0^2 + 1} + \frac{y^2}{\xi_0^2} + \frac{z^2}{\xi_0^2} = d^2 \quad (5.2.2)$$

where d represents the interfocal distance and $\epsilon = 1/\xi_0$ defines the eccentricity ellipse of the spheroid. This is shown in Fig. 13 illustrating the case of nose-on incidence on a perfectly conducting prolate spheroid.

Senior then showed that the transverse far scattered field components can be expressed as

$$E_\theta = \left(\frac{\partial P}{\partial \theta} + \frac{1}{\sin \theta} \cdot \frac{\partial \bar{P}}{\partial \theta} \right) \frac{e^{jkR}}{R} \quad (5.2.3a)$$

$$E_\phi = \left(\frac{1}{\sin \theta} \frac{\partial P}{\partial \phi} - \frac{\partial \bar{P}}{\partial \theta} \right) \frac{e^{jkR}}{R} \quad (5.2.3b)$$

where (R, θ, ϕ) are the spherical co-ordinate parameters of the observation point. Retaining only the leading term in a low frequency expansion, P and \bar{P} are given by

$$P = k^2 [(K_1 \cos \phi + K_2 \sin \phi) \sin \theta + K_3 \cos \theta] + O(k^4) \quad (5.2.4a)$$

$$\bar{P} = k^2 [(\bar{K}_1 \cos \phi + \bar{K}_2 \sin \phi) \sin \theta + \bar{K}_3 \cos \theta] + O(k^4) \quad (5.2.4b)$$

where K_j and \bar{K}_j ($j = 1, 2, 3$) are implicit functions of the geometrical parameters d and ξ_0 of the spheroid. This aforementioned formulation is valid only in a low frequency range, or equivalently for large

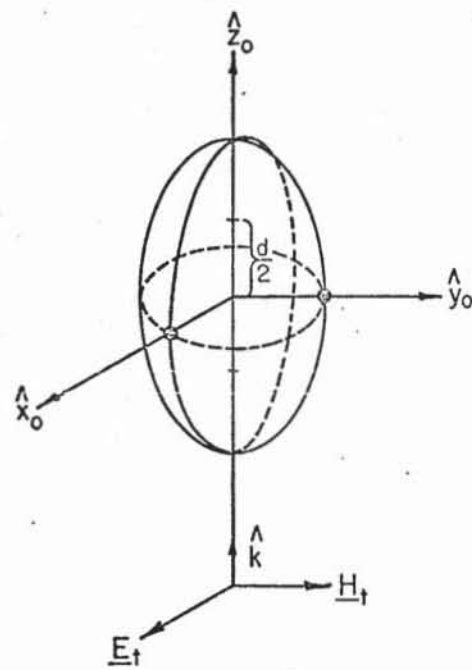


Fig. 13 Prolate Spheroid Scattering Geometry for Nose-On Incidence

dimension bodies. Following Senior⁽⁴²⁾, the coefficients K_j and \bar{K}_j can be expressed in terms of the Legendre polynomials as

$$\begin{aligned} K_1 &= -\frac{2}{3} d^3 \cdot \ell_1 \cdot \frac{P_1^1(\xi_0)}{Q_1^1(\xi_0)} & \bar{K}_1 &= -\frac{2}{3} d^3 \cdot \ell_2 \cdot \frac{P_1^1(\xi_0)'}{Q_1^1(\xi_0)'} \\ K_2 &= -\frac{2}{3} d^3 \cdot m_1 \cdot \frac{P_1^1(\xi_0)}{Q_1^1(\xi_0)} & \bar{K}_2 &= -\frac{2}{3} d^3 \cdot m_2 \cdot \frac{P_1^1(\xi_0)'}{Q_1^1(\xi_0)'} \\ K_3 &= \frac{1}{3} d^3 \cdot n_1 \cdot \frac{P_1^0(\xi_0)}{Q_1^0(\xi_0)} & \bar{K}_3 &= \frac{1}{3} d^3 \cdot n_2 \cdot \frac{P_1^0(\xi_0)'}{Q_1^0(\xi_0)'} \end{aligned} \quad (5.2.5)$$

where $P_r^s(\xi_0)$ and $Q_r^s(\xi_0)$ are the associated Legendre's functions of order r and degree s of the first and the second kind, respectively, and the primed expressions represent its first order partial derivatives with respect to ξ_0 .

Neglecting the higher order terms of $O(k^4)$, the transverse far scattered field components can be expressed in matrix form. Extracting the radial components, according to (5.2.3) and (5.2.4), the normalized field components are related to the unknown coefficients K_j and \bar{K}_j by

$$[e] = [S(\theta, \phi)] [K] \quad (5.2.6a)$$

where the transpose of the column matrix $[e]$ is given by

$$[e]^T = [e_{\theta_1}, e_{\theta_2}, e_{\theta_3}, e_{\phi_1}, e_{\phi_2}, e_{\phi_3}] \quad (5.2.6b)$$

and that of $[K]$ by

$$[K]^T = [K_1, K_2, K_3, \bar{K}_1, \bar{K}_2, \bar{K}_3] \quad (5.2.6c)$$

Since only the coefficients K_j, \bar{K}_j for $j = 1, 2, 3$ are retained in

this low-frequency expansion, measured data are required for only three bistatic angles which results in the following far scattered field matrix:

$$[S(\theta, \phi)] = \begin{bmatrix} \cos\theta_1 \cos\phi_1 & \cos\theta_1 \sin\phi_1 & -\sin\theta_1 & -\sin\phi_1 & \cos\phi_1 & 0 \\ \cos\theta_2 \cos\phi_2 & \cos\theta_2 \sin\phi_2 & -\sin\theta_2 & -\sin\phi_2 & \cos\phi_2 & 0 \\ \cos\theta_3 \cos\phi_3 & \cos\theta_3 \sin\phi_3 & -\sin\theta_3 & -\sin\phi_3 & \cos\phi_3 & 0 \\ -\sin\phi_1 & \cos\phi_1 & 0 & -\cos\theta_1 \cos\phi_1 & -\cos\theta_1 \sin\phi_1 & \sin\theta_1 \\ -\sin\phi_2 & \cos\phi_2 & 0 & -\cos\theta_2 \cos\phi_2 & -\cos\theta_2 \sin\phi_2 & \sin\theta_2 \\ -\sin\phi_3 & \cos\phi_3 & 0 & -\cos\theta_3 \cos\phi_3 & -\cos\theta_3 \sin\phi_3 & \sin\theta_3 \end{bmatrix}$$

(5.2.7)

Inspecting the properties of (5.2.7), it is valuable to note that the obtained far scattered field matrix is identical in form to that obtained for a nonsymmetrical spherical scattering geometry as given in eq.

[III-1] in Boerner and Vandenberghe⁽⁸⁾, for the particular case $m = 1(N = 3)$.

5.3 RETRIEVAL OF THE PARAMETERS OF THE GENERATING ELLIPSE

5.3.1 COMPUTATION OF THE K_j AND \bar{K}_j COEFFICIENTS

The coefficients K_j and \bar{K}_j are recovered by a standard matrix inversion procedure. The degree of accuracy is dictated only by the measurement technique employed to evaluate the far field components. To guarantee most stable inversion, an optimum distribution of aspect angles is ob-

tained by optimizing the determinant associated with the scattered field matrix defined in (5.2.7). This has been derived in Boerner and Vandenberghe⁽⁸⁾ in context with a purely nonsymmetrical spherical scattering geometry. The closed-form solution for the determinant was given in eq. [III-3] as

$$[S(\theta, \phi)] = 4^2 \sin^2 \frac{\Delta_{12}}{2} \sin^2 \frac{\Delta_{23}}{2} \sin^2 \frac{\Delta_{31}}{2} \quad (5.3.1a)$$

where $\Delta_{\mu\nu}$ is the geodesical distance between two points on the unit sphere of directions, with

$$\cos \Delta_{\mu\nu} = \cos \theta_{\mu} \cos \theta_{\nu} + \sin \theta_{\mu} \sin \theta_{\nu} \cos(\phi_{\mu} - \phi_{\nu}) \quad (5.3.1b)$$

Equation (5.3.1a) states that no two aspect angles can be alike for the inversion to be possible. To obtain the maximum accuracy on the retrieval of the coefficients K_j and \bar{K}_j , $|S(\theta, \phi)|$ needs to be maximum. This results for an equidistant distribution of the three aspect angles over the unit sphere of directions, i.e. $|\Delta_{12}| = |\Delta_{23}| = |\Delta_{31}| = 120^\circ$, for which case $|S(\theta, \phi)| = \frac{27}{4}$.

5.3.2 RETRIEVAL OF THE PARAMETERS OF THE GENERATING ELLIPSE

The incentive of this development results from the fact that all the descriptive parameters of the prolate spheroid are contained in the coefficients K_j and \bar{K}_j . Thus employing the same argumentation which in the cases of circular cylindrical and spherical scattering geometries did lead to unique expressions of recovering the radii of curvature of those scatterers, we conjecture that the geometrical features of the

prolate spheroid can be retrieved from a knowledge of these coefficients.

Senior's approach is also employed for the reason that it is our aim to merely use an expansion in spherical wave functions and to avoid the cumbersome formulations in terms of prolate spheroidal functions for which only rather limited tables seem to exist. Furthermore, and in line with the order of truncation of $O(k^4)$ in (5.2.4), only the case of nose-on incidence is treated which is satisfactory to demonstrate our model technique as previously described for the circular cylindrical and the spherical cases.

For nose-on incidence $l_1 = 1$, $m_1 = 1$, $n_1 = 0$ and thus only K_1 and \bar{K}_2 are non-vanishing identically which, however, does not affect the matrix inversion procedure for the truncated case $M = 1(N = 3)$, considered in (5.2.7), since the direction cosines do not enter the formulation of the far scattered field matrix. Senior's coefficients K_1 and \bar{K}_2 as defined in (5.2.5) are explicitly expressed in terms of d and ξ_0 employing standard series expansions of the associated Legendre's functions of the first and the second kind⁽¹⁶⁾, resulting in

$$K_1 = -\frac{2}{3} d^3 \frac{P_1^1(\xi_0)}{Q_1^1(\xi_0)} = -\frac{2}{3} d^3 \cdot \left[\frac{1}{2} \ln\left(\frac{\xi_0 + 1}{\xi_0 - 1}\right) - \frac{\xi_0}{\xi_0^2 - 1} \right]^{-1} \quad (5.3.2a)$$

$$\bar{K}_2 = -\frac{2}{3} d^3 \frac{P_1^1(\xi_0)'}{Q_1^1(\xi_0)'} = -\frac{2}{3} d^3 \cdot \left[\frac{1}{2} \ln\left(\frac{\xi_0 + 1}{\xi_0 - 1}\right) - \frac{1}{\xi_0} + \frac{1}{\xi_0(\xi_0^2 - 1)} \right]^{-1} \quad (5.3.2b)$$

Equations (5.3.2a) and (5.3.2b) represent the set of two transcendental equations involving the two unknowns, d and ξ_0 . The ratio $\frac{K_1}{\bar{K}_2}$ is independent of d , resulting in

$$\frac{K_1}{\bar{K}_2} = \frac{\ln \left(\frac{\xi_0 + 1}{\xi_0 - 1} \right) - \frac{2}{\xi_0} + \frac{2}{\xi_0(\xi_0^2 - 1)}}{\ln \left(\frac{\xi_0 + 1}{\xi_0 - 1} \right) - \frac{2\xi_0}{(\xi_0^2 - 1)}} \quad (5.3.3)$$

In Fig. 14, the right-hand side of (5.2.3) is plotted versus $\varepsilon = 1/\xi_0$ within the limits of definition $0 \leq \varepsilon \leq 1$. From inspection of Fig. 14, it is observed that a unique solution of (5.3.3) can be obtained since the right-hand side of (5.3.3) is monotonically increasing and therefore ε can always be uniquely recovered. The value of d may then be determined from

$$\frac{1}{K_1} - \frac{1}{\bar{K}_2} = \frac{3}{d^3 \xi_0 (\xi_0^2 - 1)}$$

which leads to

$$d = \left[\frac{3}{\xi_0 (\xi_0^2 - 1)} \cdot \frac{K_1 \cdot \bar{K}_2}{(\bar{K}_2 - K_1)} \right]^{1/3} \quad (5.3.4)$$

Therefore, both of the a priori unknown parameters d and $\varepsilon = 1/\xi_0$, describing the generating ellipse of the prolate spheroid, can be recovered if Senior's expansion⁽⁴²⁾ is employed.

5.4 CONCLUSIONS

The presented study clearly demonstrates the merits of the inverse

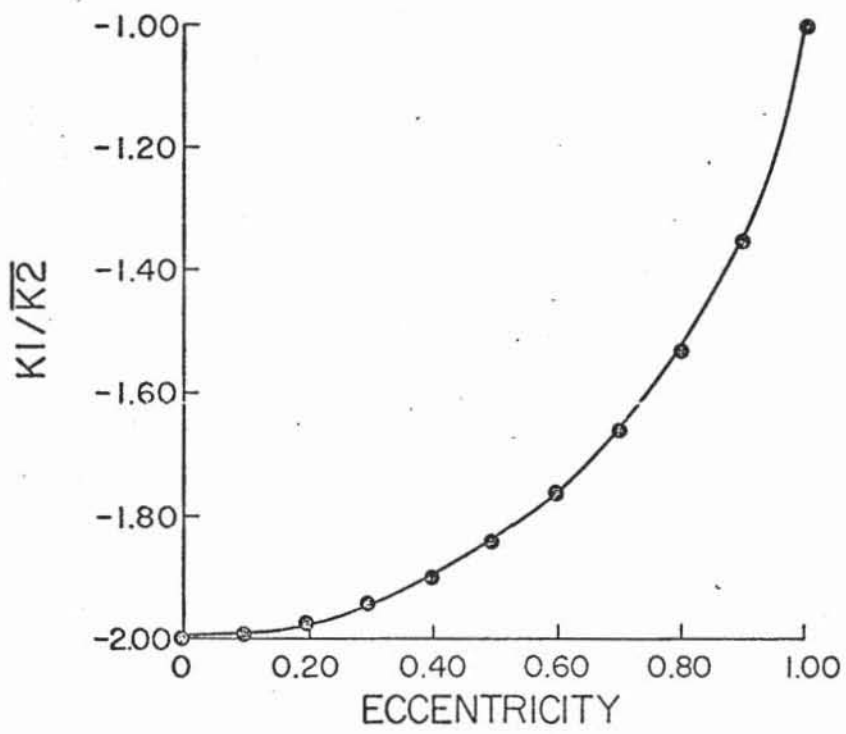


Fig.14 Characteristic Equation for the Evaluation of the Eccentricity

scattering model technique developed in *chapters two and four* to recover the salient features of a prolate spheroidal scatterer. Based on the hypothesis that all information pertaining to simple shapes are implicitly contained in the Fourier coefficients, the method provides analytical expressions defining the geometrical parameters of the scatterer's shape in terms of a limited number of these expansion coefficients. Therefore, this model technique does not require methods of analytical continuation^(55, 15) and neither the application of inverse boundary conditions⁽⁵⁵⁾ -- two techniques requiring extensive computation time.

In treating the inverse problem of scattering from a prolate spheroid, it was found advantageous to employ Senior's⁽⁴²⁾ alternative formulation of the far scattered field. This power series expansion in k has the merit of being related to spherical wave functions⁽⁴⁵⁾ instead of the complicated prolate spheroidal functions. This expansion, valid for the low-frequency case, is truncated at the order $O(k^4)$. It is thus possible to relate the normalized transverse scattered field components of only three aspect angles with Senior's coefficients via a scattered field matrix. These coefficients representing the leading terms of the low-frequency expansion are then recovered by inverting the matrix. It is valuable to note that this matrix is identical to that encountered for the nonsymmetrical spherical case in Boerner and Vandenberghe⁽⁸⁾, eqs. [III-1] and [III-3]. This cognizance also underlines the simplicity of Stevenson's and Senior's formulations of the field scattered

by a prolate spheroid. Finally, the characteristic geometrical parameters d and ξ_0 are recovered from the expressions of Senior's coefficients. This simple method of retrieving these characteristic parameters uniquely defines the shape of the prolate spheroid which was the ultimate aim of this report.

This shape has been presented mainly as an illustration of the applicability of the inverse scattering model, derived for the circular cylinder and the sphere in *chapters two and four*.

PART B

*chapter six*OPTIMIZATION PROCEDURE6.1 INTRODUCTION

In the last few years, an enormous amount of data has been compiled from satellites and space probes, contributing extensively to such varied disciplines as meteorology, atmospheric studies, outer space and planetary exploration. However, the possibility of actually using this data is quite another matter, depending upon the ability of the associated decision-making processes to correctly interpret this data. In the field of inverse scattering, where a knowledge of the far-scattered field at various aspect angles confined within a finite cone of observation constitutes the only available data, techniques must be accordingly developed in order to assimilate and digest this information so as to accurately portray the inobservable body.

In addition, although it is desirable to utilize as much information as possible to objectify the scatterer, it is ultimately essential to develop and implement some kind of computerized technique to compress this information in order to rapidly streamline the measured data to the particular decision under consideration. This is especially important whenever we employ continuous measurement techniques⁽¹⁰⁾ or when discrete measurements are performed⁽⁴⁹⁾.

The search for radar data which provides unique representation of any space object however remote has led to the use of multiple frequency and multistatic angle data. For example, applying physical optics or using Kirchhoff's approximations, it has been demonstrated that one can determine the size and shape of a scattering target for a restricted bistatic aspect angle range from the backscattered field measured at all angles⁽²⁸⁾. This general theory has been modified further to show that one can gain partial information from the measured data if frequencies are limited to a given band.

However, the problem of data selection remains a thorny one and computerized techniques must still be developed for this end. The amount of crude data necessary for the case of the rotationally symmetrical body has been drastically reduced^(51, 52, 53, 54). It is now possible to recover the shape of this geometry by an inversion of the matrix procedure, which requires the far field scattered by such bodies to be known in amplitude phase and polarization at various bistatic angles for a given incident plane wave; and also requires the far scattered field to be expressed in a series of expansions of the orthogonal scalar or vector wave functions with respect to some co-ordinate system whose origin must lie within the scatterer. Nevertheless, the problem is not completely resolved, as special attention must be focused on the distribution of the bistatic angles within a given measurement domain of observation to avoid instabilities in the matrix inversion procedure as to attain a modicum of certainty in this area.

In this part, we will examine this specific problem for scattering geometries representing the "mth" degree multipole cases with special attention being given to the circular cylinder and the sphere. A general technique is established which can be employed for maximum accuracy in the retrieval of these shapes.

This theory will not be limited to the field of electromagnetics, since it could contribute in the optimization of any polynomials, when they are expressed in terms of their root products with all roots playing identical roles. This theory greatly reduces computation time, thus making an invaluable contribution to the decision-making processes of rapidly assimilating and interpreting the vast compilation of data necessary in pattern recognition.

6.2 FORMULATION OF THE PROBLEM

It is assumed that for a given transmitted field, we can accurately obtain the field scattered from rotationally symmetrical bodies in amplitude, in phase and in polarization for a sufficiently large number 'N' of different bistatic angles $\{\phi_c, \theta_c, c = 1, 2, \dots, N\}$.

It is further assumed that the scattered field components can be expressed in a series expansion, in orthogonal scalar or in vector wave functions. In *chapters two, three and four*, such expansions have been derived employing cylindrical scalar or spherical vector wave functions.

for the circular cylinder, (2.2.1), for the elliptic cylinder, (3.4.9), and for geometries representing the 'mth' degree multipole cases, (4.2.10). With the radial part dependence extracted by normalization, the scattered field components have been related to associated expansion coefficients $\{X_\nu, \nu = 1, 2, \dots, N\}$, via a scattered field matrix,

$$\begin{bmatrix} E_{\theta_1} \\ E_{\theta_2} \\ \vdots \\ E_{\theta_N} \\ E_{\phi_1} \\ E_{\phi_2} \\ \vdots \\ E_{\phi_N} \end{bmatrix} = [S(\theta, \phi)] \cdot \begin{bmatrix} X_1 \\ X_2 \\ \vdots \\ \vdots \\ \vdots \\ \vdots \\ X_{2N} \end{bmatrix} \quad (6.2.1)$$

In particular, it has been demonstrated that the electrical radius of the cylinder and of the sphere could be recovered from these expansion coefficients, (2.4.4), (2.4.14), (4.5.5) and (4.5.7). In the case of the elliptic cylinder, the associated coefficients characterize the body's main features. Still, due to the complexity of the Mathieu wave functions, it has not been possible to derive a simple expression directly relating the electrical axes of the cylinder in terms of these coefficients.

In this analysis, the matrix $[S(\theta, \phi)]$ must be inverted to retrieve the electrical radius of the cylinder and of the sphere from the associated

coefficients $\{X_\nu, \nu = 1, 2, \dots, 2N\}$. However, to ensure a stable inversion, we are compelled to optimize the determinant $|S(\theta, \phi)|$ associated with $[S(\theta, \phi)]$. In other words, the optimal distribution of aspect angles which spreads over some limited region of space, is sought, for which $|S(\theta, \phi)|$ becomes maximum. This is indeed an obligatory procedure, if any degree of accuracy is desired in the retrieval of the coefficients $\{X_\nu, \nu = 1, 2, \dots, 2N\}$. In addition, it is further assumed that the associated determinant $|S(\theta, \phi)|$ can be written in a closed-form-solution where the θ and ϕ dependence are separated and factorized as:

$$|S(\theta, \phi)| = |\Theta| \cdot |\Phi| \quad (6.2.2)$$

where $|\Theta|$ and/or $|\Phi|$ represent a product of trigonometric functions, of the aspect angles θ and/or ϕ , which is symmetrical in $\{\phi_c, c = 1, 2, \dots, N\}$ or $\{\theta_c, c = 1, 2, \dots, N\}$ (7, 8). Only determinants of the form:

$$\prod_{\mu=1}^N \sin^{2m_\mu} \theta_\mu \cdot \prod_{\substack{N > r > s \geq 1}} (\cos \theta_r - \cos \theta_s)^2 \quad (4.3.8)$$

are subsequently optimized, since they represent the most general formulation of those determinants associated with geometries representing the 'mth' degree multipole cases.

6.3 OPTIMIZATION PROCEDURE

For the sake of demonstration, consider a product involving 'N' variables u_k ($k = 1, 2, \dots, N$), which play identical roles as in the product given by:

$$\prod_{\substack{N > r > s \geq 1}} (u_r - u_s) \quad (6.3.1)$$

where each u_k varies within the limits $(-1, +1)$. The optimal variables, consisting of specific values for which (6.3.1) is optimal, are found in solving the set of 'N' simultaneous equations. These equations express the vanishing derivatives of (6.3.1) with respect to any variable u_k . By taking the derivatives, we shall find the optimum values u_{0k} for which (6.3.1) is either maximum or minimum. A comparison between the final value of (6.3.1), when u_{0k} is employed, and a value obtained from any other distribution will remove the ambiguity.

Nevertheless, before carrying out a detailed study of the polynomials expressing the vanishing derivatives, Gauss's fundamental lemma on the root expansion of polynomials⁽⁴⁴⁾ will be reviewed with the intention of introducing the notations:

$$\text{Let } f(u) = \sum_{\mu=0}^N a_{\mu} u^{\mu} \text{ have the } N \text{ zeros } u_1, u_2, \dots, u_N, \text{ then}$$

$$f(u) = A_N (u - u_1)(u - u_2) \dots (u - u_N) = A_N \sum_{\mu=0}^N (-1)^{\mu+1} d_{N,\mu} u^{N-\mu} \quad (6.3.2)$$

where $d_{N,\mu}$, which represents the sum of $\binom{N}{\mu} = \frac{N!}{\mu! (N-\mu)!}$ products of μ different roots of (3.2), is equal to

$$d_{N,\mu} = \sum_{\binom{N}{\mu}} (u_1, u_2, \dots, u_{\mu})$$

$$= (-1)^{\mu} \frac{A_{N-\mu}}{A_N} \quad (6.3.3)$$

with

$$d_{N,-2} = 0; \quad d_{N,-1} = 0; \quad d_{N,0} = 1 \quad (6.3.4)$$

Similarly, the iterator $d_{N,\mu}^i(u_k)$ is defined as

$$d'_{N,\mu}(u_k) = d_{N,\mu} - d'_{N,\mu-1}(u_k) \quad (6.3.5)$$

where

$$d'_{N,-2}(u_k) = 0; \quad d'_{N,-1}(u_k) = 0; \quad d'_{N,0}(u_k) = 1 \quad \text{and} \quad d'_{N,N}(u_k) = 0 \quad (6.3.6)$$

This iterator, presently introduced for convenience, will later be used to further the development of the presentation.

The set of 'N' equations, expressing the derivatives of (6.3.1), is then used to build a polynomial in descending power of any variable u_k as:

$$\sum_{\mu=0}^N B_{N,\mu} u_k^\mu = 0 \quad (6.3.7)$$

in such a manner that the coefficients $B_{N,\mu}$ contain a symmetric expression of the desired solutions u_{0k} . In other words, the polynomial as defined in (6.3.7) is constructed in such a way that every coefficient $B_{N,\mu}$ depends only upon a linear combination of $d_{N,\mu}$. The result of this algorithm is the removal of the subscript (k) in (6.3.7) which is a polynomial of degree N, the roots of which are the desired solutions u_{0k} .

According to Gauss's lemma, the polynomial (6.3.7) must be identical to (6.3.2). This implies that....

$$\frac{d_{N,\mu}}{A_N} = \frac{B_{N,\mu}}{B_{N,N}} \quad (6.3.8)$$

Since by construction, the $B_{N,\mu}$ coefficients depend upon the $d_{N,\mu}$ coefficients, (6.3.8) thus represents a recurrence-relationship between the $d_{N,\mu}$ coefficients. Therefore, with (6.3.6) each $d_{N,\mu}$ coefficient can be

explicitly found and the given polynomial (6.3.7) completely defined. Subsequently, the last step consists in having a zero finding subroutine for polynomials and in obtaining the precise values of the roots u_{0k} , the object of the original search.

The theory is then largely illustrated within the following important problems, namely:

- (i) What is the best distribution of bistatic angles within a wedge angle of half-angle θ_{MC} for which (2.3.2)

$$2 \frac{N(N-1)}{2} \prod_{\substack{r \\ N-1 > r > s > 0}} (x_r - x_s) \quad \text{is maximum?}$$

- (ii) What is the best distribution of bistatic angles within a polar sector of half-angle θ_{MC} for which (4.3.8)

$$\prod_{\mu=1}^N \sin^{2m} \theta_{\mu} \cdot \prod_{\substack{r \\ N > r > s > 1}} (\cos \theta_r - \cos \theta_s)^2 \quad \text{is maximum?}$$

Further on in section (6.6.5), it will be seen that the optimization of the determinant associated with the circular cylinder is a special case encountered in the optimization of the polar part $|\Theta|$ of the determinant associated with geometries representing the 'mth' degree multipole cases. For the present, however, the former is derived primarily for better illustration purposes. The recognition of the inherent symmetrical properties within this analysis will then be assumed for the more general case.

It is interesting to note that the resolution of this problem is by no means restricted to the study of inverse scattering. Indeed, it could

be appropriate to optimize any analytical expression, written in the form of a product of band-limited functions, such as: trigonometrical, Legendre and Tchebyscheff functions of 'N' variables, as they all play identical roles. Hence the scope of its applicability widely overruns that of our specific problem; it could very well be applied in other domains of studies or in other disciplines where such expressions are encountered.

6.4 OPTIMIZATION OF THE DETERMINANT $|\phi(N)|$ AS GIVEN BY (2.3.2)

The optimal distribution of aspect angles spread over some limited wedge of the unit circle of direction is derived for which the determinant $|\phi(N)|$ becomes maximum.

By introducing the co-ordinates defined in equations (2.3.3a) to (2.3.3d) and illustrated in Fig. 3, it is shown in equation (2.3.4) that this determinant can be written in the form

$$|\phi(N)| = (\cos\alpha - \cos\beta)^{\frac{N(N-1)}{2}} \prod_{\substack{N-1 \\ r > s \geq 0}} (u_r - u_s) \quad (6.4.1)$$

which represents a distribution of cosines:

$$u_r = \frac{\cos\phi_r}{\left| \frac{\cos\alpha - \cos\beta}{2} \right|} = \frac{x_r - \left(\frac{\cos\alpha + \cos\beta}{2} \right)}{\left| \frac{\cos\alpha - \cos\beta}{2} \right|}$$

symmetrical about $\cos\phi_0$ as defined in (2.3.3b).

Since the two cosines, $\cos\alpha$ and $\cos\beta$, which correspond to the wedge limiting aspect angles α and β , are known, the number of unknowns in

equation (6.4.1) is reduced to $n = N-2$. The general situation is first considered for which no *a priori* symmetries can be assumed, so that $-1 < u_r < 1$, where, for convenience's sake, u_r is chosen larger than u_s . To find the optimal distribution of cosines for which (6.4.1) is maximum, that set of simultaneous equations, which expresses the vanishing derivatives of (6.4.1) with respect to all variables u_r , is solved.

First, the derivatives of $|\phi(N)|$ with respect to any u_r , are formulated in a closed form solution. The cases $N = 4$ and $N = 5$ are presented to illustrate the more general case.

EXAMPLE:- $N = 4, n = 2, r = 1, u_0 = 1, u_4 = -1$

$$\begin{aligned} |\phi(4)| &= (u_1 + 1)(u_2 + 1) 2 (u_2 - u_1)(1 - u_1)(1 - u_2) \\ &= 2 (1 - u_1^2)(1 - u_2^2)(u_2 - u_1) \\ \frac{\partial |\phi(4)|}{\partial u_1} &= -2 (1 - u_1^2)(1 - u_2^2)(u_1 - u_2) \cdot \left[\frac{2u_1}{1 - u_1^2} + \frac{1}{u_2 - u_1} \right] \end{aligned}$$

EXAMPLE:- $N = 5, n = 3, r = 2, u_0 = 1, u_5 = -1$

$$\begin{aligned} |\phi(5)| &= (u_1 + 1)(u_2 + 1)(u_3 + 1) 2 (u_2 - u_1)(u_3 - u_1)(1 - u_1) \\ &\quad \cdot (u_3 - u_2)(1 - u_2)(1 - u_3) \\ &= 2 (1 - u_1^2)(1 - u_2^2)(1 - u_3^2)(u_2 - u_1)(u_3 - u_1)(u_3 - u_2) \\ \frac{\partial |\phi(5)|}{\partial u_2} &= 2 (1 - u_1^2)(1 - u_3^2)(u_3 - u_1) \cdot \{-2u_2 (u_2 - u_1)(u_3 - u_2) \\ &\quad + (1 - u_2^2)(u_3 - u_2) - (1 - u_2^2)(u_2 - u_1)\} \\ &= -|\phi(5)| \cdot \left\{ \frac{2u_2}{1 - u_2^2} + \frac{1}{u_1 - u_2} + \frac{1}{u_3 - u_2} \right\} \end{aligned}$$

In the general case,

$$\frac{\partial |\phi(N)|}{\partial u_r} = |\phi(N)| \cdot \frac{\partial}{\partial u_r} \{ \text{Log } |\phi(N)| \} \quad (6.4.2a)$$

where

$$|\phi(N)| = 2 \prod_{i=1}^{N-2} (1 - u_i^2) \cdot \prod_{\substack{N-2 > i > s > 1}} (u_i - u_s) \quad (6.4.2b)$$

Equation (6.4.3a) is then equal to

$$\begin{aligned} \frac{\partial |\phi(N)|}{\partial u_r} &= |\phi(N)| \cdot \frac{\partial}{\partial u_r} \left\{ \text{Log } 2 + \sum_{i=1}^{N-2} \text{Log } (1 - u_i^2) + \sum_{\substack{s=1 \\ i \neq s}}^{N-2} \text{Log } (u_i - u_s) \right\} \\ &= - |\phi(N)| \cdot \left\{ \frac{2u_r}{1 - u_r^2} + \sum_{\substack{s=1 \\ r \neq s}}^{N-2} \frac{1}{u_r - u_s} \right\} \quad (6.4.3) \end{aligned}$$

The constant multiplier $|\phi(N)|$ is the value of the determinant and can be ignored in the subsequent derivations.

Employing the notations defined in (6.3.3), (6.3.4), (6.3.5), and in (6.3.6), the procedure used to construct the polynomial, as given by (6.3.7), is illustrated in the next example: for $n = 4$ where $u_k = u_4$.

EXAMPLE:- $n = 4, u_k = u_4$

$$\begin{aligned} &- 5u_4^4 + 4u_4^3 (u_1 + u_2 + u_3) - 3u_4^2 (u_1u_2 + u_2u_3 + \\ &u_3u_1 - 1) + 2u_4 (u_1u_2u_3 - u_1 - u_2 - u_3) + \\ &(u_1u_2 + u_3u_1 + u_3u_2) = 0 \end{aligned}$$

According to (6.3.3) and to (6.3.5)

$$\begin{aligned}
 d_{4,-1} &= 0; \quad d_{4,0} = 1; \quad d_{4,1} = u_1 + u_2 + u_3 + u_4 \\
 d_{4,2} &= u_1 u_2 + u_2 u_3 + u_3 u_1 + u_1 u_4 + u_2 u_4 + u_3 u_4 \\
 d_{4,3} &= u_1 u_2 u_3 + u_1 u_2 u_4 + u_2 u_3 u_4; \quad d_{4,4} = u_1 u_2 u_3 u_4
 \end{aligned}$$

and

$$\begin{aligned}
 d'_{4,-2}(u_4) &= 0; \quad d'_{4,-1}(u_4) = 0 \\
 d'_{4,0}(u_4) &= 1; \quad d'_{4,1}(u_4) = u_1 + u_2 + u_3 \\
 d'_{4,2}(u_4) &= u_1 u_2 + u_2 u_3 + u_3 u_1 \\
 d'_{4,3}(u_4) &= u_1 u_2 u_3; \quad d'_{4,4}(u_4) = 0
 \end{aligned}$$

Therefore, for $n = 4$, (6.4.3) can be rewritten as:

$$\begin{aligned}
 &(-1)^5 5u_4^4 [d'_{4,0}(u_4) - d'_{4,-2}(u_4)] + (-1)^4 4u_4^3 [d'_{4,1}(u_4) - d'_{4,-1}(u_4)] \\
 &+ (-1)^3 3u_4^2 [d'_{4,2}(u_4) - d'_{4,0}(u_4)] + (-1)^2 2u_4 [d'_{4,3}(u_4) - d'_{4,1}(u_4)] \\
 &+ (-1)^1 1 [d'_{4,4}(u_4) - d'_{4,2}(u_4)] = 0
 \end{aligned}$$

.....by inspection of the given example, it follows that (6.4.3) can be expressed in the form:

$$\sum_{v=0}^n (-1)^{v+1} u_r^{n-v} (n-v+1) \cdot [d'_{n,v}(u_r) - d'_{n,v-2}(u_r)] = 0 \quad (6.4.4)$$

Substituting $d'_{n,v-2}(u_r)$ by its value given in terms of $d_{n,v-1}$ in

(6.3.5), the equation (6.4.4) is reduced to

$$\sum_{v=0}^n (-1)^{v+1} \{(n-v+1) u_r^{n-v} [d_{n,v} - u_r d_{n,v-1} - (1-u_r^2) d'_{n,v-2}(u_r)]\} \quad (6.4.5)$$

which can be written as

$$\sum_{v=0}^n (-1)^{v+1} (n-v+1) u_r^{n-v} \{d_{n,v} - u_r d_{n,v-1} (1-u_r^2) \cdot \sum_{t=1}^{v-1} (-1)^{t-1} u_r^{t-1} d_{n,v-t-1}\} = 0 \quad (6.4.6)$$

by expressing $d'_{n,v-2}(u_r)$ in terms of $d_{n,v}$.

This expression can then be ordered in u_r by adding the different contribution of each terms at the u_r^{n-v} power.

The coefficient of u_r^{n-v} is given by

$$\begin{aligned} & [(n-v+1) d_{n,v} - (n-v+1) d_{n,v-2} \\ & + (n-v) d_{n,v} - (n-v) d_{n,v-2} \\ & + \dots \\ & + d_{n,v} - d_{n,v-2}] \\ & = \frac{(n-v+1)(n-v+2)}{2} \cdot (d_{n,v} - d_{n,v-2}) \quad (6.4.7) \end{aligned}$$

Therefore, (6.4.6) can be re-ordered as

$$\sum_{v=0}^n (-1)^{v+1} u_r^{n-v} \left[\frac{(n-v+2)(n-v+1)}{2} \right] \cdot (d_{n,v} - d_{n,v-2}) = 0 \quad (6.4.8)$$

which is the proper form as given by (6.3.7)..except for the two known roots +1 and -1, which we have extracted from the beginning.. The subscript r may now be removed, since (6.4.8) is absolutely symmetric in terms of u_0 .

According to Gauss's lemma, (6.4.8) must be identical to

$$A_n \sum_{v=0}^n (-1)^{v+1} u_r^{n-v} d_{n,v} = 0 \quad (6.4.9)$$

Therefore, a unique relationship results between factor $d_{n,v}$ and factor $d_{n,v-2}$, and that, for general 'n'

$$\frac{d_{n,v}}{d_{n,0}} = \frac{\left[\frac{(n-v+2)(n-v+1)}{2} \right] \cdot (d_{n,v} - d_{n,v-2})}{\frac{(n+2)(n+1)}{2} \cdot (d_{n,0} - d_{n,-2})} \quad (6.4.10a)$$

Since $d_{n,-2} = 0$ and $d_{n,0} = 1$, (6.4.10a) is rearranged to give a recurring connection between $d_{n,v}$ and $d_{n,v-2}$ in the form

$$d_{n,v} = \frac{(n-v+2)(n-v+1)}{v(2n-v+3)} \cdot d_{n,v-2} \quad (6.4.10b)$$

Furthermore, according to (6.4.10b) starting from $d_{n,-1}$, all coefficients for odd values of v are zero; this, in turn, implies that the roots of the polynomial (6.4.9) appear in symmetrical pair about $u_r = 0$, with the constraint $-1 < u_r < +1$. Also, the fact follows straightforwardly that (6.4.6) has only one set of solutions u_{0r} and that if the u_{0r} takes symmetrical values with respect to zero, then the coefficients $d_{n,v}$ for odd values of 'v' are zero. If another set of solutions was found, where the coefficients $d_{n,v}$ for odd values of 'v' were again zero, for unsymmetrical u_{0r} , two different sets of solutions would then satisfy (6.4.6). Such an hypothesis is hence rejected. The present demonstration is readily self-explicated in the following example:-

Let us consider the polynomial $f(u)$ defined by

$$f(u) = (u-u_1)(u-u_2)(u-u_3)(u-u_4)$$

where

$$\begin{aligned} d_{n,1} &= u_1 + u_2 + u_3 + u_4 \\ d_{n,3} &= u_1u_2u_3 + u_1u_2u_4 + u_1u_3u_4 + u_2u_3u_4 = 0 \end{aligned} \quad (6.4.11)$$

In the first place, it is obvious that the symmetrical pair of u_r , with respect to zero, satisfied equation (6.4.11). Nevertheless, let us

consider the existence of another set of solutions which would meet the requirements of equation (6.4.11). From (6.4.11), we have

$$\begin{aligned} u_1 + u_3 &= -(u_2 + u_4) \\ (u_1 u_3 - u_2 u_4) \cdot (u_2 + u_4) &= 0 \end{aligned}$$

Since $u_2 = u_4$, we must have $-u_1 u_3 = u_2 u_4$ and $-u_1 + u_3 = (-u_2 + u_4)$ order to satisfy equation (6.4.11). This leads to $-u_1^2 + u_1(u_2 + u_4) + u_2 u_4 = 0$ and to

$$\begin{aligned} -u_1 &= -u_2 \\ u_1 &= -u_4 \end{aligned} \tag{6.4.12}$$

which were rejected by hypothesis and therefore proves the aforementioned conclusion. Taking this symmetry into consideration, it appears convenient to introduce the new variable μ , so that $\nu = 2\mu$. With $d_{n,0} = 1$, all the coefficients $d_{n,2\mu}$ can be determined by successive iteration of (6.4.10b) as

$$\begin{aligned} d_{n,2\mu} &= (-1)^\mu \frac{\prod_{t=1}^{\mu} (n - 2t + 2)(n - 2t + 1)}{\prod_{t=1}^{\mu} 2t (2n - 2t + 3)} \\ &= (-1)^\mu \frac{[n(n-2) \dots (n-2\mu+2)] [(n-1)(n-3) \dots (n-2\mu+1)]}{2^{\mu} \mu! [(2n+1)(2n-1) \dots (2n-2\mu+3)]} \\ &= (-1)^\mu \frac{n!(2n-2\mu+1)!!}{(2\mu)!!(n-2\mu)!(2n+1)!!} \end{aligned} \tag{6.4.13}$$

and therefore, (6.4.3) with $\nu = 2\mu$, becomes

$$B_n \sum_{\mu=0}^{n/2} (-1)^{\mu+1} u_r^{n-2} \frac{n!(2n-2\mu+1)!!}{(2\mu)!!(n-2)!(2n+1)!!} = 0 \tag{6.4.14}$$

Before going further into the presentation, a similar derivation is

undertaken by assuming an *a priori* symmetry which could have been rendered feasible directly from (6.4.1). The determinant, as given by (6.4.1) represents a distribution of cosines u_r , symmetrical about $\cos\phi_0$ as defined by:

$$\cos\phi_0 = \frac{\cos\alpha + \cos\beta}{2} \quad (2.3.3b)$$

Because of the assumed symmetry and due to the fact that two or three solutions have already been put forward (+1 and -1 for the 'N' even case; three +1, 0, -1 for the 'N' odd case), the number of unknowns in equation (6.4.1) can be reduced to

$$\left. \begin{aligned} p &= \frac{N-2}{2}, \text{ Neven} \\ p &= \frac{N-3}{2}, \text{ N odd} \end{aligned} \right\} \quad (6.4.15)$$

Considering the range $0 < u_r < 1$, where u_i is chosen greater than u_j for convenience, (6.4.1) thus takes on the following form:

$$|\phi(\text{Neven})| = 2^{\frac{N}{2}} (\cos\alpha - \cos\beta)^{\frac{(N-1)N}{2}} \left[\prod_{t=1}^p (1 - u_t^2) \sqrt{u_t} \prod_{\substack{p \geq i > j \geq 1}} (u_i^2 - u_j^2) \right]^2 \quad (6.4.16)$$

and

$$|\phi(\text{N odd})| = 2^{\frac{N-1}{2}} (\cos\alpha - \cos\beta)^{\frac{(N-1)N}{2}} \left[\prod_{t=1}^p (1 - u_t^2) u_t^{3/2} \prod_{\substack{p \geq i > j \geq 1}} (u_i^2 - u_j^2) \right]^2$$

The derivatives of (6.4.10), with respect to $v_r = u_r^2$, can be rearranged as polynomials of degree 'p':

$$\frac{\partial}{\partial v_r} |\phi(p)| = A \left[(2 \mp 1) - \frac{4v_r}{1-v_r} + 4v_r \left(\sum_{\substack{i=1 \\ j \neq i}}^p \frac{1}{(v_i - v_j)} \right) \right] \equiv 0 \quad (6.4.17)$$

where A stands for a front-end constant multiplier. The upper and lower signs refer to even and odd values of p respectively. The

following derivations are presented for the case p even, since the odd case is easily derived with the definition of (6.4.16). Employing the same procedure which led to (6.4.4), equation (6.4.16) may be expressed in the form

$$\sum_{v=0}^{\frac{\ell-1}{2}} (-1)^{\frac{\ell-2v-1}{2}} (2\ell-4v-1) v_r^{\frac{\ell-2v-1}{2}} [d'_{\ell,v-1}(v_r) + d'_{\ell,v}(v_r)] = 0$$

$p = \text{even}, \ell = 2p + 1 = N - 1$ (6.4.17)

With the substitution of $d'_{\ell,v-1}(v_r)$ by its value given in terms of $d_{\ell,v}$, equation (6.4.17) reduces to

$$\sum_{v=0}^{\frac{\ell-1}{2}} (-1)^{\frac{\ell-2v-1}{2}} (2\ell-4v-1) v_r^{\frac{\ell-2v-1}{2}} (d_{\ell,v-1}(x_r) + (\ell - v_r) \sum_{t=1}^v (-1)^{t-1} \cdot v_r^{t-1} d_{\ell,v-1}) = 0$$

(6.4.18)

which can be ordered in v_r as

$$\sum_{v=0}^{\frac{\ell-1}{2}} (-1)^{\frac{\ell-2v-1}{2}} v_r^{\frac{\ell-2v-1}{2}} (d_{\ell,v-1} + d_{\ell,v}) \sum_{t=v}^{\frac{\ell-1}{2}} (2\ell - 4t - 1) = 0$$

(6.4.19)

However, according to Gauss's lemma, equation (6.4.19) must be identical to

$$\sum_{v=0}^{\frac{\ell-1}{2}} (-1)^{\frac{\ell-2v-1}{2}} v_r^{\frac{\ell-2v-1}{2}} d_{\ell,v} = 0$$

and, therefore, a unique relationship, between the factors $d_{\ell,v}$ and $d_{\ell,v-1}$, results for general ℓ .

$$\frac{d_{\ell,v}}{d_{\ell,0}} = \frac{(d_{\ell,v-1} + d_{\ell,v}) \cdot \sum_{t=v}^{\frac{\ell-1}{2}} (2\ell - 4t - 1)}{(d_{\ell,-1} + d_{\ell,0}) \cdot \sum_{t=0}^{\frac{\ell-1}{2}} (2\ell - 4t - 1)} \tag{6.4.20}$$

Since $d_{\ell,-1} = 0$ and $d_{\ell,0} = 1$, (6.4.20) is rearranged in the form

$$d_{\ell,v} = d_{\ell,v-1} \frac{\sum_{t=v}^{\frac{\ell-1}{2}} (2\ell - 4t - 1)}{\sum_{t=0}^{\frac{\ell-1}{2}} (2\ell - 4t - 1)} = d_{\ell,v-1} \frac{(\ell - 2v)(\ell + 1 - 2v)}{2v(2\ell - 2v + 1)} \tag{6.4.21}$$

With $d_{\ell,0} = 1$, all the coefficients $d_{\ell,v}$ can be determined by successive iteration of (6.4.21) as

$$\begin{aligned} d_{\ell,v} &= \frac{\prod_{r=1}^v \sum_{t=r}^{\frac{\ell-1}{2}} (2\ell - 4t - 1)}{\prod_{r=0}^{v-1} \sum_{t=0}^r (2\ell - 4t - 1)} = \frac{\prod_{r=1}^v (\ell - 2r)(\ell - 2r + 1)}{2^v \prod_{r=0}^{v-1} (r + 1)(2\ell - 2r - 1)} \\ &= \frac{[(\ell - 2)(\ell - 4) \dots (\ell - 2v)] [(\ell - 1)(\ell - 3) \dots (\ell + 1 - 2v)]}{2^v \cdot v! \cdot |(2\ell - 1)(2\ell - 3) \dots (2\ell + 1 - 2v)|} \\ &= \frac{(\ell - 1)! (2\ell - 2v - 1)!!}{(2v)!! (\ell - 2v - 1)! (2\ell - 1)!!} \tag{6.4.22} \end{aligned}$$

and, therefore, (6.4.16) becomes for even 'p'

$$\sum_{v=0}^{\frac{\ell-1}{2}} (-1)^{\frac{\ell-2v-1}{2}} \frac{(\ell - 1)! (2\ell - 2v - 1)!!}{(2v)!! (\ell - 3v - 1)! (2\ell - 1)!!} u_r^{\frac{\ell-2v-1}{2}} = 0 \tag{6.4.23}$$

which is identical to (6.4.14) when $(\ell-1)$ is replaced by 'n' in (6.4.24), to balance with the definition of 'n', given in the earlier

derivations; namely,

$$n = N - 2 = (N - 1) - 1 = \ell - 1$$

This derivation analytically proves that the roots u_{0r} take on symmetric values with respect to zero and it has been presented for the sake of completeness. It also shows that, if an *a priori* symmetry can be detected, the derivation of a polynomial, of the type given in (6.3.7) is appreciably facilitated.

While including the known roots, -1 and $+1$, (6.4.14) or (6.4.23) are multiplied by the factor $(1 - u^2)$; and multiplying each side of equation (6.4.14) or of equation (6.4.23), by the chosen constant:

$$\frac{(2n + 2)!}{2^{n+1} (n+1)! (n)!} \quad (6.4.24)$$

the following optimization function ensues:

$$(1-u_r^2)^{1/2} P_{n+1}^1(u_r) = O_N^1(u_r) = (1-u_r^2)^{1/2} \left[\frac{(2n+2)! (1-u_r^2)^{1/2}}{2^{n+1} n! (n+1)!} \sum_{v=0}^n (-1)^v \cdot \frac{(n)! (2n-2v+1)!!}{(2v)!! (n-2v)! (2n+1)!!} u_r^{n-2v} \right] \quad (6.4.25)$$

where (6.4.25) is identical to (2.3.5).

The expression in the square brackets represents the associated Legendre function $P_{n+1}^1(u_r)$ of the first kind and of the first degree, as well as order $(n + 1)$ with $n = N - 2$; where the explicit formulation of $P_n^1(u)$ follows from the definition given in Jahnke and Emde⁽¹⁶⁾.

6.5 OPTIMIZATION OF THE DETERMINANT ASSOCIATED WITH THE GEOMETRIES
REPRESENTING THE 'mTH' DEGREE MULTIPOLE CASES

Let us proceed now with the derivation of the optimal distribution of the aspect angles (θ_μ ; $\mu = 1, 2, \dots, N$), which are spread over some limited polar angle of the unit sphere of directions and for which the polar part $|\Theta|$ of the determinant $|S_N(\theta, \phi)|$ becomes maximum. This is permissible since, as found in (4.3.8), the polar part θ and the azimuth ϕ part are independent from each other. Neglecting the multiplicative constant in (4.3.8), the polar part $|\Theta|$, which needs to be optimized may be formulated as (4.4.4a):

$$|\Theta_{N \text{ even}, p}| = \left[\prod_{k=1}^p (1 - u_k^2)^{m/2} u_k^{1/2} \prod_{\substack{i > j > 1 \\ p}} (u_i^2 - u_j^2) \right]^4 \quad (4.4.4a)$$

where only the case 'N even' is considered. The 'odd case' results from the definition of (4.4.4b).

The set of derivatives of part (4.4.4a), with respect to all 'p' variables, is then solved as outlined in section (6.3).

$$\frac{\partial}{\partial v_k} |\Theta_{N \text{ even}, p}| = \left[1 - \frac{2mv_k}{1-v_k} + 4v_k \sum_{\substack{j=1 \\ j \neq i}}^{p-1} \frac{1}{v_i - v_j} \right] = 0 \quad (6.5.1)$$

where $v_k = u_k^2$.

With $\ell = N - 1$, (6.5.1) may be written as

$$\sum_{\mu=0}^{\frac{\ell+1}{2}} (-1)^{\frac{\ell-2\mu+1}{2}} v_k^{\frac{\ell-2\mu+1}{2}} \{(2\ell + 2 + 2m - 4\mu + 1) d'_{\ell,\mu}(v_k) + (2\ell + 2 + 1 - 4\mu) d'_{\ell,\mu-1}(v_k)\} = 0 \quad (6.5.2)$$

Employing the relationship between the $d'_{\ell,\mu}(v_k)$ and the $d_{\ell,\mu}$ coefficients, equation (6.5.2) can be written as

$$\sum_{\nu=0}^{\frac{\ell+1}{2}} (-v_k)^{\frac{\ell-2\nu+1}{2}} \{(2\ell + 2m - 4\nu - 1) d_{\ell,\nu} - (2\ell + 2m - 4\mu - 1) v_k d'_{\ell,\mu-1}(v_k) + (2\ell - 4\nu + 3) d'_{\ell,\nu-1}(v_k)\} \quad (6.5.3)$$

and further reduces to

$$\sum_{\nu=0}^{\frac{\ell+1}{2}} (-v_k)^{\frac{\ell-2\nu+1}{2}} \{d_{\ell,\nu} [2\ell + 2m - 4\nu + 1] + \sum_{t=\nu+1}^{\frac{\ell+1}{2}} (2\ell + 2m - 4t - 1) + d_{\ell,\nu-1} \sum_{t=\nu}^{\frac{\ell+1}{2}} (2\ell - 4t + 3)\} = 0 \quad (6.5.4)$$

But, according to Gauss's lemma, (6.5.4) must be identical to

$$\sum_{\nu=0}^{\frac{\ell+1}{2}} (-v_k)^{\frac{\ell-2\nu-1}{2}} d_{\ell,\nu} \equiv 0 \quad (6.5.5)$$

Equating (6.5.4) and (6.5.5) results in a unique relationship between factor $d_{\ell,\nu}$ and factor $d_{\ell,\nu-1}$ with

$$\begin{aligned} d_{\ell,\nu} &= d_{\ell,\nu-1} \frac{\sum_{t=\nu}^{\frac{\ell+1}{2}} (2\ell - 4t + 3)}{[4\nu \sum_{t=1}^{\nu} (2\ell + 2m - 4t - 1)]} \\ &= d_{\ell,\nu-1} \frac{(\ell - 2\nu + 2)(\ell - 2\nu + 3)}{2\nu(2\ell + 2m - 2\nu + 1)} \quad (6.5.6) \end{aligned}$$

Since $d_{\ell,-1} = 0$, $d_{\ell,0} = 1$, an analytical expression of $d_{\ell,v}$ in terms of ℓ, m and v results, namely

$$d_{\ell,v} = \frac{\sum_{r=1}^v (\ell - 2r + 2)(\ell - 2r + 3)}{\sum_{r=1}^v (2r)(2\ell + 2m - 2r + 1)} \quad (6.5.7)$$

$$= \frac{[\ell(\ell - 2) \dots (\ell - 2v + 2)][(\ell + 1)(\ell - 1) \dots (\ell - 2v + 3)]}{(2v)!![(2\ell + 2m - 1)(2\ell + 2m - 3) \dots (2\ell + 2m - 2v + 1)]} \quad (6.5.8)$$

$$= \frac{(\ell + 1)!(2\ell + 2m - 2v - 1)!!}{(2v)!!(\ell - 2v + 1)!(2\ell + 2m - 1)!!}$$

$$d_{\ell,v} = \frac{[(\ell + m) - (m - 1)]![2(\ell + m) - 2v - 1]!!}{(2v)!![(1 + m) - (m - 1) - 2v]![2(\ell + m) - 1]!!} \quad (6.5.9)$$

and hence, (6.5.5) is equal to

$$\sum_{\mu=0}^{\frac{\ell+1}{2}} (-v_k) \frac{\ell-2\mu-1}{2} \frac{[(\ell + m) - (m - 1)]![2(\ell + m) - 2\mu + 1]!!}{(2\mu)!![(\ell + m) - (m - 1) - 2\mu]![2(\ell + m) - 1]!!} \quad (6.5.10)$$

Comparing the resulting expression with the expansion of the associated Legendre function of the first kind, of the degree 'm' and of the order ℓ , i.e.

$$P_{\ell}^m(u_k) = \frac{(2\ell)!}{2^{\ell} \ell! (\ell - m)!} (1 - u_k^2)^{\frac{m}{2}} \sum_{t=0}^{\frac{\ell-m}{2}} (-1)^t \frac{(\ell - m)!(2\ell - 2t - 1)!! u_k^{\ell - m - 2t}}{(2t)!! (\ell - m - 2t)! (2\ell - 1)!!} \quad (6.5.11)$$

it follows that the optimization function given by (6.5.11), when multiplied by the constant

$$\frac{2(\ell + m)}{2^{\ell+m} (\ell + m)! (\ell + 1)!} \quad (6.5.12)$$

equals:

$$O_N(u_k) = \frac{1}{(1-u_k^2)^{\frac{m-1}{2}}} P_{n+m}^{m-1}(u_k); \quad n = N - 1 \quad (6.5.13)$$

whose 'N' zeros representing the 'N' optimization cosines being sought.

It is to be noted that, for $m = 2$, (6.5.13) is identical with the expression obtained for the cylindrical case; except for the factor $(1 - u_k^2)$ in the denominator which appears in equation (6.5.13). This results because in this more general derivation both roots -1 and $+1$ needed to be removed.

6.6 RELEVANCE TO THE MEASUREMENT TECHNIQUE

Although no measurements have been carried out, the optimization technique derived here gives basic constraints upon the location of the bistatic measurement angles. These locations are important in obtaining maximum accuracy on the retrieval of the associated coefficients representing the field scattered by the various shapes considered. These constraints are summarized in Theorem I (section (4.3.4)) and in Theorem II (section (4.4)) for the spherical case; section (2.3.2) for the circular case.

Such theorems are of great importance to those engaged in the measurement of the scattered field since they simplify the compilation of the data by providing the exact locations where the measurements will be meaningful.

*chapter seven*SUMMARY AND CONCLUSIONS

This thesis has been only concerned with the establishment of an electromagnetic inverse scattering model, applicable to simple bodies of revolution. The incentive was not to unravel the extremely complex inverse scattering problem in its general formulations, but rather to bring some insight into the existing relationships between the shape of the scatterer and the far scattered field as observed for a known incident field.

Whereas most of the classical approaches to the problem, relying on inverse scattering boundary conditions⁽⁵³⁾ or on a method of analytical continuations^(55, 31), require the retrieval of the near field to recover the shape of the scatterers, it is emphasized and demonstrated that this procedure is not necessarily standard since all pertinent information concerning the geometry of the scatterers is implicitly contained within the far scattered field components. For simple shapes, the inverse scattering problem can then be solved much more directly. This particular aspect seems to have been neglected in the current literature and we have thus attempted here to present a serviceable theory and practical technique to fill this gap. The scope of this field has a vast range and the reader should remember that what is provided here is no more than the formulation of a particular method and some of its applications (for example, only perfectly conductive bodies, the sur-

face of which are describable by complete geometric co-ordinate surfaces have been discussed.) They are, in order: the circular cylinder, the elliptic cylinder, the sphere and the prolate spheroid. The analysis has been confined to these geometries because they are the simplest forms amenable to direct solutions and, therefore, they best exemplify the relevance of our theory. They are also commonly considered as the basic shapes to test methods of more general applicability; and it was hence natural to choose them in this presentation. Of course, it must be assumed at all times that the total scattered field is known in amplitude, phase and polarization at all points - with respect to a given co-ordinate system whose origin lies at the centre of the scatterer.

The development has been divided into two parts. The first part deals primarily with the recovery of the various shapes from far scattered field data. The second part comes, naturally, as a complement to the first one, insofar as it determines the location of the receiver's direction. Its main purpose is to obtain the best possible degree of accuracy in the portrayal of the scatterers. Although no measurements have been carried out, this part constitutes an important contribution to the field of inverse scattering, since it gives reliable information, thus ensuring a reasonable amount of certainty in prediction of the delineation of the object. Therefore, it deserves to be singled out into a separate section.

The investigation of the circular cylinder far exceeds the analysis of

the other geometric shapes, both in scale and in value. The reason for this is that it has been the subject of extensive research in earlier decades, due to its two-dimensional nature and to the simplicity of its shape, as well as to the fact that the spherical case can be traced back to the simple circular cylindrical case.....as shown in section (4.5). To say, finally, that the inverse scattering model, presented in this thesis, has originated from the careful investigation of this geometry, readily justifies the extent of the analysis.

Primarily, the scattered field has been expressed in a series expansion of circular wave functions. The truncated set of the unknown expansion coefficients has been related via the far scattered field matrix to the far scattered field components for non-identical aspect angles. The associated coefficients have been recovered by a matrix inversion procedure. The instabilities inherent in this procedure have been studied from the properties of the closed-form representation of the associated scattered field determinant. The location of the receiver's directions has been discriminated to obtain maximum accuracy in this procedure. This follows a novel, determinate optimization procedure derived in part B. Employing the results of this optimization procedure, it has been demonstrated that the electrical radius of the cylinder could be recovered from the associated expansion coefficients, for all polarization cases.

In the case where the domain of observation is restricted to a small wedge angle, a rather tedious derivation has been initiated to palliate

the decrease in accuracy of the obtained expansion coefficients. This also applies when the electrical radius of the cylinder is much larger than unity. Finally, when it becomes almost impossible to determine the expansion coefficients accurately due to the unstable nature of the far scattered field matrix, an iterative averaging method has been introduced in section (2.7). Such a method is essentially based upon the dependence of the back scattering cross-section of the scatterer with the magnitude of the scattered electric field. This technique gives good results to all of the cases encountered, i.e. ka varying between 1 and 15.

The study of the elliptic cylinder is carried out in the same manner as that of the circular cylinder. However, in contrast with the former instance, no simple relations exist between the two electrical axes and the associated wave function coefficients. This follows from the description of the far scattered field, in terms of Mathieu functions, which are much more difficult to manipulate. For this geometry, which covers a wider latitude of interest than that of the circular cylinder, only the iterative averaging method is conclusive, namely that the radius of curvature can be recovered via a comparative study with a circular cylinder of identical curvature. It is then anticipated that this technique could be successfully applied to retrieve the main radii of curvature of smooth-convex shapes.

The three-dimensional problem is then approached with a study of the

spherical case. It is shown, in particular, that the electrical radius can be recovered again from the associated expansion coefficients. The formulae here obtained are quite similar to those obtained for a circular geometry. The reason for this is that the Hansen's wave functions, employed in the case of the sphere, depend upon the spherical Bessel functions, while the circular wave functions depend upon the cylindrical Bessel functions...the latter being simply related to the former. The determinant associated with the scattered field matrix which relates a finite set of transverse field components to the truncated set of expansion coefficients, has also been optimized in part B.

Finally, the problem of the prolate spheroid is broached using a new formulation of the scattered field, in terms of Legendre polynomials as given by Stevenson⁽⁴⁵⁾. Due to the lack of tables, no computations can be presented...although the inverse scattering model used for the other geometries is successfully applicable. Much more research should be devoted to the study of the direct, as well as the inverse, problem concerning the prolate spheroid, but it would exceed the scope of this thesis. It has been of interest to show how our model could be applied to various shapes; this example is hence only illustrative.

In conclusion, the electromagnetic inverse scattering model presented here relates the shape of the scatterer to the expansion coefficients employed in the formulation of the far scattered fields, in terms of orthogonal wave functions. Although it is not as general a conclusion

as those of: Weston, Bowman and Ar⁽⁵⁷⁾; Weston and Boerner⁽⁵⁵⁾; Lewis⁽²⁸⁾; Millar⁽³⁰⁾; and Imbriale and Mittra⁽¹⁵⁾it does, however, bring some fundamental relationships which could be applied to other sophisticated inverse scattering models and techniques. Those relations could prove to be of great importance, for example, in the formulation of the direct problem of scattering -- where one coefficient could be expressed in terms of the others; or again, it might be possible to relate the various creeping waves, which originate in the formulation of the direct problem of scattering by simple shapes, since each of these depend upon such expansion coefficients. It may turn out to be of some interest in the convergence problem, where the higher order creeping waves could be expressed in terms of the lower order creeping waves. Moreover, magnetic and electric expansion coefficients are also related to one another. It is thereby anticipated that the scattered field could be uniquely expressed in terms of only one set of expansion coefficients, associated with either the electric type wave functions or with the magnetic type wave functions if such a similar relationship could be found among these wave functions. This particular aspect requires further investigation.

In addition, while none of the geometries encountered in this thesis duplicate practical shapes, the inverse scattering model, developed here, could be applied to obstacles, for which the formulation of the scattered field can be expressed in terms of "surface harmonic wave functions multiplied by appropriate expansion coefficients". In the

same line of thought...dielectric coated objects should be investigated as well, since all information relative to these objects is indeed included in the far scattered field. For instance, it is conjectured that one can retrieve the electrical radius, the electrical depth of the layer and the dielectric constant of a dielectric coated cylinder or sphere by employing our inverse scattering model. In these cases, more expansion coefficients would be necessary in comparison to the above mentioned cases, to recover, uniquely, both information. However, it is anticipated that relationships similar to (2.4.4), (2.4.14), (4.5.5), and (4.5.7) should exist.

Finally, the optimization procedure, as developed in part B, can be applied to many other areas of research. It should, in particular, be profitable to those dealing with matrix inversion procedure since it permits the elimination of instabilities in the inversion, and that, whenever the matrix elements are following a Vandermonde type pattern. Its applicability is therefore not restricted to the electromagnetic theory. It could prove to be a very efficient tool in optimizing determinants whose elements are trigonometric, Legendre, Tschebycheff or other band-limited functions.

To conclude, extensive research is still required in this field of "inverse scattering", if a comprehensive understanding of its actual mechanism is desired, and especially since the vast majority of objects encountered in practice are not the simple shapes we have examined. It is, however, our hope that this contribution, partial as it may be,

will bring some insight into this extremely complex field and contribute to the ultimate goal of defining the shape of any obstacle. Indeed, this model could be employed as an additional radar signature which would allow significant reduction of ambiguity in the portrayal of simple shapes....when correlated with other models. It is also our hope that this technique will open up new avenues in this area, and hasten the eventual resolution of this problem in its entirety.

REFERENCES

1. Abramowitz, M. and Stegun, I. A., "Handbook of Mathematical Functions with Formulas, Graphs, and Mathematical Tables", Dover Publications, Inc., New York, 1954.
2. Altman, J. L., Bates, R. H. T. and Fowle, E. N., "Introductory Notes Related to Electromagnetic Inverse Scattering", The MITRE Corporation Contract No. AF 19(628)-2390, Project No. 496.0, 1964, pp. 1 - 203.
3. Atkinson, F. V., "On Sommerfeld's 'Radiation Condition'", Philos. Mag., vol. XL, 1949, pp. 645 - 651.
4. Bargmann, V. A., "On the Connection between Phase Shifts and Scattering Potential", Rev. Modern Physics, vol. 21, 1949, pp. 448 - 493.
5. Boerner, W. M. and Antar, Y. M., "Aspects of E.M. Pulse Scattering from a Grounded Dielectric Slab", to be published in Archiv der Elektrischen Übertragung, 1972.
6. Boerner, W. M., Aboul-Atta, O. A. and Vandenberghe, F. H., "General Properties of the Scattered Field Matrix in Spherical Coordinates", to be published in Applied Mathematical Journal.
7. Boerner, W. M., Vandenberghe, F. H. and Hamid, M. A. K., "Determination of the Electrical Radius ka of a Circular Cylindrical Scatterer from the Scattered Field", Can. Journal of Physics, vol. 49, No. 7, 1971, pp. 804 - 819.
8. Boerner, W. M. and Vandenberghe, F. H., "Determination of the Electrical Radius ka of a Spherical Scatterer from the Scattered Field", Can. Journal of Physics, vol. 49, No. 11, 1971, pp. 1507 - 1535.
9. Bojarski, N. N., "Three-dimensional Electromagnetic Short Pulse Inverse Scattering", Syracuse University, Res. Corp., Syracuse, New York, 1967.
10. Crispin, J. W., Hiatt, Jr. R. E., Sleator, F. B. and Siegel, K. M., "The Measurement and Use of Scattering Matrices", University of Michigan, 1961, purchase order No. SC-11334.
11. Einarson, O., Kleinman, R. E., Laurin, P. and Uslenhi, P. L. E., "Studies in Radar Cross Section L-Diffraction and Scattering by Regular Bodies IV: The Circular Cylinder", University of Michigan Radiation Laboratory, Report No. 7133-3T, 1966.

12. Erma, V. A., "An Exact Solution for the Scattering of Electromagnetic Waves from Conductors of Arbitrary Shape. I. Case of Cylindrical Symmetry", *The Physical Review*, Vol. 173, No. 5, 1968, pp. 1243 - 1257.
13. Faddeyev, L. D., "On Inverse Problem in Quantum Theory of Scattering", *J. Math. Phys.*, Vol. 4, 1963, pp. 72 -
14. Freedman, A., "The Portrayal of Body Shape by a Sonar or Radar System", *The British Institution of Radio Engineers*, Vol. 25, 1963, pp. 51 - 64.
15. Imbriale, W. A. and Mittra, R., "The Two-dimensional Inverse Scattering Problem", *Antenna Lab., University of Illinois*, Report No. 69-6, 1969.
16. Jahnke, E. and Emde, F., "Tables of Functions with Formulae and Curves", (Dover Publications, New York).
17. Kazarinoff, N. D. and Ritt, R. K., "Scalar Diffraction by an Elliptic Cylinder", *IRE Trans.*, AP-7, 1959, pp. 521 - 527.
18. Kazarinoff, N. D. and Ritt, R. K., "On the Theory of Scalar Diffraction and Its Application to the Prolate Spheroid", *Annals of Physics*, Vol. 6, 1959, pp. 277 - 299.
19. Karp, S. N., "A Convergent 'Farfield' Expansion for Two-dimensional Radiation Functions", *Comm. Pure Appl. Math.*, Vol. XIV, 1961, pp. 427 - 434.
20. Karp, S. N., "Far Field Amplitude and Inverse Diffraction Theory" appearing in "Electromagnetic Waves", *Proc. of a Symposium at the University of Wisconsin*, April, 1961, pp. 291 - 300.
21. Kay, J., "The Inverse Scattering Problem when the Reflection Coefficient is a Rational Function", *Comm. Pure Appl. Math.*, Vol. 13, 1960, pp. 375 - 393.
22. Kell, R. E., "On the Derivation of Bistatic Cross-Section from Monostatic Measurements", *Proc. of the IEEE*, Vol. 53, Part I, 1965, pp. 983 - 992.
23. Keller, J. B., "The Inverse Scattering Problem in Geometrical Optics and the Design of Reflectors", *IRE Trans.*, AP-7, 1959, pp. 146 - 149.
24. Kennaugh, E. M. and Moffat, D. L., "Transient and Impulse Response Approximation", *IEEE Trans.*, AP-17, Vol. 53, No. 8, 1965, pp. 893 - 901.

25. Kowalewski, G., "Einführung in die Determinanten Theorie (Chelsea Publ. Co., New York, 1948).
26. Levy, B. R., "Diffraction by an Elliptic Cylinder", Jour. of Math. and Mech., Vol. 9, 1960, pp. 147 - 165.
27. Levy, B. R. and Keller, J. B., "Diffraction by a Spheroid", Can. Jour. of Physics, Vol. 38, 1960, pp. 28 - 144.
28. Lewis, R. M., "Physical Optics Inverse Diffraction", IEEE Trans., AP-17, No. 3, 1969, pp. 308 - 314.
29. McLahlan, N. W., "Theory and Application of Mathieu Functions", (Dover Publications, Inc., New York, 1963).
30. Millar, R. F., "Rayleigh Hypothesis in Scattering Problems", Electronic Letters, Vol. 5, No. 17, 1969, pp. 416 - 417.
31. Mittra, R. and Imbriale, W. A., "The Two-dimensional Inverse Scattering Problem", Laboratory Report No. 69-6, Department of Electrical Engineering, University of Illinois, Urbana, Illinois, 1969.
32. Mittra, R. and Wilton, D. R., "A Numerical Approach to the Determination of Electromagnetic Scattering Characteristics of Perfect Conductors", Proceedings of the IEEE, 1969, pp. 2064 - 2065.
33. Mitzner, H. M., "An Integral Equation Approach to Scattering From a Body of Finite Conductivity", Radio Science, Vol. 2, (New Series), No. 12, 1967, pp. 1459 - 1470.
34. Morse, P. M. and Feshbach, H., "Methods of Theoretical Physics, Vol. I and Vol. II", McGraw-Hill Book Co., Inc., New York, 1953).
35. Moses, H. E. and de Ridder, C. M., "Properties of Dielectrics from Reflection Coefficients in One Dimension", Technical Report No. 322, Lincoln Laboratory, M.I.T., 1965.
36. Müller, C., "Radiation Patterns and Radiation Fields", Jour. Rat. Mech. and Anal., Vol. 4, 1955, pp. 235 - 246.
37. Müller, C., "Electromagnetic Radiation Patterns and Sources", IRE Trans., AP- 4, No. 3, 1956, pp. 224 -232.
38. Petrina, D. Ia., "Solution of the Inverse Scattering Problem", Ukrainakii Matematicheskii Zhurnal (U.S.S.R.), Vol. 12, No. 2, 1960, pp. 476 - 479 (Translation: OTS 62-11505; AD 255678).
39. Ross, R. A., "Scattering by a Finite Cylinder", Proc. IEEE, Vol. 114, No. 7, 1967, pp. 864 - 868.

40. Saunders, W. K., "On Solutions of Maxwell's Equations in an Exterior Region", Proc. Nat. Acad. Sci. U.S.A., Vol. 38, 1952, pp. 342 - 348.
41. Schultz, F. V., "Scattering by a Prolate Spheroid", Report UMM-42, Willow Run Research Center, University of Michigan, 1950.
42. Senior, T. B. A., "The Scattering of an Electromagnetic Wave by a Spheroid", Can. Jour. of Physics, Vol. 44, No. 7, 1966, pp. 1353 - 1359.
43. Shafai, L., "An Improved Integral Equation for the Numerical Solution of Two-dimensional Diffraction Problems", Can. Jour. of Physics, Vol. 48, No. 8, 1970, pp. 954 - 963.
44. Smirnow, W. I., "Lehrgang der Höheren Mathematik, Teil I", (VEB Deutscher Verlag der Wissenschaften, Berlin).
45. Stevenson, A. F., "Solution of Electromagnetic Scattering Problems as Power Series in the Ratio (Dimension of Scatterer)/Wave-Length", Journal of Applied Physics, Vol. 24, No. 9, 1953, pp. 1134 - 1151.
46. Stratton, J., "Electromagnetic Theory", McGraw-Hill Book Co., Inc., New York, 1941.
47. Vandenberghe, F. and Boerner, W. M., "On the Inverse Problem of Scattering from a Perfectly Conducting Prolate Spheroid", to be published in Can. Jour. of Physics, 1972.
48. Waterman, J. C., "New Formulation of Acoustic Scattering", Jour. of the Acoustical Society of America, Vol. 45, No. 6, 1969, pp. 1417 - 1429.
49. Waterman, P. C. and McCarthy, C. V., "Numerical Solution of Electromagnetic Scattering Problems", The MITRE Corp., 1968.
50. Weinstein, L. A. and Fedorov, A. A., "Scattering of Plane and Cylindrical Waves on an Elliptical Cylinder and Conception of Diffraction Rays", Radiotekhnika i Elektronika 6, No. 1, 1961, pp. 31 - 46.
51. Weston, V. H., Boerner, W. M. and Dolph, C. H., "Inverse Scattering Investigation", University of Michigan, 1967, Contract AF 19(628)-67-C-0190.
52. Weston, V. H. and Boerner, W. M., "Inverse Scattering Investigation", University of Michigan, 1968, Contract AF 19(628)-67-C-0190.
53. Weston, V. H. and Boerner, W. M., "University of Michigan Radiation Laboratory Report", No. 8579-I-F, ESD-TR-67-517 (see also ESD-TR-67-517 Reports, Vols. 1 - 4), 1968.

54. Weston, V. H. and Boerner, W. M., "Inverse Scattering Investigation Final Report", University of Michigan Radiation Laboratory Report No. 8579-I-F, ESD-TR-67-517, 1968.
55. Weston, V. H. and Boerner, W. M., "An Inverse Scattering Technique for Electromagnetic Bistatic Scattering", Can. Jour. of Physics, Vol. 47, 1969, pp. 1177 - 1183.
56. Weston, V. H. and Bowman, J. J., "Inverse Investigation", 1 April - 30 June, 1966, University of Michigan, 1966, Contract AF 19(628)-4884.
57. Weston, V. H., Bowman, J. J. and Ergun, Ar., "Inverse Scattering Investigation", Final Report, 10 October, 1965 - 30 September, 1966, University of Michigan, 1966, Contract AF 19(628)-4884.
58. Weston, V. H. and Einarsson, O., "Inverse Scattering Investigation", 1 October - 31 December, University of Michigan, 1966, Contract AF(628)-4884.
59. Weyl, H., "Die Natürlichen Randwertaufgaben im Aussenraum für Strahlungsfelder Beliebiger Dimension und Beliebigen Ranges", Math. Z., Vol. 56, No. 12, 1952, pp. 105 - 119.
60. Wilcox, C. H., "An Expansion Theorem for Electromagnetic Fields", Comm. Pure Appl. Math., Vol. 9, 1956, pp. 115 - 134.

appendix A.1

RETRIEVAL OF THE POLARIZATION ANGLE δ

Assuming normal incidence with respect to the cylinder axis, then the ambiguity still exists in the proper recovery of the polarization angle δ , defined in (2.2.1) and illustrated in Fig. 1. If $\delta \neq 0$ or $\frac{\pi}{2}$ both (2.2.3) and (2.2.4) must be used for recovering "ka". The cases for which δ is known, have been treated in section 2.4 and here it is shown that δ can be uniquely recovered although it may not be known with precision.

Thus, instead of employing (2.2.5b) and (2.2.6b), the unknown expansion coefficients may now be defined as

$$a'_n = a_n \cos \delta \quad (\text{A.1.1})$$

$$b'_n = b_n \sin \delta \quad (\text{A.1.2})$$

such that (2.2.5b) and (2.2.6b) are replaced by

$$a''_n = a'_n H_n^{(1)}(kR) \quad \text{and} \quad b''_n = b'_n H_n^{(1)'}(kR)$$

resulting in no changes in the matrix formulation of (2.2.11) or in the inversion procedure of section 2.3. Thus, for a fixed computational co-ordinate system and a non-singular distribution of aspect angles, the coefficients a'_n and b'_n can be obtained to the degree of accuracy dictated only by the measurement and the inversion techniques. If the recovered coefficients a'_n are inserted in (2.2.4), the resulting expression for "ka" is identical with that using the coefficient a_n . This is so, since

$a'_n = a_n \cos \delta$ and therefore the constant multiplier $\cos \delta$ cancels in (2.2.4). Assuming that the proper value of "ka" is found, then a_n can be recalculated from the cylindrical radial functions as

$$a_n = - \frac{J_n(ka)}{H_n^{(1)}(ka)} \quad (2.2.5b)$$

and therefore

$$\cos \delta = \frac{a'_n}{a_n} \quad (A.1.3)$$

To determine δ uniquely, the three degenerate cases, defined by (A.3.2), (A.3.16) and (A.3.17), may be employed if the coefficients $a'_0, a'_1, a'_2, b'_0, b'_1, b'_2, b'_3,$ and b'_4 are known to the aforementioned degree of accuracy.

From (A.1.1), (A.1.2), (2.2.5b), (2.2.6b), and (A.3.2), another relationship for the polarization angle δ is found

$$\tan \delta = \frac{b'_0}{a'_1} \quad (A.1.4)$$

Similar relationships are obtained from (A.3.16) and (A.3.17) where in (A.3.16) the expression on the left hand side is related to that on the right hand side by

$$\tan \delta = \frac{a'_0(b'_v)}{a'_1} \quad (A.1.5)$$

and similarly for (A.3.17)

$$\tan \delta = \frac{a'_2(b'_v)}{a'_1} \quad (A.1.6)$$

Similar expressions can obviously be obtained for all higher order a'_n employing $(n + 1)$ th order iterations of (2.4.8) in terms of the known b'_n coefficients.

Since (A.1.3) to (A.1.6) are determinate relationships, it may be of practical interest to note that δ can be uniquely recovered using only two sets of measurements.

appendix A.2

PROPERTIES OF THE VANDERMONDE DETERMINANT

It is to be shown that the determinant $|\phi(N)|$ of a matrix $[\phi(N)]$ which is generated from a Vandermonde matrix $[W(w_{\mu\nu} = x_{\mu}^{\nu-1}, \nu = 1, 2, \dots, N)]$, by adding to consecutive column vectors, preceding column vectors times some constant multipliers $q_{\nu t}$ as follows

$$[\phi] = [w_1, w_2 + q_{12}w_1, w_3 + q_{23}w_2 + q_{13}w_1, \dots, w_n + \dots + q_{1n}w_1] \quad (\text{A.2.1})$$

is given by

$$|\phi| = \text{Det} \cdot [\phi] = |w_1, w_2, w_3, \dots, w_n| = |W| \quad (\text{A.2.2})$$

where in particular

$$|W(w_{\mu\nu} = x_{\mu}^{\nu-1}, \nu = 1, 2, 3, \dots, N)| = (-1)^{\frac{(N-1)N}{2}} \prod_{\substack{N > r > s > 1}} (x_r - x_s) \quad (\text{A.2.3})$$

The statement (A.2.2) can easily be proven from the following property of determinants⁽²⁵⁾.

The determinant $|\phi|$ of a matrix $[\phi]$ which is generated from a matrix $[\psi]$ of non-identical column vectors ψ_{ν} , by adding to consecutive column vectors, preceding column vectors times some constant multiplier $p_{\nu t}$ as follows

$$[\phi] = [\psi_1, \psi_2 + p_{12}\psi_1, \psi_3 + p_{23}\psi_2 + p_{13}\psi_1, \dots, \psi_n + \dots + p_{1n}\psi_1] \quad (\text{A.2.4})$$

is given by

$$|\phi| = \text{Det} \cdot [\phi] = |\psi_1, \psi_2, \psi_3, \dots, \psi_n| = |\psi| \quad (\text{A.2.5})$$

which follows directly from the expansion of the determinant.

Statement (A.2.3) follows from the properties of the Vandermonde determinant associated with the Vandermonde matrix⁽²⁵⁾, where

$$\begin{aligned}
 & \begin{vmatrix} x_1^{N-1} & x_1^{N-2} & \dots & x_1^{N-\nu} & \dots & x_1^0 \\ x_2^{N-1} & x_2^{N-2} & \dots & x_2^{N-\nu} & \dots & x_2^0 \\ \vdots & \vdots & & \vdots & & \vdots \\ x_\mu^{N-1} & x_\mu^{N-2} & \dots & x_\mu^{N-\nu} & \dots & x_\mu^0 \\ \vdots & \vdots & & \vdots & & \vdots \\ x_N^{N-1} & x_N^{N-2} & \dots & x_N^{N-\nu} & \dots & x_N^0 \end{vmatrix} = \\
 & = (-1)^{\frac{(N-1)N}{2}} \begin{vmatrix} x_1^0 & x_1^1 & \dots & x_1^{\nu-1} & \dots & x_1^{N-1} \\ x_2^0 & x_2^1 & \dots & x_2^{\nu-1} & \dots & x_2^{N-1} \\ \vdots & \vdots & & \vdots & & \vdots \\ x_\mu^0 & x_\mu^1 & \dots & x_\mu^{\nu-1} & \dots & x_\mu^{N-1} \\ \vdots & \vdots & & \vdots & & \vdots \\ x_N^0 & x_N^1 & \dots & x_N^{\nu-1} & \dots & x_N^{N-1} \end{vmatrix} = \\
 & (-1)^{\frac{N(N-1)}{2}} \prod_{\substack{N > r > s > 1}} (x_r - x_s) \quad (\text{A.2.6})
 \end{aligned}$$

appendix A.3

FORMULATION OF THE a_0 , a_1 AND a_2 COEFFICIENTS IN TERMS OF THE b_n
COEFFICIENTS

It is now demonstrated that the three contiguous coefficients a_0 , a_1 and a_2 can be determined in terms of a finite number of b_ν coefficients. Using the well-known properties of cylindrical wave functions

$$Z_{-\nu} = (-1)^\nu Z_\nu, \quad Z'_{-\nu} = (-1)^\nu Z'_\nu \quad (\text{A.3.1})$$

gives $a_{-n} = a_n$ and $b_{-n} = b_n$. This may be employed to relate a_1 and b_0 , since from (2.4.5), (A.3.1), (2.2.5b) and (2.2.6b), $Z'_0 = -Z_1$, therefore,

$$a_1 \equiv b_0 \quad (\text{A.3.2})$$

This represents the single degenerate case in which one b_ν coefficient is related to one a_ν coefficient. Employing either (2.4.4), (2.4.14) or (2.4.16), a_0 and a_2 must be related to a finite number of b_ν coefficients. Otherwise, the higher order a_n coefficients cannot be obtained in terms of the b_ν coefficients from higher iterations of (2.4.18). One additional degenerate relationship results from (2.4.15) with $\nu = 2$, i.e.

$$4Z'_3 = \rho/2 [Z'_4 - Z'_0] \quad (\text{A.3.3})$$

which yields with (2.2.6b)

$$\frac{\rho}{2} = \frac{4Z'_3}{Z'_4 - Z'_0} = \frac{4H_3^{(1)'}}{H_4^{(1)' } - H_0^{(1)'}}$$

$$\frac{4J'_3}{J'_4 - J'_0} = \frac{4b_3 H_3^{(1)'}}{b_4 H_4^{(1)' } - b_0 H_0^{(1)'}} \quad (\text{A.3.4})$$

and

$$\frac{H_4^{(1)'}}{H_0^{(1)'}} = -\frac{b_0 - b_3}{b_3 - b_4} = -\frac{b_{03}}{b_{04}} \quad (\text{A.3.5})$$

where in the following the notation $b_{\mu\nu} = b_\mu - b_\nu$ is used, thus satisfying the identity transformation

$$b_{rs} b_{uv} = b_{ru} b_{sv} + b_{rv} b_{us} \quad (\text{A.3.6})$$

On the other hand, the ratio of (A.3.5) can be expressed, with further algebraic transformations, as

$$\frac{H_4^{(1)'}}{H_0^{(1)'}} = \frac{H_4^{(1)'}}{H_2^{(1)'}} \cdot \frac{H_2^{(1)'}}{H_0^{(1)'}} = \frac{-b_{20}(a_5 - a_3)}{(a_5 - b_4)(a_3 - b_2)} \quad (\text{A.3.7})$$

which, with successive applications of (2.4.8), can be expressed in terms of a_2 and a finite number of b_ν coefficients as

$$\frac{H_4^{(1)'}}{H_0^{(1)'}} = -\frac{[(a_2 - b_0)b_{32} - (a_2 - b_3)b_{20}](a_2 - b_0)}{(a_2 - b_0)(a_2 - b_3)b_{42} - (a_2 - b_4)(a_2 - b_3)b_{20} - (a_2 - b_2)(a_2 - b_0)b_{34}} \quad (\text{A.3.8})$$

Equating (A.3.5) and (A.3.8) yields

$$\begin{aligned} & \{+(a_2 - b_0)(a_2 - b_3)b_{02}b_{34} - (a_2 - b_0)(a_2 - b_0)b_{23}b_{34} + \\ & (a_2 - b_0)(a_2 - b_3)b_{24}b_{03} - (a_2 - b_3)(a_2 - b_4)b_{02}b_{03} + \\ & (a_2 - b_0)(a_2 - b_2)b_{03}b_{34}\} \equiv 0 \end{aligned} \quad (\text{A.3.9})$$

With $\alpha_0 = (a_0 - b_0)$ and $\alpha_1 = (a_0 - b_1)$ and further application of (2.4.18), equation (A.3.9) is reduced to an expression explicit in a_0 and a finite number of b_ν coefficients:

$$\begin{aligned} & [\alpha_0^2 L_1 + \alpha_0 \alpha_1 M_1 + \alpha_1^2 N_1] = [\alpha_0^2 \{+ b_{01} b_{01} b_{23} b_{34} + b_{01} b_{02} b_{13} b_{34} + b_{01} b_{03} b_{13} b_{24} \\ & + b_{02} b_{03} b_{13} b_{14} + b_{01} b_{03} b_{12} b_{34}\} + \alpha_0 \alpha_1 \{b_{01} b_{02} b_{03} b_{34} + b_{01} b_{02} b_{03} b_{34} + \\ & b_{01} b_{03} b_{03} b_{24} + b_{02} b_{03} b_{03} b_{14} + b_{02} b_{03} b_{04} b_{13}\} + \alpha_1^2 b_{02} b_{03} b_{03} b_{04}] \equiv 0 \end{aligned} \quad (\text{A.3.10})$$

However, to find a relationship for a_2 or a_0 in terms of b_v , another relationship is found by equating (2.4.14a) and (2.4.14b) for $n = 2$

$$\frac{b_{01}(a_2 - b_3)}{b_{02}(a_2 - b_1)} = 3 \frac{(a_3 - b_3)}{(a_3 - b_2)} \quad (\text{A.3.11})$$

which, with repeated application of (2.4.18) results in

$$[b_{01}(a_2 - b_3)(a_2 - b_2) - 3b_{02}(a_2 - b_3)(a_2 - b_1) + 3b_{23}(a_2 - b_0)(a_2 - b_1)] \equiv 0 \quad (\text{A.3.12})$$

or

$$[\alpha_0^2 L_2 + \alpha_0 \alpha_1 M_2 + \alpha_1^2 N_2] = [\alpha_0^2 b_{12} b_{13} + \alpha_0 \alpha_1 \{b_{12} b_{03} - 3b_{23} b_{01} - 2b_{13} b_{02}\} - \alpha_1^2 2b_{02} b_{03}] \equiv 0 \quad (\text{A.3.13})$$

Since $\alpha_0, \alpha_1 \neq 0$, a relationship for a_0 results from (A.3.10) and (A.3.13) by eliminating the quadratic term α_1^2 :

$$\alpha_0 \{ \alpha_0 (2L_1 + b_{03} b_{04} L_2) + \alpha_1 (2M_1 + b_{03} b_{04} M_2) \} \equiv 0 \quad (\text{A.3.14})$$

By employing (A.3.6), the constant multipliers in (A.3.14) reduce to

$$(2L_1 + b_{03} b_{04} L_2) = b_{13}^L = b_{13} \{ + 8 b_{02} b_{03} b_{14} - 4 b_{02} b_{04} b_{13} - b_{03} b_{04} b_{12} \} \quad (\text{A.3.15a})$$

and

$$(2M_1 + b_{03} b_{04} M_2) = b_{03}^M = b_{03} \{ + 8 b_{02} b_{03} b_{14} - 7 b_{02} b_{04} b_{13} + 2 b_{03} b_{04} b_{12} \} \quad (\text{A.3.15b})$$

Therefore, the desired relationships for $a_2, a_1,$ and a_0 are given by

$$a_0(b_v) \equiv \frac{[b_0 b_{13}^L + b_1 b_{03}^M]}{[b_{13}^L + b_{03}^M]} \quad (\text{A.3.16})$$

$$a_1 \equiv b_0, \quad (\text{A.3.2})$$

$$a_2(b_v) \equiv \frac{[b_0 b_{13}^L - b_1 b_{03}^M]}{[b_{13}^L - b_{03}^M]} \quad (\text{A.3.17})$$

where the denominators in (A.3.16) and (A.3.17) will only vanish simultaneously if $b_0 = b_3$ and $b_1 = b_3$. For that particular case, it is found that $L = M$, $a_0 = b_0 = b_1$, and $a_2 = 0$. Thus, the existence of two contiguous coefficients (i.e. $a_0 = a_0(b_v)$ and $a_1 = a_1(b_v)$ or $a_1 = a_1(b_v)$ and $a_2 = a_2(b_v)$) is guaranteed in all cases.

appendix A.4

FORMULATION OF $\{a_{n+4}, n \geq 0\}$ IN TERMS OF $\{a_0, a_1, a_2, a_3\}$

To decrease the size of the matrix $[\phi(N)]$, the coefficient $a_{n+4}, n \geq 0$ has to be expressed as a linear combination of the set $\{a_0, a_1, a_2, a_3\}$. It is shown that this is not the case, but that a_{n+4} can be related to that set in a very sophisticated manner.

With the definitions given in (2.6.8), A_4 and B_4 are written as

$$\begin{aligned} A_4 &= T_4 = 3 a_{20} A_3 - A_2 B_4 = 3 a_{21} a_{20} \\ B_4 &= U_4 = 3 a_{20} B_3 - B_2 B_4 = a_{32} a_{10} \end{aligned} \quad (\text{A.4.1})$$

In order to obtain a more specific description of the iterative formula (2.6.5), and to induct a formation law for the coefficient A_{n+4} and B_{n+4} , the case $n = 1$ is treated separately. For $n = 1$, equations (2.6.1) and (2.6.2) result in

$$a_5 = \frac{a_4 T_5 - a_3 U_5}{T_5 - U_5} = \frac{a_4 [4a_{32} a_{31}] - a_3 [2a_{43} a_{21}]}{4a_{32} a_{31} - 2a_{43} a_{21}} \quad (\text{A.4.2})$$

After substitution of a_4 by its value as given in (2.6.3), with

$$a_{43} = a_4 - a_3 = \frac{a_3 A_4 - a_2 B_4}{A_4 - B_4} - a_3 = \frac{a_{32} B_4}{A_4 - B_4} \quad (\text{A.4.3})$$

the coefficient a_5 is expressed as:

$$a_5 = \frac{\left[\frac{a_3 A_4 - a_2 B_4}{A_4 - B_4} \right] 4a_{32} a_{31} - a_3 \left[\frac{2a_{32} B_4}{A_4 - B_4} \right] a_{21}}{4a_{32} a_{31} - 2a_{21} \left[\frac{a_{32} B_4}{A_4 - B_4} \right]}$$

$$= \frac{a_3 [2a_{31} A_4 - a_{21} B_4] - a_2 [2a_{31} B_4]}{[2a_{31} A_4 - a_{21} B_4] - [2a_{31} B_4]} \quad (\text{A.4.4})$$

According to (2.6.5), a_5 formulated as

$$a_5 = \frac{a_3 [2a_{31} A_4 - A_3 B_4] - a_2 [2a_{31} B_4 - B_3 B_4]}{[2a_{31} A_4 - A_3 B_4] - [2a_{31} B_4 - B_3 B_4]} \quad (\text{A.4.5})$$

is identical with

$$\frac{a_3 A_5 - a_2 B_5}{A_5 - B_5} \quad (\text{A.4.6})$$

(A.4.5) and (A.4.6) verify that

$$\begin{aligned} A_5 &= 2a_{31} A_4 - A_3 A_4 \\ B_5 &= 2a_{31} B_4 - B_3 B_4 \end{aligned} \quad (\text{A.4.7})$$

which is in accordance with the general law as stated in (2.6.6).

Assuming that a_{n+4} , $n \geq 0$ can always be written in the form (2.6.5),

the coefficient a_{mp} for $m > p \geq 2$ can be expressed as

$$\begin{aligned} a_{mp} &= a_m - a_p = \frac{a_3 A_m - a_2 B_m}{A_m - B_m} - \frac{a_3 A_p - a_2 B_p}{A_p - B_p} \\ &= a_{32} \frac{A_p B_m - B_p A_m}{[A_m - B_m][A_p - B_p]} \end{aligned} \quad (\text{A.4.8})$$

and for any n , (2.6.1) can be formulated as:

$$\frac{\left[\frac{a_3 A_{n+3} - a_2 B_{n+3}}{A_{n+3} - B_{n+3}} \right]^{(n+3)} \left[\frac{A_{n+1} B_{n+2} - A_{n+2} B_{n+1}}{[A_{n+1} - B_{n+1}][A_{n+2} - B_{n+2}]} \right] \left[\frac{A_n B_{n+2} - A_{n+2} B_n}{[A_{n+2} - B_{n+2}][A_n - B_n]} \right]}{\left[\frac{A_{n+1} B_{n+2} - A_{n+2} B_{n+1}}{[A_{n+1} - B_{n+1}][A_{n+2} - B_{n+2}]} \right] \left[\frac{A_n B_{n+2} - A_{n+2} B_n}{[A_{n+2} - B_{n+2}][A_n - B_n]} \right]}$$

$$\begin{aligned}
& \frac{\left[\frac{a_3 A_{n+2} - a_2 B_{n+2}}{A_{n+2} - B_{n+2}} \right] \left[\begin{matrix} [n+1] \\ \left[\frac{A_{n+1} B_{n+3} - A_{n+3} B_{n+2}}{[A_{n+3} - B_{n+3}] [A_{n+2} - B_{n+2}]} \right] \left[\frac{A_n B_{n+1} - B_n A_{n+1}}{[A_n - B_n] [A_{n+1} - B_{n+1}]} \right] \end{matrix} \right]}{\left[\begin{matrix} [n+1] \\ \left[\frac{A_{n+1} B_{n+3} - A_{n+3} B_{n+2}}{[A_{n+3} - B_{n+3}] [A_{n+2} - B_{n+2}]} \right] \left[\frac{A_n B_{n+1} - B_n A_{n+1}}{[A_n - B_n] [A_{n+1} - B_{n+1}]} \right] \end{matrix} \right]} \\
& \hspace{15em} (A.4.9)
\end{aligned}$$

which is written more concisely as

$$a_{n+4} = \frac{a_3 \left[\frac{A_{n+3} z_{n+3} - A_{n+2} y_{n+2}}{A_{n+3} z_{n+3} - A_{n+2} y_{n+2}} \right] - a_2 \left[\frac{B_{n+3} z_{n+3} - B_{n+2} y_{n+2}}{B_{n+3} z_{n+3} - B_{n+2} y_{n+2}} \right]}{\left[\frac{A_{n+3} z_{n+3} - A_{n+2} y_{n+2}}{A_{n+3} z_{n+3} - A_{n+2} y_{n+2}} \right] - \left[\frac{B_{n+3} z_{n+3} - B_{n+2} y_{n+2}}{B_{n+3} z_{n+3} - B_{n+2} y_{n+2}} \right]} \quad (A.4.10)$$

where z and y are defined comprehensively.

Since equation (A.4.10) is valid for $n = 1$, and $n = 2$, it is first concluded that (A.4.10) is valid for any n .

From (A.4.10), it is further evident that any common multiplier to z_{n+3} and y_{n+2} can be extracted and removed. In order to deduct the formation law for A_{n+4} and B_{n+4} , we examine the specific cases $n = 2$ and $n = 3$ separately.

For $n = 2$, z_5 and y_4 are respectively equal to

$$\begin{aligned}
z_5 &= 5 \left[\frac{A_3 B_4 - A_4 B_3}{A_3 B_4 - A_4 B_3} \right] \left[\frac{A_2 B_4 - A_4 B_2}{A_2 B_4 - A_4 B_2} \right] \\
y_4 &= 3 \left[\frac{A_4 B_5 - A_5 B_4}{A_4 B_5 - A_5 B_4} \right] \left[\frac{A_2 B_3 - B_2 A_3}{A_2 B_3 - B_2 A_3} \right]
\end{aligned} \quad (A.5.11)$$

Substituting A_4 and B_4 in z_5 by their respective expressions given in (A.4.1) results in:

$$z_5 = 5 \left[\frac{A_3 B_4 - A_4 B_3}{A_3 B_4 - A_4 B_3} \right] \left[3a_{21} a_{20} \right] = 5 \left[\frac{A_3 B_4 - A_4 B_3}{A_3 B_4 - A_4 B_3} \right] 3a_{20} \left[\frac{A_2 B_3 - B_2 A_3}{A_2 B_3 - B_2 A_3} \right] \quad (A.4.12)$$

Similarly, y_4 is given by

$$\begin{aligned} y_4 &= 3 [A_4 (2a_{31} B_4 - B_3 B_4) - (2a_{31} A_4 - A_3 B_4) B_4] [A_2 B_3 - B_2 A_3] \\ &= 3B_4 [A_3 B_4 - A_4 B_3] [A_2 B_3 - B_2 A_3] \end{aligned} \quad (\text{A.4.13})$$

and therefore, after reduction of the common factor in z_5 and y_4 , the coefficient A_6 and B_6 are found to be equal to

$$\begin{aligned} A_6 &= 5a_{20} A_5 - A_4 B_4 \\ B_6 &= 5a_{20} B_5 - B_4 B_4 \end{aligned} \quad (\text{A.4.14})$$

The coefficients z_6 and y_5 are also derived comprehensively

$$\begin{aligned} z_6 &= 6 [A_4 B_5 - A_5 B_4] [A_3 B_5 - A_5 B_3] \\ &= 6 [A_4 B_5 - A_5 B_4] [A_3 (2a_{31} B_4 - B_3 B_4) - (2a_{31} A_4 - A_3 B_4) B_3] \\ &= 6 [A_4 B_5 - A_5 B_4] [2a_{31}] [A_3 B_4 - A_4 B_3] \end{aligned} \quad (\text{A.4.15})$$

and

$$\begin{aligned} y_5 &= 4 [A_5 B_6 - A_6 B_5] [A_3 B_4 - A_4 B_3] \\ &= 4 [A_5 (5a_{20} B_5 - B_4 B_4) - (5a_{20} A_5 - A_4 B_4) B_5] [A_3 B_4 - A_4 B_3] \\ &= 4 B_4 [A_4 B_5 - A_5 B_4] [A_3 B_4 - A_4 B_3] \end{aligned} \quad (\text{A.4.16})$$

which after proper reduction of the common factors, leads to

$$\begin{aligned} A_7 &= 3a_{31} A_6 - A_5 B_4 \\ B_7 &= 3a_{31} B_6 - B_5 B_4 \end{aligned} \quad (\text{A.4.17})$$

The general case is derived by induction of (A.4.1), (A.4.7), (A.4.14) and (A.4.17) and is given in (2.6.6), (2.6.7), and (2.6.8).

appendix A.5

FORMULATION OF THE FAR SCATTERED FIELD FROM AN ELLIPTIC CYLINDER

For an incident plane wave given by

$$\underline{E}_z^i = \underline{E}_0 e^{jk \cdot \underline{R}} \quad (\text{A.5.1})$$

the far scattered field \underline{E}_z^s is expressed as

$$\begin{aligned} \underline{E}_z^s = \sum_{n=0}^{\infty} [& C_{2n} \text{Me}_{2n}^{(1)}(\xi) \cdot \text{ce}_{2n}(\eta) \cdot \text{ce}_{2n}(\theta) + C_{2n+1} \text{Me}_{2n+1}^{(1)}(\xi) \cdot \text{ce}_{2n+1}(\eta) \cdot \\ & \text{ce}_{2n+1}(\theta) + S_{2n+1} \text{Ne}_{2n+1}^{(1)}(\xi) \cdot \text{se}_{2n+1}(\eta) \cdot \text{se}_{2n+1}(\theta) + S_{2n+2} \text{Ne}_{2n+2}^{(1)}(\xi) \cdot \\ & \text{se}_{2n+2}(\eta) \cdot \text{se}_{2n+2}(\theta)] \quad (\text{A.5.2}) \end{aligned}$$

following McLahlan notation⁽²⁹⁾.

In (A.5.2),

$$\begin{aligned} \text{Me}_m^1(\xi) &= \text{Ce}_m(\xi) + j\text{Fey}_m(\xi) \\ \text{Ne}_m^1(\xi) &= \text{Se}_m(\xi) + j\text{Gey}_m(\xi) \end{aligned} \quad (\text{A.5.3})$$

and in this formulation, ce_m and se_m are the even and odd solutions of order m of the regular Mathieu differential equation,

$$\frac{d^2 y}{dx^2} + (m^2 - 2q \cos 2x)y = 0 \quad (\text{A.5.4})$$

and p_m and s_m are constant multipliers defined in (29). $\text{Ce}_m(\xi)$ and $\text{Se}_m(\xi)$, $[\text{Fey}_m(\xi)$ and $\text{Gey}_m(\xi)]$, are the even and odd solutions of the first kind, [second kind], of order m of the modified Mathieu differential equation,

$$\frac{d^2 y}{dx^2} - (m^2 - 2q \cosh x)y = 0 \quad (\text{A.5.5})$$

The coefficients C_m and S_m are determined from the boundary condition for the total field \underline{E}_z , i.e.,

$$\underline{E}_z = \underline{E}_z^i + \underline{E}_z^s = 0 \text{ at } \xi = \xi_0 \quad (\text{A.5.6})$$

It is shown in McLahlan⁽²⁹⁾ that the scattered field \underline{E}_z^s under the condition (A.5.6) results in:

$$\begin{aligned} \underline{E}_z^s = -2E_{z0} \sum_{n=0}^{\infty} \{ & \alpha_{2n}(\xi_0) \cdot \frac{Me_{2n}^{(1)}(\xi)}{p_{2n}} \cdot ce_{2n}(\eta) \cdot ce_{2n}(\theta) + \beta_{2n+2}(\xi_0) \cdot \\ & \frac{Ne_{2n+2}^{(1)}(\xi)}{s_{2n+2}} \cdot se_{2n+2}(\eta) \cdot se_{2n+2}(\theta) + j \left[\gamma_{2n+1}(\xi_0) \cdot \frac{Me_{2n+1}^{(1)}(\xi)}{p_{2n+1}} \cdot \right. \\ & \left. ce_{2n+1}(\eta) \cdot ce_{2n+1}(\theta) + \delta_{2n+1}(\xi_0) \cdot \frac{Ne_{2n+1}^{(1)}(\xi)}{s_{2n+1}} \cdot se_{2n+1}(\eta) \cdot se_{2n+1}(\theta) \right] \} \end{aligned} \quad (\text{A.5.7})$$

where

$$\begin{aligned} \alpha_{2n}(\xi_0) &= \frac{Ce_{2n}(\xi_0)}{Me_{2n}^{(1)}(\xi_0)} ; \quad \beta_{2n+2}(\xi_0) = \frac{Se_{2n+2}(\xi_0)}{Ne_{2n+2}^{(1)}(\xi_0)} \\ \gamma_{2n+1}(\xi_0) &= \frac{Ce_{2n+1}(\xi_0)}{Me_{2n+1}^{(1)}(\xi_0)} ; \quad \delta_{2n+1}(\xi_0) = \frac{Se_{2n+1}(\xi_0)}{Ne_{2n+1}^{(1)}(\xi_0)} \end{aligned} \quad (\text{A.5.8})$$

In the far field, i.e. for large values of ξ , the confocal ellipses are approximately concentric circles and the following relations hold:

$$\frac{-2Me_{2n}^{(1)}(\xi)}{p_{2n}} = -2j \frac{Ne_{2n+1}^{(1)}(\xi)}{s_{2n+1}} = 2 \sqrt{\frac{2}{\pi kR}} e^{j(kR+3/4)} \quad (\text{A.5.9})$$

which results with (A.5.7) in (3.2.7).

The expansion of the Mathieu functions of the first kind which appear in (3.2.9) and (3.2.11) are given next in terms of their coefficients A_m^n and B_m^n . Although they are not entering directly in the derivation of the far scattered field, they will be referred to in section (3.4.2) and are presented here for convenience. The functions

$$ce_{2n}(\phi, q) = \sum_{r=0}^{\infty} A_{2r}^{2n} \cos 2r\phi, \quad n = 0, 1, 2, \dots \quad (\text{A.5.10})$$

are periodical, modulo π , even in the angle ϕ , and hence have a constant term in the series expansion which is function of q . The functions

$$ce_{2n+1}(\phi, q) = \sum_{r=0}^{\infty} A_{2r+1}^{2n+1} \cos(2r+1)\phi, \quad n = 0, 1, 2, \dots \quad (\text{A.5.11})$$

are periodical, modulo 2π , and even in the angle ϕ . The functions

$$se_{2n+1}(\phi, q) = \sum_{r=0}^{\infty} B_{2r+1}^{2n+1} \sin(2r+1)\phi, \quad n = 0, 1, 2, \dots \quad (\text{A.5.12})$$

are periodical, modulo 2π , and odd in ϕ , and the functions

$$se_{2n+2}(\phi, q) = \sum_{r=0}^{\infty} B_{2r+2}^{2n+2} \sin(2r+2)\phi, \quad n = 0, 1, 2, \dots \quad (\text{A.5.13})$$

are periodical, modulo 2π and odd in ϕ . The employed notation is that of McLahlan and is such that ce_{2n} , ce_{2n+1} , se_{2n+1} , se_{2n+2} have n zeros in $0 < \phi < \pi/2$.